

Cost Optimization of Power-to-Methane Process with Dynamic Modelling

Elisa Konttila

School of Chemical Engineering

Thesis submitted for examination for the degree of Master of
Science in Technology.

Espoo 15.7.2022

Supervisor

Prof. Annukka Santasalo-Aarnio

Advisors

MSc Henri Karimäki

MSc Juho Piispa

Copyright © 2022 Elisa Konttila

Author Elisa Konttila

Title Cost Optimization of Power-to-Methane Process with Dynamic Modelling

Degree programme Advanced Energy Solutions

Major Industrial Energy Processes and Sustainability **Code of major** CHEM3044

Supervisor Prof. Annukka Santasalo-Aarnio

Advisors MSc Henri Karimäki, MSc Juho Piispa

Date 15.7.2022 **Number of pages** 107 **Language** English

Abstract

Two major crisis, climate change and Russian war on Ukraine, disturb the stability of the current energy system. Alternative fuels must be developed to limit the global warming and to ensure the energy security in European countries. Synthetic natural gas (SNG) can respond to these needs because of its renewable origin and its properties that match the ones of fossil natural gas.

Because of the increasing amount of fluctuating renewable energy, demand response will play a large role in the future energy system. Therefore, it is important to study the dynamic properties of the production of SNG, process called Power-to-Methane, and if the process could adjust its load according to electricity prices.

In this thesis, the dynamic capabilities of Power-to-Methane were reviewed, as well as the requirements that must be fulfilled in order to the participate to demand response. It was concluded that electrolysers have the best dynamic properties of the process components and are able to participate to most of the market places in the Finnish electricity system. A Simulink model was created to study the optimal dynamic operation method of the electrolyser with regards to decreasing electricity costs of the operation. In addition, an optimal intermediate hydrogen storage size was found with which the total costs of the process were the lowest. The optimal storage size was 3100 or 4650 kg depending on the electricity price scenario that was modelled.

The results of the economic analysis show that the costs of the process can be significantly reduced with dynamic operation when electricity is bought with spot market prices. However, current electricity prices are too high to be able to profit from the production even with dynamic operation. When electricity prices from the beginning of 2021 were utilized, the production was profitable. The most profitable process was achieved with steady operation with average PPA-price from Finland.

Dynamic operation with the most fluctuating electricity prices resulted in the largest cost reductions. When increasing the share of renewable electricity, the prices evolve to be cheaper and more volatile due to the low generation cost and intermittent nature of renewable energy. Therefore, dynamic operation can be a more cost-effective method to produce SNG in the future. Additionally, increasing natural gas prices contribute to this process becoming more feasible.

Keywords Power-to-Methane, Dynamic modelling, Demand response, Electrolyser, Hydrogen storage, Simulink

Tekijä Elisa Konttila

Työn nimi Power-to-Methane Prosessin Kuluoptimointi Dynaamisella Mallinnuksella

Koulutusohjelma Advanced Energy Solutions

Pääaine Industrial Energy Processes and Sustainability **Pääaineen koodi** CHEM3044

Työn valvoja Prof. Annukka Santasalo-Aarnio

Työn ohjaaja DI Henri Karimäki, DI Juho Piispa

Päivämäärä 15.7.2022

Sivumäärä 107

Kieli Englanti

Tiivistelmä

Kaksi merkittävää kriisiä, ilmastonmuutos ja Venäjän sota Ukrainaa vastaan, horjuttavat nykyisen energiajärjestelmän vakautta. Vaihtoehtoisia uusiutuvia polttoaineita on kehitettävä ilmaston lämpenemisen rajoittamiseksi ja Euroopan maiden energiavarmuuden varmistamiseksi. Synteettinen maakaasu (SNG) voi vastata näihin tarpeisiin uusiutuvan alkuperänsä ja maakaasua vastaavien ominaisuuksien vuoksi.

Kysyntäjoustolla tulee olemaan suuri rooli tulevaisuuden energiajärjestelmässä uusiutuvan energian määrän lisääntymisen vuoksi. Sen vuoksi on tärkeää tutkia SNG:n tuotannon, Power-to-Methane prosessin, dynaamisia ominaisuuksia ja sitä, voisiko prosessin kuormaa säätää sähkön hinnan mukaan.

Tässä diplomityössä tarkasteltiin mahdollisuuksia operoida Power-to-Methane prosessia dynaamisesti sekä vaatimuksia, jotka on täytettävä, jotta se voi osallistua kysyntäjousto. Todettiin, että elektrolyysereillä on parhaat dynaamiset ominaisuudet prosessikomponenteista ja ne pystyvät osallistumaan suurimmalle osalle Suomen sähköjärjestelmän markkinapaikoista. Simulink-mallilla tutkittiin elektrolyysilaitteen optimaalista dynaamista ajotapaa prosessin sähkökustannusten alentamiseksi. Lisäksi löydettiin optimaalinen välivarastokoko, jolla prosessin kokonaiskustannukset olivat alhaisimmat. Optimaalinen varastokoko oli 3100 tai 4650 kg riippuen mallinnetusta sähkön hintaskenaariosta.

Taloudellisen analyysin tulokset osoittavat, että prosessin kustannuksia voidaan merkittävästi alentaa dynaamisella ajotavalla, kun sähköä ostetaan spot-markkinahinnoilla. Nykyiset sähkön hinnat ovat kuitenkin liian korkeat, jotta tuotanto olisi kannattavaa edes dynaamisella operointitavalla. Tuotanto oli kannattavaa, kun 2021 alun sähköhintoja hyödynnettiin. Kannattavin prosessi saavutettiin tasaisella operoinnilla Suomen keskimääräisellä PPA-hinnalla.

Dynaaminen operointitapa tiheimmillä sähkön hinnanvaihteluilla johti suurimpiin kustannussäästöihin. Sähkön hinnat tulevat tulevaisuudessa muuttumaan halvemmiksi ja epäsäännöllisimmiksi uusiutuvan energian alhaisten tuotantokustannusten ja ajoittaisen luonteen vuoksi. Siksi dynaaminen ajotapa voi tulevaisuudessa olla kustannustehokkaampi tapa tuottaa SNG:tä. Myös maakaasun korkealle nousseet hinnat edesauttavat prosessin kehitystä kannattavammaksi.

Avainsanat Power-to-Methane, Dynaaminen mallinnus, Kysyntäjousto, Elektrolyyseri, Vetyvarasto, Simulink

Alkusanat

Tätä kirjottaessani siitä on melkein tasan viisi vuotta, kun sain tietää päässeeni opiskelemaan kemian tekniikkaa Aalto-Yliopistoon. Muistan olleeni epävarma siitä mitä opinnot tulevat pitämään sisällään, koska minulla ei etukäteen ollut oikeastaan mitään tietoa alasta. Nyt viisi vuotta myöhemmin pystyn sanomaan, että alan valinta meni täysin nappiin, vaikka sen tekikin vähän summa mutikassa. Kiitokset avusta alan valinnassa menee Noralle, joka tiesi paremmin kuin itse tiesin mikä ala minulle sopisi, ja äidilleni, joka tiesi Noran tietävän tämän ja organisoii tapaamisen. Itse opinnot sisälsivät paljon hyvää: mielenkiintoisia kursseja, uusia ystäviä, paljon oppimista sekä opiskelijatapahtumia, mutta olen myös enemmän kuin innokas aloittamaan työurani tässä energiamurroksen kulta-ajassa.

Haluan kiittää ohjaajiani Henri Karimäkeä ja Juho Piispaa kaikesta avusta ja ohjauksesta, joita sain diplomityöni aikana. Kommunikointiväylä oli aina avoin ja apua oli aina tarvittaessa saatavilla, mikä auttoi luomaan miellyttävän työskentelyilmapiirin. Kiitokset kuuluu myös valvojalleni Annukka Santasalo-Aarniolle, joka varmisti työn menevän Aallon protokollan mukaisesti. Hän myös vahvisti kiinnostustani tähän aiheeseen jo ensimmäisten maisterikurssien aikana kiinnostavilla luennoillaan. Haluan myös kiittää kollegoitani X-ahead projektin alla avusta mm. oikolukemisen ja vertaistuen muodossa. Olen myös erittäin kiitollinen Tommi Rintamäelle, Henri Karimäelle ja Petri Laaksolle mahdollisuudesta päästä tekemään diplomityötä erittäin kiinnostavasta aiheesta.

Erittäin suuri kiitos kuuluu kaikille perheenjäsenilleni, jotka toimivat suurimpana kannustusjoukkonani koko opiskeluideni ajan ja vahvistivat näin uskoa itseeni. Heidän kiinnostuksensa opiskeluihini oli lakkaamatonta ja tiesin, että heille on helppo jakaa sekä hyvät että huonot uutiset. Haluan kiittää myös kumppaniani kannustuksesta ja kaikista myönnytyksistä, joita hän on tehnyt varmistaaksemme opiskelurauhan minulle kahden vuoden etä(korona)opiskeluiden aikana. Myös ystäväni, yhdessä kumppanini kanssa, ovat olleet tärkeä voimavara, jonka avulla olen saanut siirrettyä ajatuksia muualle vapaa-aikanani. Kiitos, että olette!

Otaniemi, 15.7.2022

Elisa Konttila

Contents

Abstract	3
Tiivistelmä	4
Alkusanat	5
Contents	6
Symbols and abbreviations	8
1 Introduction	10
2 Power-to-Methane	12
2.1 Demand Response	14
2.2 Sector Coupling	19
3 Carbon Capture	22
3.1 Absorption Process	22
3.2 Point Sources	24
3.3 Dynamic Properties	26
4 Water Electrolysis	31
4.1 Alkaline Electrolysis	32
4.2 Proton-Exchange Membrane Electrolysis	33
4.3 Solid Oxide Electrolysis	34
5 Synthesis	36
5.1 Methane	36
5.1.1 Catalytic Methanation	36
5.1.2 Biological Methanation	45
5.2 Alternative Synthesis Technologies	48
5.2.1 Methanol	48
5.2.2 Fischer-Tropsch	49
6 Hydrogen Storage	51
7 Dynamic Modelling	54
7.1 State-of-the-Art Dynamic Modelling	54
7.2 Simulation Software	58
8 Methods	59
8.1 Process Model	59
8.1.1 Water Electrolysis	64
8.1.2 Hydrogen storage	65
8.1.3 Carbon capture	65

8.1.4	Methanation	66
8.1.5	Demand Response Payments	66
8.1.6	Methodology and Model validation	66
8.2	Economic analysis	68
9	Results	73
9.1	Optimized Operation Parameters for the Electrolyser	73
9.2	Capital Expenditures	77
9.3	Operating Expenditures	78
9.4	Levelized Cost of Synthetic Natural Gas	81
9.5	Net Present Value	85
10	Conclusions	91
	References	94

Symbols and abbreviations

Symbols

F	Faraday's constant, [C/mol]
I	Current, [A]
M	Molar mass, [g/mol]
m	Mass, [kg]
\dot{m}	Mass flow rate, [kg/s]
N	Number of objects, [-]
n	Amount of substance, [mol]
\dot{n}	Molar flow rate, [mol/s]
P	Power, [W]
p	Pressure, [bar]
R	Universal gas constant, [$J/(molK)$]
r	Discount rate, [%]
T	Temperature, [K], [$^{\circ}C$]
V	Volume, [m^3]
Z	Compressibility factor, [-]
γ	Diatomic constant, [-]
η	Efficiency, [%]
ρ	Density, [kg/m^3]

Operators

$\frac{\partial}{\partial t}$	Partial derivative with respect to variable t
\sum_i	Sum over index i

Abbreviations

AEL	Alkaline Electrolysis
a-FRR	Automatic frequency restoration reserve
CAPEX	Capital expenditure
CHP	Combined heat and power
CMP	Capacity market program
CSTR	Continuous stirred tank reactor
CZA	Copper-zinc-alumina
DB	Demand bidding
DEA	Diethanolamine
DLC	Direct load control
DR	Demand response
E-fuel	Electrofuel
EU ETS	European emission trading system
FCR	Frequency containment reserve
FCR-D	Frequency containment reserve for disturbances
FCR-N	Frequency containment reserve for normal operation
FFR	Fast frequency reserve
FLH	Full load hours
FRR	Frequency restoration reserve
FT	Fischer-Tropsch
GHSV	Gas hourly space velocity
I/C	Interruptible/Curtailable Service
IEA	International Energy Agency
IRR	Internal rate of return
LCES	Liquid carbon dioxide energy storage system
LCOCO ₂	Levelized cost of carbon dioxide
LCOH ₂	Levelized cost of hydrogen
LCOSNG	Levelized cost of synthetic natural gas
LHV	Lower heating value
LOHC	Liquid organic hydrogen carrier
MDEA	N-methyldiethanolamine
MEA	Monoethanolamine
m-FRR	Manual frequency restoration reserve
NPV	Net present value
OPEX	Operating expenditure
PEM	Proton-exchange membrane
PPA	Power purchase agreement
PtH	Power-to-Hydrogen
PtM	Power-to-Methane
PtX	Power-to-X
RE	Renewable energy
RWGS	Reverse water-gas-shift
SNG	Synthetic natural gas
SOE	Solid oxide electrolysis
TBR	Trickle-bed reactor
TOU	Time-of-use
TSO	Transmission system operator
VRE	Variable renewable energy
YSZ	Yttria stabilized zirconia

1 Introduction

Global energy transition is experiencing large contributions from major historical events in the 2020s. Due to Covid-19 pandemic, energy-related carbon dioxide emissions decreased heavily in 2020 and then again increased after the pandemic started to ease in 2021. This increase corresponds to two-thirds of the pandemic-related reductions and it is the second largest single rise in the history with a 4 % increase in the emissions. This requires actions to steer the change back to downward trend to stay on track with the climate goals, specifically limiting the temperature rise to 1.5 °C. [1]

Additionally, Russia's war on Ukraine in 2022 forces majority of the other countries to reconsider their energy security. Russia is one of the top three crude oil producers and the second-largest natural gas producer globally. [2] In Finland, Russian imports covered 44.6 % of total fossil fuel demand, corresponding to about 57.6 TWh. When only natural gas is considered, the percentage grows to 67.8 %, which corresponds to about 13.8 TWh. However, the natural gas imports have come down to this value from 100 % quite recently. [3, 4] To lower the dependency of Russia's imports even further, actions need to be taken. International energy agency, IEA, has written a 10-point plan to reduce the reliance and suggests actions such as accelerating the development of green alternatives and making the most of the current low emission energy sources, such as bioenergy and nuclear. [5]

Natural gas is a versatile fuel that has many applications in different sectors. These sectors include industry, power generation, heating and transportation. [6] However, utilization of natural gas is compromised due to the sudden decreased availability of it and climate goals that require the transition from fossil sources to renewable ones. Therefore, there is a need for a fuel that could replace fossil natural gas. synthetic natural gas (SNG) is a fuel that can be produced from renewable sources and its properties match the ones of natural gas [7].

Power-to-X (PtX) is a concept where renewable electricity is used to produce various products. The variety and increasing amount of the different products is denoted as "X". These products include essentials such as fuels, chemicals, heat or energy carriers for storage. [8, 9] PtX technology has multiple benefits in addition to replacing of fossil fuels. With PtX, energy security can be improved by balancing electricity supply and demand, and thus electricity grid. PtX also offers a possibility to store electricity in the final product. In this thesis, the focus is on the production of SNG, a process called Power-to-Methane (PtM).

Electricity prices as well as availability of electricity are becoming more and more volatile as the amount of variable renewable energy (VRE) is increasing. Due to this change in the energy system, electricity producers may not be able to control the production as much as needed and thus more flexibility is required from consumers to help to stabilize the grid. Therefore, an important aspect to study is the ability of the PtM process to respond to the changes in electricity system. [8] The aim of this thesis is to research if the PtM process could be operated dynamically based on variations in electricity price and if this kind of operation could be economically feasible. Transient operation of PtM requires an intermediate hydrogen storage that

has an effect on the costs of the process. Therefore, optimal size of the hydrogen storage is studied. With flexible operation, there is a possibility to participate to demand response (DR) markets, if the market requirements are fulfilled. In addition, the effect of transient operation to sector coupling possibilities are reviewed. The research questions of the thesis are:

- What are the limitations of flexible operation of Power-to-Methane process and can the limitations be improved?
- What are the market requirements for dynamic operation of Power-to-Methane in demand response and in sector coupling?
- What is the optimal size of intermediate hydrogen storage to achieve the highest economical feasibility of the transient operation of Power-to-Methane and how will the feasibility of that compare to the feasibility of steady operation with wholesale or power purchase agreement -prices?

This thesis is divided into three parts: literature review, Simulink model and economic analysis. The literature review includes explanation on the dynamic properties of the process components and the market requirements for the transient operation. The scope of the literature review includes each PtM component: water electrolyser, CO₂ capture and methane synthesis. For electrolysis, all three main technologies: alkaline, proton-exchange membrane and solid oxide electrolyser, and their dynamic properties are reviewed. One technology, amine based absorption, is chosen for carbon capture. Methanation is divided into catalytic and biological methanation. In addition, different hydrogen storage technologies are shortly reviewed but the focus is on pressurized vessels. Market requirements for demand response in the Finnish electricity system are reported as well as sector coupling possibilities from the context of grid injection of the produced SNG.

The created Simulink model is used to study the effect of transient operation on the electricity costs of the electrolyser. In the model, only dynamic operation of the electrolyser is taken into account and methanation is kept stable with the intermediate storage. Different electricity price data, called electricity price mixes, from years 2021 and 2022 are used as a input for the model, and for each mix, different hydrogen storage capacities are modelled. It will be investigated how the storage capacity affects to the electricity costs of the process. In addition, a comparison between the electricity price mixes is done and it will be studied how electricity price variation frequency and magnitude affect to the costs of the process.

In the economic analysis, profitability of the different scenarios are examined. Capital and operating expenditures as well as levelized cost of synthetic natural gas (LCOSNG) and net present value (NPV) are calculated for each scenario. From the results, the optimal hydrogen storage size can be concluded. The profitability of the dynamic cases, and in particular the optimal cases, are compared to profitability of steady operation with wholesale prices and power purchase agreement (PPA) prices. Finally, the thesis concludes with a discussion on the feasibility of the transient PtM process and following that, final conclusions will be drawn and presented.

2 Power-to-Methane

Power-to-Methane is a process where synthetic natural gas is produced from renewable electricity. This process consists of an electrolyser, a carbon capture unit and a synthesis reactor. Renewable electricity is used to power the electrolyser that converts water into green hydrogen. Carbon dioxide is captured from flue gases, directly from air or by digestion of biomass. Hydrogen and carbon dioxide are then converted into methane. This process is one of the many alternatives under the Power-to-X technology.

The ongoing energy transition has sped up the development of PtX technologies, including PtM. Many commercial projects have already arisen around the world. Europe being the leading region in the initialized projects. The commissioned PtX projects in Europe are presented in a diagram in Figure 1. It can be seen that the interest started to rise in 2011 and has since experienced a wave like pattern. 2018 and 2020 being the years that stand out with the highest number of commissioned projects. Germany has the largest share, 44 %, of the PtX projects in Europe. The capacity of the projects is classified by the electrolyser capacity. Most of the projects are above 1 MW scale, however, also multiple smaller, 5 - 100 and 100 - 500 kW, projects have been initialized. The energy source was specified to be either direct or surplus renewable energy or renewable energy in the form of certificates in most of the projects. However, in some of the projects, national grid is used, which may result in quite low usage of renewables. [10]

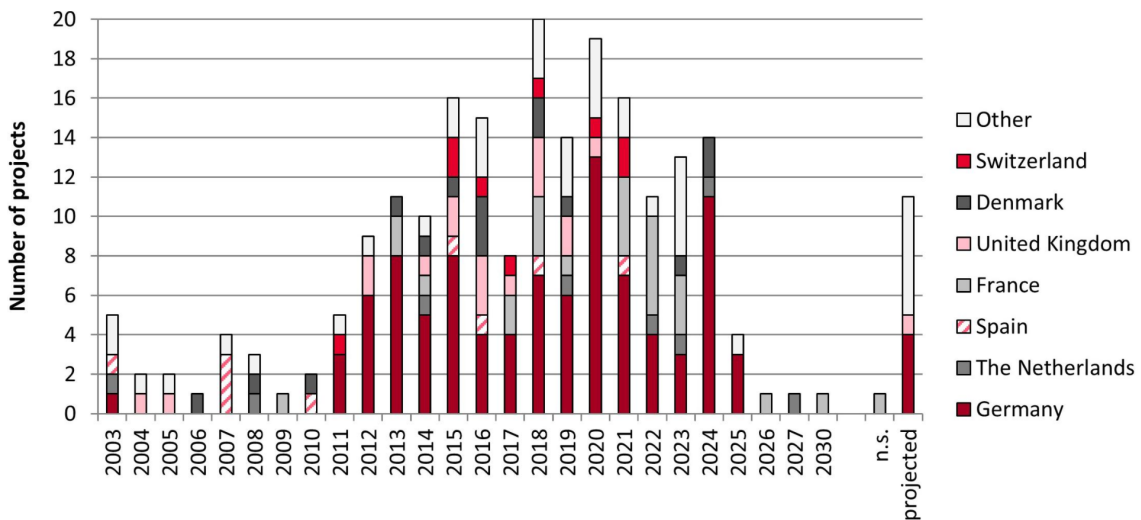


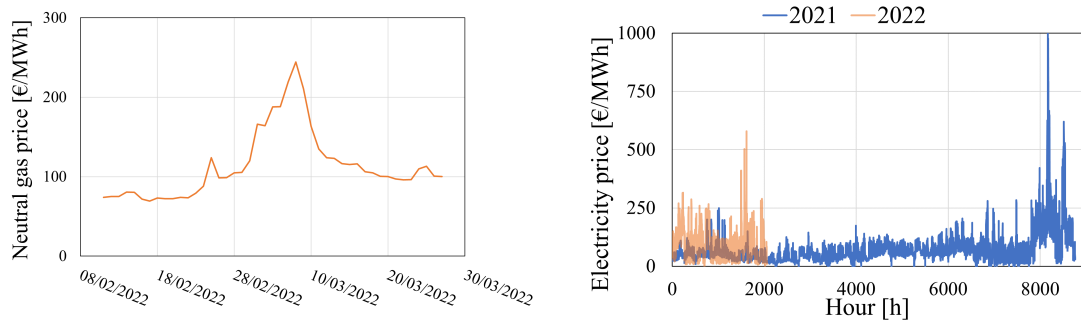
Figure 1: Commissioned Power-to-X projects in Europe. n.s. not specified. [10]

Hydrogen is used to produce methane in 22 % of the European PtX projects. PtM being then the second most utilized PtX technology. Only Power-to-Hydrogen (PtH) being ahead of PtM with a large share of 69 % of the projects. The benefit of PtH is that the additional processing of the produced hydrogen can be neglected and carbon capture is not needed. Therefore, the complexity and the cost of the plant decrease. [10] However, PtM is preferred because of the ready infrastructure for the

product and the increased safety of methane in comparison with hydrogen [11, 12]. Hydrogen has wider flammability range and lower ignition energy than methane. In addition, due to its small size, hydrogen can escape structures more easily and be exposed to oxygen which increases the risk of explosion. [12]

The challenge of PtM is related to the costs of producing SNG versus the cost of fossil natural gas. The largest contributor to the SNG cost is the electricity price. Guilera et al. [11] calculated the cost of SNG to be 70 - 125 €/MWh depending on the electricity price of a particular region. Electricity prices from 2016 were used in the calculations and it was considered that the plant was operated continuously. The cost of SNG was calculated to be 2 - 7 times higher than that of natural gas. In future scenarios, it was estimated that SNG could reach costs as low as 40 €/MWh with efficiency improvements and policies. This cost was competitive with the natural gas price at that time. [11]

However, the prices of natural gas and electricity have changed recently due to the newest worldwide crisis, Russia's war in Ukraine. Natural gas prices varied between 16 - 62 €/MWh in the study of Guilera et al. [11] in 2018. After the Russian invasion of Ukraine, the gas prices have reached record high values, the European 20-day average being 132.8 €/MWh according to TTF neutral gas price index in March of 2022 [13]. In addition to the war, natural gas prices started to increase already in 2021 because of low natural gas supply in Europe [14]. Electricity prices have also gone up considerably during 2021 and 2022 mainly due to the high natural gas prices in electricity generation. In addition, the decreased hydropower generation due to dry weather and low reserves have increased the electricity prices as have the high CO₂ prices. [15, 16] However, the effect of high CO₂ prices had a minimal effect when compared to the high fossil gas prices [16]. Average wholesale market price of electricity in the end of 2021 was four times higher than the 2015-2020 average [15]. The TTF neutral gas price index evolution during February and March of 2022 as well as electricity spot prices in Finland in 2021 and 2022 are shown in Figure 2.



(a) TTF neutral gas prices in Europe. Data from [17].

(b) Electricity prices in Finland in 2021 & 2022. Data from [18].

Figure 2: Natural gas and electricity price evolution.

Due to the major price fluctuations of natural gas and electricity, it is hard to estimate the feasibility of SNG in the future. However, because most of the world's

natural gas supplies have been compromised due to Russia’s invasion, alternative sources for natural gas are required to replace the Russian imports. These alternatives include also synthetic natural gas. [5] Therefore, the development of PtM enables energy transition to renewable sources and also strengthens the energy security of European countries.

2.1 Demand Response

Demand response (DR) is a method to respond to the increasing amount of VRE by evening out the time-dependent changes in electricity consumption with demand side management. Due to the intermittent nature of the weather-based renewable energy sources, supply can not always follow demand. Therefore, it is important that demand can be changed according to the available supply. DR is divided into load shedding and load following measures. In load shedding, the electricity consumers reduce load in times of peak demand, and in load following, they shift the consumption to a time of lower demand or higher VRE generation. These measures are necessary to avoid demand surpassing supply or excess curtailment of VRE. [19] However, to be able to participate to the DR actions, flexibility and dynamic capabilities are required from the consumer.

As the economic feasibility of SNG is uncertain due to the volatile electricity prices, measures to increase the feasibility are needed. Demand response can provide possibilities for a PtM plant to increase its economic feasibility. Different demand response programs have been developed around the world to balance the electricity consumption. The demand response programs used in the United States are listed in Figure 3. [20] In EU, there is no uniform program structure because the electricity markets are not integrated. However, some of the time-based and incentive-based programs listed in Figure 3 are also known in EU, for example Time-of-Use (TOU), Direct Load Control (DLC) and Demand Bidding (DB). [21, 22] Time-based programs, also called implicit programs, refer to measures where electricity price is varied dynamically. At times of high demand, the price is increased which compels some of the customers to decrease their consumption. This way, the consumers receive cost reductions in the form of lower production costs. However, incentive-based, or explicit, programs may be more tempting because they offer incentives for industrial consumers to lower their load at specific times. Therefore, in an explicit method, the consumer gains savings in the forms of reduced production cost and direct payments in exchange to load reductions. [20, 21] Some of the incentive-based programs are mandatory after contracts have been signed, for example Interruptible/Curtailable Service (I/C) and Capacity Market Program (CMP). In these programs consumers are subject to penalties if they do not come up to expectations regarding load curtailment. However, other programs offer freer demand response possibilities. For example in demand bidding consumers bid how much load they would be ready to curtail with given incentives. [20] Implicit and explicit demand response programs are not replacements for each other, but both of them are required to tempt different consumers to participate in demand response [21].

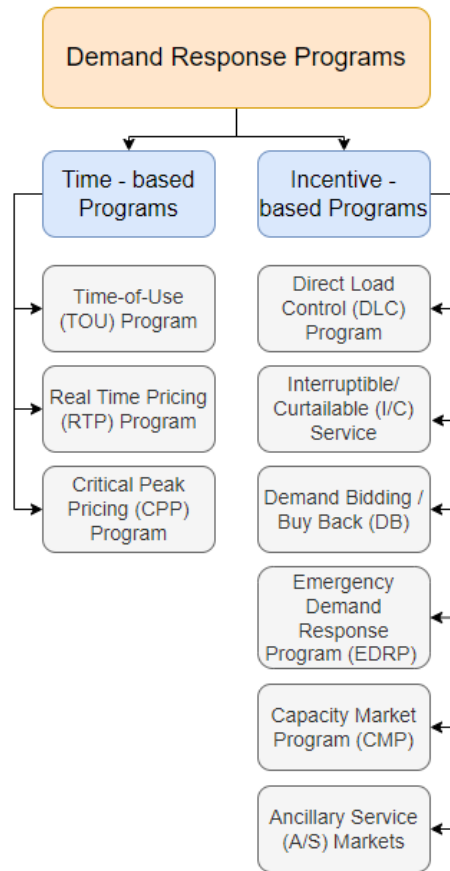


Figure 3: Demand response programs. Modified from [20].

In Finland, demand response can participate in all of the market places in the electricity system [21]. These markets include reserve products from the Finnish transmission system operator (TSO) such as frequency containment reserve (FCR), frequency restoration reserve (FRR) and fast frequency reserve (FFR). The aim of these products is to balance the frequency of the electricity grid to stay on 50 Hz. The purpose of FCR is to contain the 50 Hz frequency whereas FRR restores it after changes. FCR is divided into products for normal operation (FCR-N) and for disturbance (FCR-D). FRR is divided into automatic (a-FRR) and manual (m-FRR). [23] Under manual frequency restoration reserve, there are markets, such as balancing energy market and balancing capacity market [21]. Fast frequency reserve is developed for disturbances in low inertia situations. [24] In addition to market places provided by the TSO, demand response can also be applied in the Nordic Wholesale market. The reserve market places of Fingrid are presented in Figure 4 and the amount of demand response utilized in the Finnish electricity system on 1.2.2022 is shown in Figure 5.

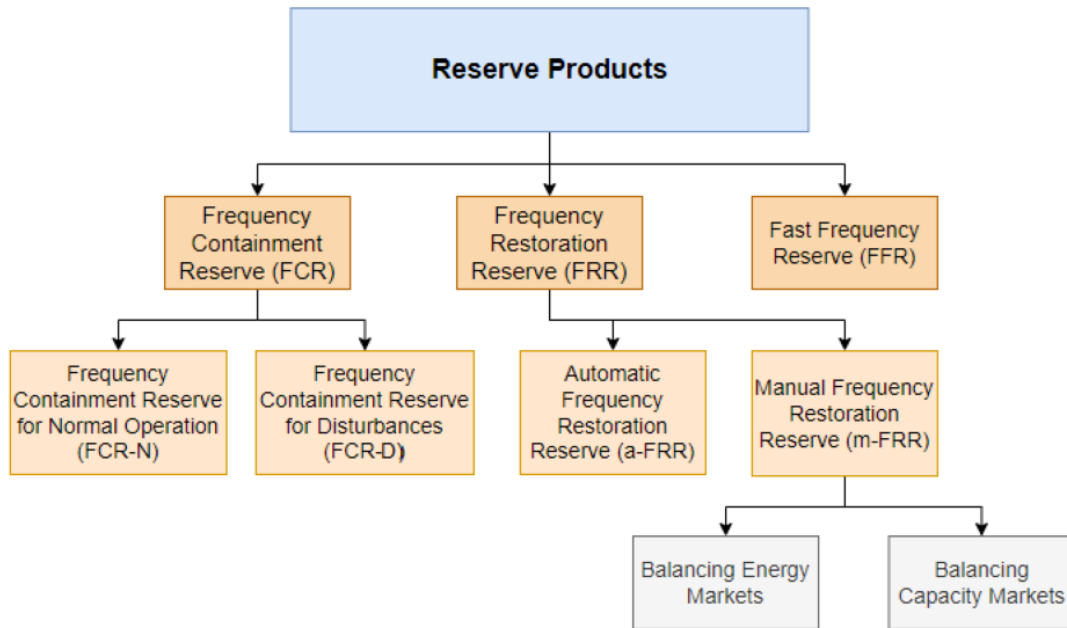


Figure 4: Reserve Markets in Finland. Data from [21, 23].

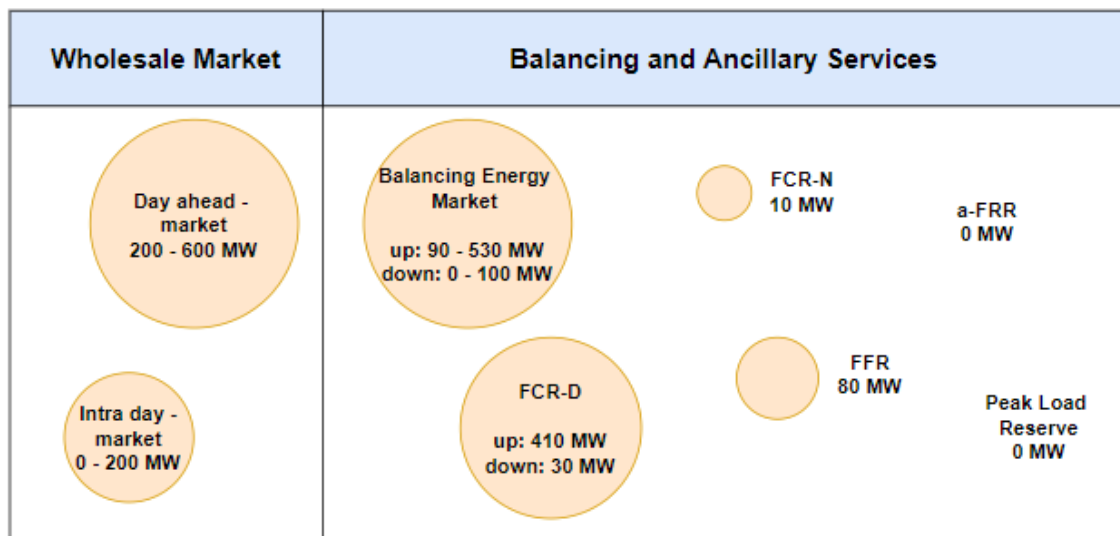


Figure 5: Demand Response in Finnish Electricity Market. Modified from [21, 25].

From Figure 5, it can be seen that the participation of DR is the highest in the wholesale markets, m-FRR and FCR-D whereas for the a-FRR and peak load reserve it is non-existing [25]. Therefore, a-FRR and peak load reserve are not covered in this thesis. There are requirements for the energy curtailment size and ramping rate to participate in these markets. The lowest electricity consumption curtailment, 0.1 MW, is accepted in the Wholesale markets and in FCR-N. The highest one is required in the balancing energy market, a minimum of 5 MW curtailment in the

energy consumption must succeed in 15 minutes to take part in this market. The fastest response time is expected in the FFR, the load must be activated from zero to nominal in 1.3 seconds when the frequency drops under 49.7 Hz, and even faster rates are required for lower frequencies. In the Wholesale markets, the demand is controlled with implicit method whereas in the TSO's reserve markets, the explicit, or incentive-based method is more common, particularly demand bidding -method [26, 24]. The payments received from the TSO are based on bids given by the generators and consumers. The price equals the highest bid that was taken into use on that particular hour or year depending on if the bids have been given in the hourly or yearly markets. In hourly markets, the price varies every hour and in the yearly markets, the same price is used throughout the year. In balancing market the price is at least the spot price. Additionally, in the balancing energy market and in FCR-D Down market, consumers can also participate in the down-regulating market by accepting low-cost energy bids to increase the consumption at certain times. [24, 27] The payments received from demand response behaviour and requirements for participation in the markets are shown in Table 1. The payments for down-regulating markets are marked with minus sign to represent the money transferred to the generator. For the hourly market payments, average price of the year 2022 until 6.4.2022 was used.

Table 1: Requirements and payments for participating in electricity markets.

Market	Contract Type	Minimum Bid Size	Ramp Requirement	Activation	Activation Frequency	Payment	Source
FCR-N	Hourly /Yearly	0.1 MW	3 min / 100 %	After +/- 0.1 Hz change	Constantly	19.85 €/MW / 12.24 €/MW/h	[28, 29, 26]
FCR-D Up	Hourly /Yearly	1 MW	5 s / 50 % 30 s / 100 %	After frequency change from 49.9 to 49.5 Hz After frequency change from 50.1 to 50.5 Hz	Multiple times a day Couple times a year	2.6 €/MW / 1.9 €/MW/h 23.95 €/MW / 10 €/MW/h	[28, 29, 26] [28, 29, 26]
Balancing Energy	Hourly	5 MW (1 MW if electronic activation is used)	15 min / Min. Bid	Manual	Depends on the bids and balancing needs	Up: 107.28 €/MWh	[27, 30, 26]
FFR	Hourly	-	Activation: 1.3 s / 100 % 1 s / 100 % 0.7 s / 100 %	Below 49.7 Hz, 49.6 Hz, 49.5 Hz	Depends on the inertia of the electricity system	17 €/MW	[24, 31]
Day Ahead	Hourly	0.1 MW	-	12 h	-	Market price	[21, 26]
Intra day	Hourly	0.1 MW	-	1 h	-	Market price	[21, 26]

Alternatively, a power purchase agreement (PPA) could be used to stabilize the electricity cost of the process. PPA is a long-term agreement between power producer and consumer on a stable electricity price and consumption. These contracts are usually made to avoid the uncertainty that comes from fluctuating VRE for both producer and consumer. [32] For the consumer the benefit is that the electricity price does not increase above the agreed price. However, a relatively higher price has to be paid when electricity would otherwise be cheap. To utilize the stabilized electricity price of PPA, flexible operation is not required. However, in theory, the feasibility of the agreement could be increased even further with flexible operation. When the wholesale price of electricity would be very high, the load of the process could be reduced and electricity could be sold with the higher price. This way, profit would be made by selling the cheap PPA electricity with more expensive wholesale prices. However, in practise, this method does not support grid stabilization as it shifts the electricity consumption elsewhere at times of high demand instead of reducing the consumption or shifting it to times of lower demand. In addition, the resale of the PPA-bought electricity could be challenging for transient operation as the resale occurs often via a "back-to-back" PPA, meaning that the resale contract has similar terms as in the initial PPA [33, 34]. This means that the reseller should be able to engage to selling a constant amount of electricity, which is not reasonable as the electricity consumption of the reseller varies. Additionally, selling of electricity may be regulated to only certain utilities depending on the national law [34]. However, steady operation with PPA will be taken as a comparison case in addition to steady operation with wholesale electricity prices. These comparisons are made to expand the understanding of the feasibility of transient operation of PtM and how it compares with steady operation.

2.2 Sector Coupling

Sector coupling is a method to interconnect power producing sector to energy consuming ones to increase the rate of decarbonisation within the consumers side. Energy consumers, such as industry and transportation, are heavily dependent on fossil fuels. With new technologies and sector coupling, the dependency of fossil fuels can be decreased by powering the consuming sectors with renewable electricity. [35] Practical examples of sector coupling are electric vehicles, which use the electricity directly, and e-fuels from PtX, which serve as energy carriers [10].

The benefit of Power-to-X technology in sector coupling is the wide range of applications it can be adapted to. The higher number of application possibilities, the better decarbonisation potential the technology has. The field of applications of the commissioned PtX projects in Europe are presented in Figure 6. These applications are industrial processes, combined heat and power plants, fuels and natural gas grid injections. Fuel applications becoming the majority of PtX applications in Europe is quite a recent trend that started in 2018. Before that, natural gas blending was the most common application, meaning that the product of PtX was blended to the natural gas grid. Even though blending and combined heat and power (CHP) projects have not yet been scheduled after 2023, those projects can still arise. Synthetic

natural gas from PtM can be utilized in all of the applications shown in Figure 6. [10]

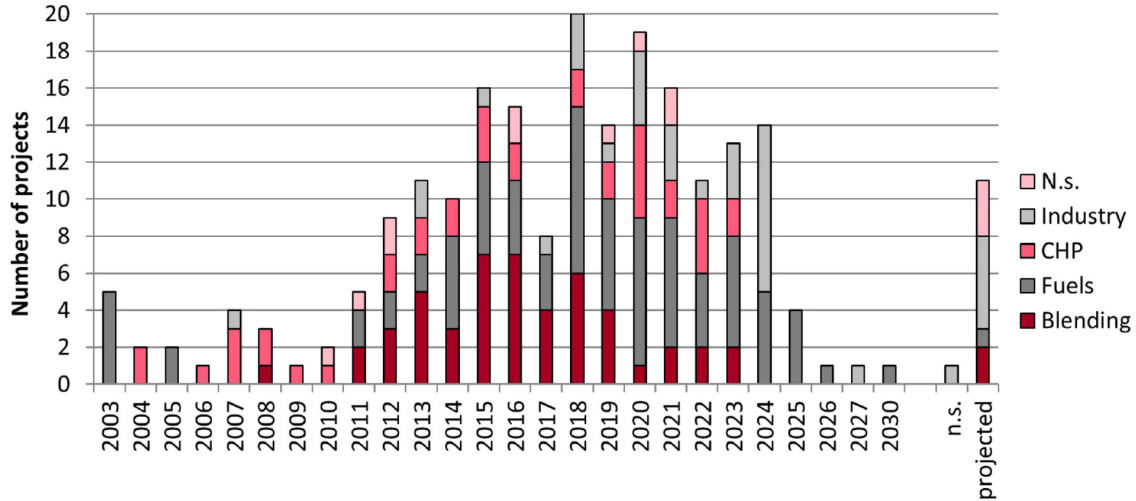


Figure 6: Field of application of the commissioned PtX projects. n.s. not specified. [10]

The produced gas has to be transferred to these different customers. Natural gas can be transferred in compressed or liquefied form [36]. Compressed natural gas is usually transferred to the different consumers by natural gas grid. The Finnish natural gas grid covers the areas in the South and Southeast Finland. [37] If the consumer is outside the range of the grid, natural gas can be transported there by compressed gas transportation containers or in liquefied form by ships, railways or trucks [36]. As SNG has the same properties as natural gas, these transportation methods apply also for it. In this thesis, the focus is on natural gas grid transmission and the requirements to inject SNG to the grid.

Gasgrid Finland is the TSO of the natural gas grid in Finland. They have set quality requirements for the injected natural gas and biomethane. These requirements are applied because it must be ensured that the customers receive fuel that is applicable for their use. Biomethane must contain at least 95 mol-% of methane and at maximum 3 mol-% of carbon dioxide. [38] If the injected biomethane is produced with some other technology than digestion of biomass, the quality limits and eligibility of the gas are agreed individually for each case [39]. Here, it is assumed that the requirements for digested biomethane apply also for SNG from catalytic methanation. Therefore, the PtM process must be operated in a manner that the quality of the product is at high enough level most of the time. This must be the case also in dynamic operation.

Gasgrid Finland sells transmission capacity to traders and shippers, who are responsible of selling the gas energy itself. Transmission capacity is expressed in kWh/h. Gas can be sold via gas exchange or over the counter with another participant. Shippers and traders are responsible of maintaining their own commercial balance in the grid, meaning that the injections and withdrawals are equal. However, Gasgrid Finland is responsible of the physical balance of the grid. [40] Shippers are required

to report their nominations of the gas quantities they plan to transmit each hour of the day. The nominations have to be submitted by certain deadline, after which renominations are still possible to change the injection quantity for the rest of the day. The renomination rounds begin every hour. In the baltconnector line, renomination is limited to some percentage of the nominal nomination. The nominations can not exceed the bought capacity. The TSO can reject the nominations if there is lack of information in the nomination or if it was submitted late. The nominations can also be reduced if there is a shortage of transmission capacity due to maintenance or disruption or if the quality of the gas does not meet the expectations. There will be a fee if the shipper fails to carry out the approved nominations or renominations. [39] To avoid the fees and buying excess transmission capacity, the SNG production should be predicted well in the dynamic operation. The requirements for dynamic operation in sector coupling as well as in demand response are summarised in Table 2.

Table 2: Summary of market requirements in Demand Response and in Sector Coupling.

Demand Response	Sector Coupling (Natural Gas Grid Injection)
- High enough ramping rate	- Product quality must meet grid quality requirements
- Enough capacity for minimum bid size	- Production must be forecasted for the following day

3 Carbon Capture

Carbon capture is an important part of those Power-to-X -processes where carbon based products are made. Captured carbon dioxide can be converted into products such as synthetic methane, methanol or gasoline when it reacts with hydrogen. In addition to being a crucial part of PtX, carbon capture has also a major impact on the environment. Power production and industries, such as cement and steel production and refineries emit large amounts of CO₂ each year. For example power production from fossil sources emits 10 000 MtCO₂/year which is about 45 % of the worldwide emissions [41, 42]. Additionally, the CO₂ emissions from fossil fueled energy production have increased over 50 % since the year 2000 [43]. Capturing the CO₂ from these point sources is one method to curb the emissions of them and enable synthetic fuel production.

Carbon capture can be divided into three categories based on the type of process used. The categories are pre-combustion, post-combustion and oxyfuel combustion. [44] Pre-combustion refers to a process where carbon is extracted from the fuel prior to the combustion with gasification and water-gas-shift reaction, whereas in the post-combustion, carbon dioxide is extracted from the flue gases. In oxyfuel combustion, the fuel is combusted with rich oxygen feed instead of air which results in higher concentration of carbon dioxide in the flue gases. Of these processes post-combustion is the one with the highest maturity. [45] Depending on the process, different technologies, such as absorption, adsorption or membrane separation, can be utilized to capture the carbon dioxide. [44] In this chapter, the focus is on post-combustion amine-based absorption process and its dynamics. More detailed information of other technologies is provided in [41, 42, 45, 46].

3.1 Absorption Process

Absorption is a process where a solute, or in this case carbon dioxide, enters a solid or liquid material called solvent. Absorption can be divided into chemical or physical absorption. The process is called chemical absorption if the solvent forms chemical bonds with CO₂ and physical if there are no chemical reactions occurring and the solvent physically solutes the CO₂. Amine-based solvents are classified under chemical absorption. [46]

Alkanolamines are safe and inexpensive chemicals that are already widely used as solvents for CO₂ capture. They can be categorized to primary, secondary and tertiary amines. Examples of these are monoethanolamine (MEA), diethanolamine (DEA) and N-methyldiethanolamine (MDEA), respectively. MEA is the most well-known amine-based solvent. [47] Important properties that describe the performance of the solvents are for example absorption capacity, cyclic capacity, absorption rate and heat release. Absorption capacity, or CO₂ loading, is defined as the mole-based ratio of the absorbed CO₂ to the solvent. The CO₂ loading is the highest for tertiary amines, being 1 mole of CO₂ per one mole of amine for MDEA. Whereas for MEA and DEA it varies between 0.5 - 1 which is still adequate for carbon capture applications. [48] Cyclic capacity describes the difference in CO₂ loading between rich and lean

solvent. The cyclic capacity is the highest for MDEA, being 43.9 g CO₂ per liter of solvent when the difference is measured between solvents at 40 °C and 120 °C. This means that MDEA absorbs and releases more CO₂ in one cycle than MEA and DEA. Absorption rate describes the rate of CO₂ transfer from gas phase to liquid phase, and it is separate from reaction rate. It is calculated at a point where the loading capacity is 50 % of the maximum, and it is the highest for MEA. [49] In addition to absorption rate, reactivity and reaction rates are also the highest for MEA [48]. Reaction heat is defined as the heat released when one mole of CO₂ is absorbed, and it increases with increasing absorption rate. Therefore, also reaction heat is the highest for primary amines. Lower reaction heats are preferred to achieve higher CO₂ loading and to minimize the energy consumption of the regeneration. [49] These above mentioned properties of the amines are summarized in the Table 3. In this chapter, the dynamic properties of 30 wt% MEA solvent absorption are reviewed more closely because it is the most common solvent used.

Table 3: Properties of alkanolamines.

Solvent	Loading capacity	Cyclic capacity (g CO ₂ /l)	Absorption rate (g CO ₂ /l/min)	Reaction heat (kJ/mol CO ₂)
MEA	0.5	37.2	5.37	86.9
DEA	0.7 - 1	41.9	3.04	68.9
MDEA	1	43.9	1.56	58.8

A major issue with alkanolamine-based chemical absorption is the degradation of alkanolamines. The degradation can be divided into thermal and oxidative degradation. [48, 47] A 2.2 kg replacement of MEA per 1 tonne of captured CO₂ is required due to the degradation. This causes economic, operational and environmental issues. [48] Additionally, corrosion is a large issue with alkanolamines. Degradation of MEA and corrosion are closely tied to each other because the degradation products of MEA increase the corrosion rate. Corrosion causes the lifetime of the surrounding equipment to decrease which again increases cost. [50]

Post-combustion CO₂ capture with amine-based absorption consists of an absorber, a heat exchanger, a stripper and a reboiler. A diagram of the process is presented in Figure 7. Flue gas with CO₂ enters the absorber column from the bottom whereas the lean solvent is fed from the top. The gas stream flows from the bottom to the top against the counter-current lean solvent stream. CO₂ is then absorbed into the solvent and CO₂ rich solvent exits the absorber from the bottom. Rest of the flue gases are released from the top of the absorber. Rich solvent goes then through a heat exchanger where it is heated by hot lean solvent. After the heat exchanger, rich solvent is fed to the top of the stripper where it flows against a counter-current flow of hot steam which heats it further and causes the CO₂ to desorb from it. The hot steam is heated in the reboiler and fed to the stripper from the bottom. After the stripper, the mixture of CO₂ and steam goes through a condenser where steam condenses and is fed back to the reboiler. The produced CO₂ is compressed and moves on to storage or synthesis process. The lean solvent exits from the bottom

of the stripper and continues its loop by entering the heat exchanger. [44] Makeup streams can be deployed because of the possible losses of water and lean solvent in the condenser and absorber, respectively [51].

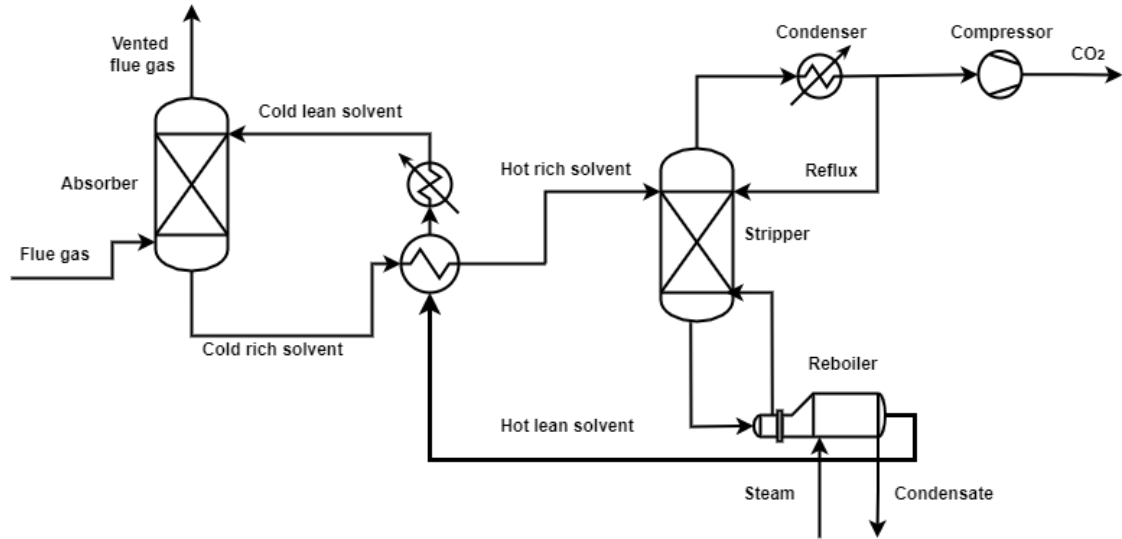


Figure 7: Process diagram of post-combustion CO₂ capture

3.2 Point Sources

As stated previously, possible point sources for CO₂ capture are power plants and industrial emitters such as steel and iron production, refineries and cement industry. However, the operation of these industrial processes is stable because the demand for products such as steel, iron and gasoline does not vary as much as electricity demand. This thesis is focused on the dynamic operation of PtX process. Therefore only power production as a point source is taken into account in this chapter.

Fossil fuel based power plants have usually been a steady base load to produce electricity, however, as the renewable and intermittent energy sources are increasing, also the base load plants have to increase their flexibility to avoid excess curtailment of green energy. [52] According to the IEA, power plants equipped with carbon capture are expected to provide flexibility to the energy system in addition to renewables. Additionally, various control and monitoring technologies have already been developed to improve the ability of power plants to operate in a flexible manner. [53] In the Figure 8, the flexibility provided to the energy system by source for different regions is presented. The power generation mix in Germany in January 2019 is illustrated in Figure 9. From the Figure 8, it can be seen that gas and coal based power plants correspond to a large share of the whole system's flexibility in all of the regions. This is concretised in Figure 9 where the fluctuating electricity production from power plants in Germany is presented. Coal and gas based power plants adapt to the intermittent renewable sources by changing their load depending on how much renewable energy is available. This implies that the flue gas flow rates from the power plants can vary and affect directly to the input of the CO₂ capture plant.

[54] However, it is important to mention that the flexibility of fossil fueled power plants depends highly on the region. In countries where the flexibility relies more on hydropower, the importance of power plants in terms of flexibility is decreased. [52] For instance in Finland, the fossil fueled power production is quite stable without a few exceptions in the data [55]. Finnish electricity production by source on 1.6.2022 is illustrated in Figure 10, from which the stability of power plants and increased amount of hydro power is seen.

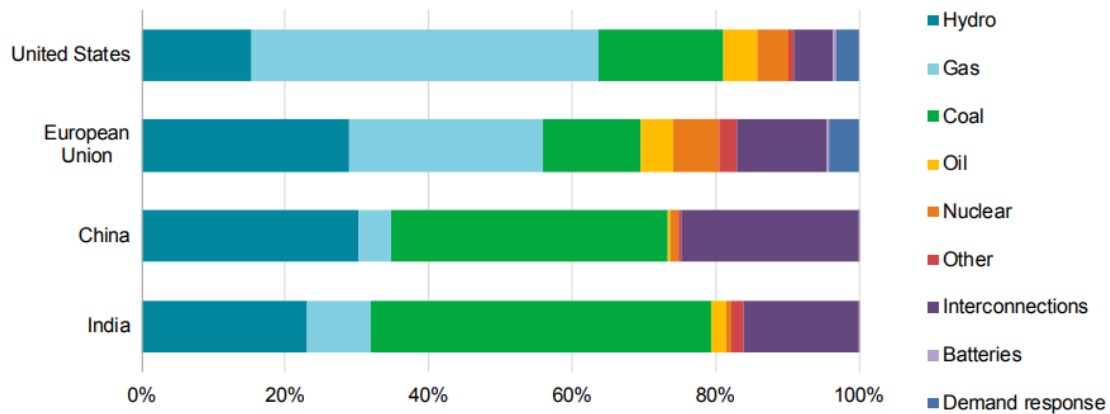


Figure 8: Flexibility provided to the energy system by source in 2018 [53].

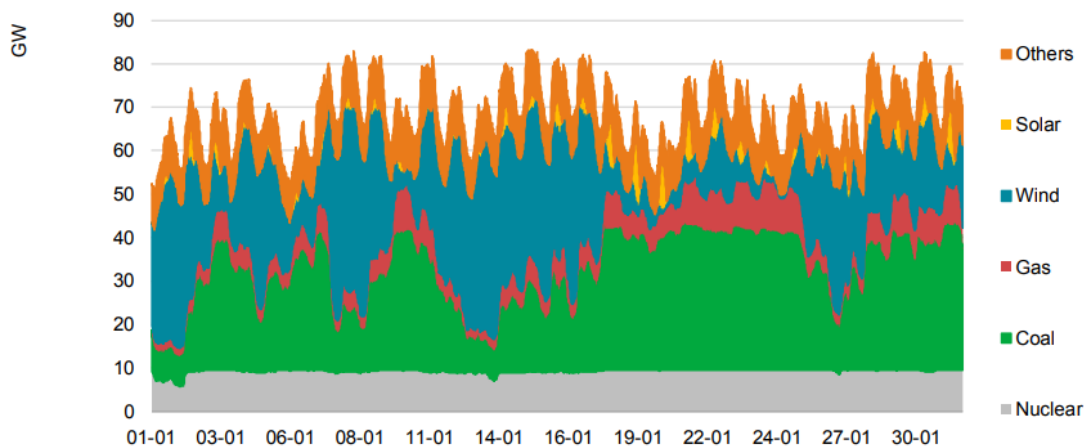


Figure 9: Power generation mix in Germany in January of 2019 [53].

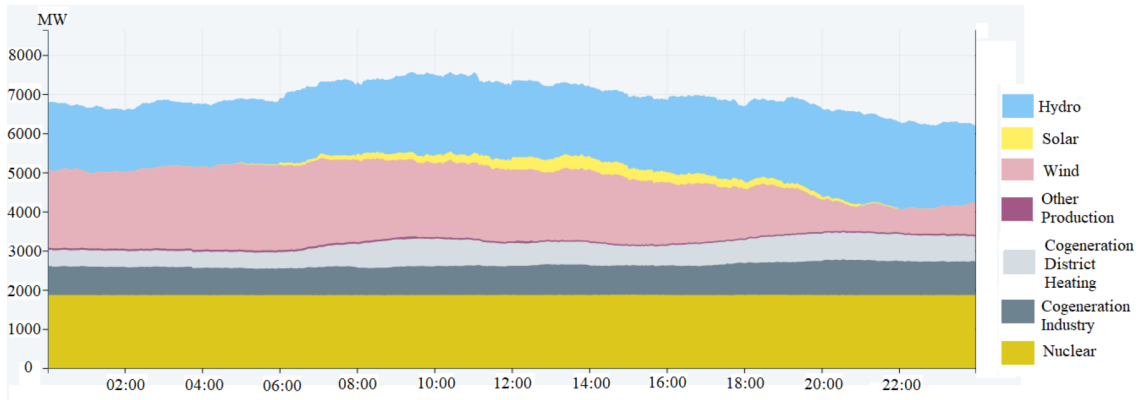


Figure 10: Power generation mix in Finland on 1.6.2022. Modified from [55].

3.3 Dynamic Properties

It is important that the CO₂ capture unit can respond to the possible fluctuations in the flue gas flow. In addition, the possibilities for the capture plant to respond to high electricity prices or demand by lowering the load could be studied. Even though this might not be reasonable due to losing the carbon neutrality of the process when doing so. In this section, different possibilities for flexible operation of CO₂ capture are discussed.

Two different concepts for the flexible operation have been studied by Cohen et al. [56]. In these concepts, it is assumed that the source of CO₂ is a power plant and that the reboiler of the integrated CO₂ capture unit consumes 30 - 50 % of the steam generated. This decreases the net electricity output by 20 - 30 %. Therefore, it would be necessary to decrease the load of the capture unit at the times of peak electricity demand. In the first option, the rich solvent flow to the stripper is reduced by circulating it back to the absorber. In this way, almost all CO₂ is vented and the steam demand in the stripper reduces. The plant is not completely shut-down but the steam required for amine scrubbing can be used to generate more electricity in peak load periods. [56] However, the effects of mixing regenerated and unregenerated solvents have not been studied [54]. The second concept requires more additional infrastructure but it enables CO₂ capture even in the periods when stripping load is reduced. The lean solvent is directed to the absorber from a storage tank and the rich solvent is also stored after the absorber instead of feeding it to the stripper. This way the CO₂ is captured but the stripper is not running and the steam can be directed elsewhere. Additional storage tanks for the solvents are required in this concept. [56]

In both of these concepts the gas and liquid throughput of the absorber stays in normal conditions but for the stripper it varies considerably and causes problems. Fractional capacity is a parameter that describes the ratio of the operation gas velocity and the flooding velocity or the maximum gas velocity. It is used to indicate the hydraulic conditions in a packed column. Usually columns are designed so that the fractional capacity is around 70-80 %. However, in the flexible operation of CO₂ capture plant, the fractional capacity of the stripper can decrease significantly. For

example, 50 % bypass of the flue gases causes the fractional capacity to decrease to less than 40 %. Another important parameter is the liquid-gas ratio in the columns. Major changes in the operational and design values of the columns can cause poor wetting of the packing and therefore low efficiency and unstable operation. [54] Therefore, the minimum load of the CO₂ capture plant is limited by the dewetting of the columns whereas the maximum load is limited by the flooding of the columns. Herrmann et al. [57] identified a capacity range of 78-125 % in their Aspen Plus model. Within this range, there were no signs of dependency between load and efficiency. [57] In addition to the columns, the compressors will also suffer from the flexible operation of the capture plant. Compressor will surge if the gas flow rate is considerably lower than the design value. This can be prevented with anti-surge system that increases the energy demand which is in contrary to what was targeted with the flexible operation of the plant. [54]

A solution for the unstable hydraulic conditions of the stripper has been found by Lin et al. [54]. Instead of bypassing the stripper, the solvent CO₂ loading, could be changed. In practice, this is done by changing the reboiler heat duty in the stripper. When less heat is fed to the stripper, all of the absorbed CO₂ is not desorbing and the loading of the solvent decreases in the next loop. This way, the amount of CO₂ captured can be decreased or increased without affecting the liquid throughput and the wetting. However, the gas flows in the stripper and in the compressor change because of the varying amount of CO₂ produced. The flow in the stripper can be stabilized by implementing a CO₂ recycle stream back to the bottom of the stripper column. [54] Lin et al. [54] used a 1 % capture rate/min ramp rate for their model whereas about 0.7 % capture rate/min rate was achieved in a model by Bui et al. [58] by turning off the hot water flow to the reboiler and turning it on again. The model results from Bui et al. [58] corresponded well to data from a pilot plant. A process flow diagram of the CO₂ capture unit with control of lean solvent loading is presented in Figure 11.

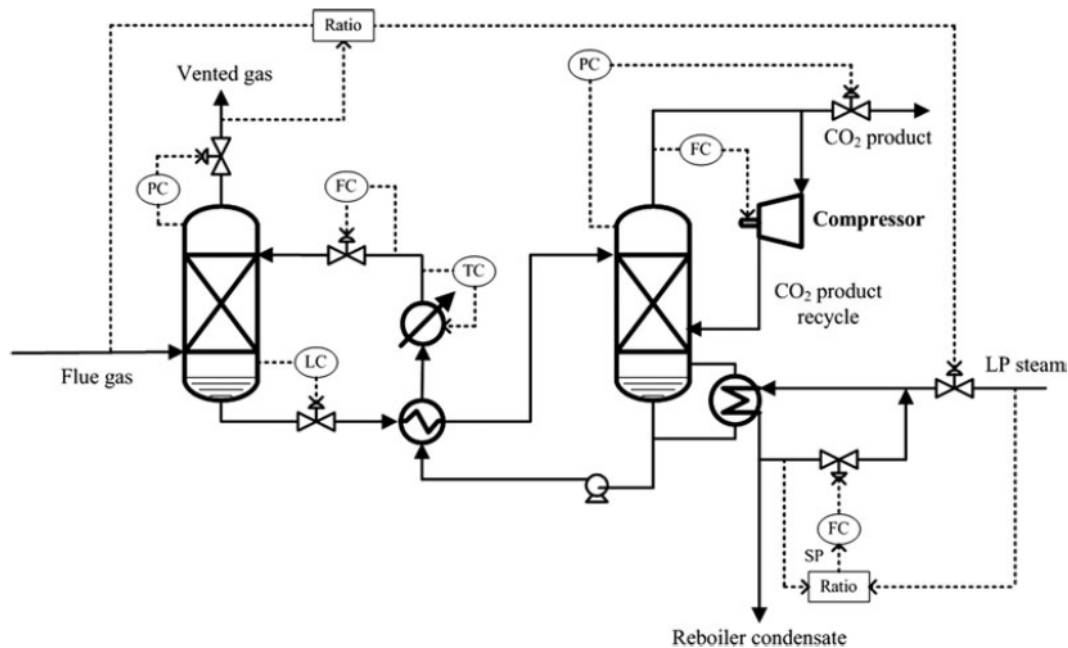


Figure 11: Process flow diagram of CO₂ capture with lean solvent loading control [54]

Nittaya et al. [51] studied different control mechanisms for flexible operation of post-combustion amine absorption and noticed that changing the reboiler heat duty is a slow control mechanism. This is because after the change in the heat duty, there is still recycled lean solvent with different concentrations of CO₂ flowing into the absorber. The amount of CO₂ in the lean solvent will not be completely changed until the whole loop has passed. A faster response time would be achieved with changing the lean solvent flow. When the flow of flue gases increases, the flow of lean solvent can be increased to achieve higher carbon capture rate and vice versa. This method also requires some additional storage for the lean solvent to be able to change the flow. In this method, the reboiler temperature should also be controlled to adapt to the decreasing or increasing amount of solvent that should be regenerated. [51] Changing of the solvent flow rate also changes the liquid throughput of the columns and the fractional capacity [54]. Therefore, this control strategy could be used only when the part-load, and thus the solvent flow, doesn't decrease significantly [59]. Bui et al. [58] ramped the flue gas mass flow approximately 2.4 %/min and controlled the CO₂ capture with lean solvent flow without causing problems to the operation. The process flow diagram of control system for varying the lean solvent flow is presented in Figure 12.

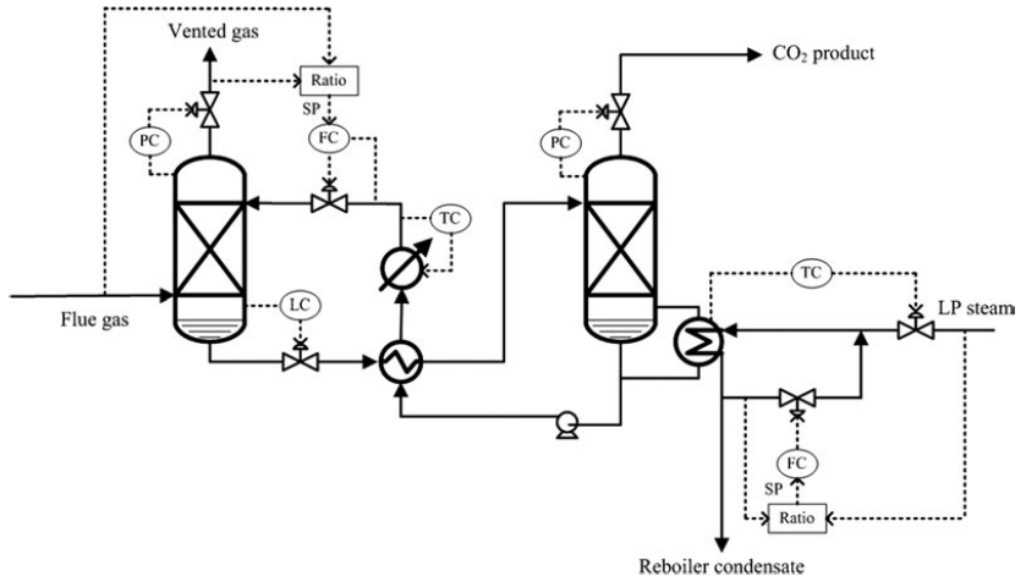


Figure 12: Process flow diagram of CO₂ capture with lean solvent flow control [54]

A combined control strategy of lean solvent flow and lean loading has been proposed to achieve lower part-loads by controlling the solvent loading after the minimum solvent flow has been reached. However, this strategy caused major instability and oscillations to the process because of the dynamic switching and the time delay between the control schemes. [59] Therefore Mechleri et al. [59] proposed that only one control strategy would be used and that the best alternative would be the lean solvent flow -strategy. In Figure 13, the difference in the response times of these control mechanisms are shown for different flue gas flow rates (50 - 95 % of the nominal value). It can be seen that at time 50 min, when +1 % change to different variables is done, the CO₂ capture rate changes. When solvent flow rate is changed, the response is immediate whereas when reboiler duty is increased, the CO₂ capture increases slowly. When flue gas flow is increased and other variables are not changed, the CO₂ capture decreases because of the increased lean solvent loading.

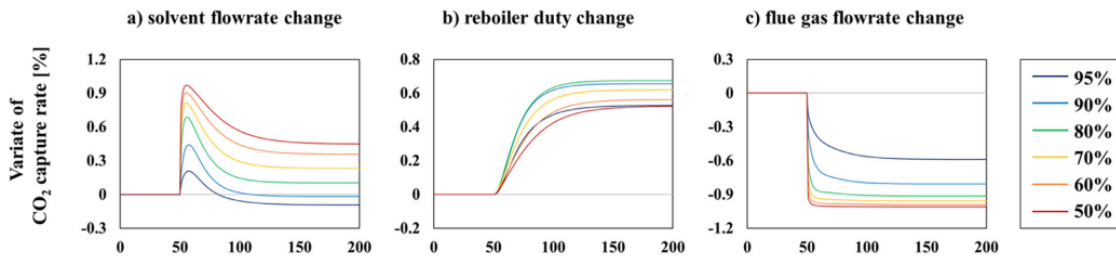


Figure 13: Response times of CO₂ capture when a) solvent flow, b) reboiler duty and c) flue gas flow are changed. The lines represent different flue gas flow rates before they are changed. [60]

In a case where it is necessary to shut down the CO₂ capture plant instead of

running it on part-load, it is important to study the start-up dynamics. The start-up process is initialized by turning on the solvent pumps to wet the columns. After the wetting is complete, the heating steam can be supplied. The time-consuming part of the process is the heating of the stripper to the operating temperature. By setting the solvent flow and heat input values to their steady state values from the start, the slowest start-up time is measured. The start-up time can be optimized by varying the values during start-up. The fastest time can be achieved with a couple of simple control mechanisms. The solvent flow rate is decreased to the lowest possible value right after the wetting is sufficient to achieve faster rate for the heating of the reboiler and the stripper. After the heating is complete, the solvent flow rate is increased to its steady state value. This way, Marx-Schubach & Schmitz [61] decreased the start-up time from 1.5 hours to 49 minutes in their optimization model. In the model, it was assumed that also the power plant supplying the heat was shut down and it takes time before the heating can be started. The dynamic properties of amine-based carbon capture are summarised in Table 4.

Table 4: Dynamic properties of amine-based absorption.

Control strategy	Ramp rate	Cold start-up	Minimum load
Lean solvent loading	0.7 - 1 % capture rate / min	-	78 %
Lean solvent flow	2.4 % flue gas flow / min	49 min	78 %

4 Water Electrolysis

One of the main components of a Power-to-X process is an electrolyser. Water electrolysis is an electrochemical process where water molecules are split into hydrogen and oxygen. The reaction is endothermic and non-spontaneous and therefore requires thermal and electrical energy to occur. [62] The share of thermal energy rises with increasing temperature in the cell, making the electricity demand smaller, and vice versa [63].

By using renewable energy sources to power the electrolyser, green hydrogen can be produced from water. This is an important benefit of producing hydrogen via electrolysis as the conventional methods use fossil feedstocks, such as natural gas or oil which are not sustainable or reasonable considering the limited reserves of them. Other advantage of water electrolysis is the high purity of the produced hydrogen. [64] However, only 4 % of hydrogen in 2019 was produced with electrolysers [64]. This is because of the low economical feasibility of them. The energy consumption of water electrolysis is 7 times larger than in steam reforming of natural gas, and therefore, the OPEX of water electrolysis is significantly larger. [65]. Nevertheless, the increasing interest in green hydrogen and its applications, in for example PtX, will boost the commissioning of needed policies and continuous development of electrolysers [64, 65].

Hydrogen production from electrolyser is approximately proportional to the current density of the cells according to Faraday's law. Therefore, part- and overloads are achieved by changing the current density. Current losses affect the proportionality especially at lower current densities. Hence, Faraday's law should be extended with Faraday's efficiency that describes the ratio of actual to theoretical hydrogen production rate. Close to nominal current densities, the Faraday's efficiency is 100 %. The final extended equation is presented in equation (1). In this equation \dot{n}_{H_2} is the molar flow rate of produced hydrogen, η_F describes the Faraday's efficiency and F is Faraday's constant. The number of electrolysis cells is denoted as N_c and current density (or alternatively, current) is marked as I . [63]

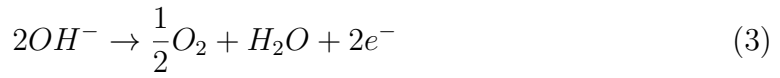
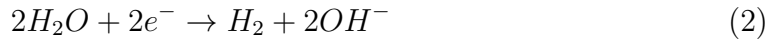
$$\dot{n}_{H_2} = \eta_F \cdot \frac{N_c I}{2F} \quad (1)$$

In addition to hydrogen production rate, current density affects also efficiency of the electrolyser: in lower current densities, the efficiency increases. This means that the part-load operation of an electrolyser cell is more efficient than full-load operation. However, the performance of the whole system may decrease as the efficiency of the utilities decrease in lower part-loads. [63]

This chapter continues with explanations of main electrolyser technologies and their dynamic properties. The focus being in the dynamic features. Important properties related to dynamic operation are minimum and maximum loads and load ramp speed as well as the start-up times. More detailed information on the other aspects of electrolysers is provided in [64, 62, 66, 67, 63].

4.1 Alkaline Electrolysis

Alkaline electrolyzers (AEL) are the most developed electrolyzers that exist. They are already widely used industrially in scales up to megawatts, and they use cheap and abundant materials. Therefore, the cost of AEL is low compared to other electrolyser types. [64, 65] Its investment cost varies in the range of 500 - 1100 €/kW_{el} [68, 69, 70, 71]. In addition, its working principle is simple. Water is broken down at cathode to hydrogen and hydroxide ion. Hydroxide acts as a charge carrier and goes through electrolyte and separating membrane to anode where it is converted to oxygen and water. [72] The reactions occurring at cathode and anode are presented in equations (2) and (3), respectively.



The operation temperature of an alkaline electrolyser is usually 40 - 90 °C and pressure is up to 30 bar [72, 66]. However, the efficiency of the electrolyser is higher in atmospheric pressures [67]. The LHV-based efficiency of an AEL electrolyser varies between 65-79 % [63]. The lifetime expectancy of the stack is in the magnitude of 55,000 - 96,000 h with a degradation rate of 0.25 - 1.5 %/a. [67, 63]. The electrolyte that is commonly used is an aqueous solution with 20-40 w-% NaOH or KOH [64], of which KOH solution is corrosive which causes increase in the maintenance frequency [67]. In addition to the corrosiveness of the electrolyte, other disadvantages of an AEL are for example its low working pressure and its low current density [73]. Commercial AELs can reach maximum current densities of 0.45 A/cm² [63].

AEL has adequate transient properties. Its minimum part-load is 15 - 20 % depending on the source. Therefore, the operating range of AEL is quite wide which supports the transient operation of the whole PtX chain. [67, 74, 75] However, at the minimum part-load, the purity of H₂ as well as the system efficiency decreases [76]. The minimum load is limited to the value of 15 - 20 % because below that the gas conductivity of the diaphragm causes H₂ to enter the O₂ stream in critical amounts resulting in flammable mixture [66]. Therefore, it is necessary to shutdown the electrolyser below this limit. Safety shutdowns are usually carried out when the hydrogen contamination in the oxygen stream exceeds 1-2 % [63].

Cold start-up time of AEL is quite long, it takes about 0.5 - 2 hours because the complete system must be purged. Therefore, continuous operation above the minimum load is better alternative than shutdowns even though it may increase the cost. [67, 75] Modular designs of the electrolyser can improve the dynamic properties of AEL. Individual modules enable lower part-loads which would minimize the issue of long cold start-up times. [66] Warm start-up times are much faster, taking about 1-5 minutes which would not cause large issues for transient operation, however, keeping the electrolyser warm for long times is not feasible [75].

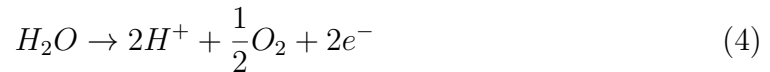
In addition to the long start-up times, on-off operation of the electrolyser causes problems in the rate of degradation, which increases from steady-state value of 3

mV/1000h to over 10 mV/1000h and may decrease the lifetime expectancy [76]. The ability to ramp load quickly is poorer for AEL than for other electrolyser technologies. The ramp-up speed is at maximum only 20 %/s which is caused by the inertia of the ionic transport through liquid electrolytes. [74, 62]

4.2 Proton-Exchange Membrane Electrolysis

Proton-Exchange Membrane (PEM) electrolyser was developed to overcome the disadvantages of AEL such as the low current densities and difficulties in the transient operation. However, its development is still mainly in stage of pre-commercial and small-scale applications even though a couple of MW scale PEMs have become available. [73, 67] PEMs operate at current densities between 1-2 A/cm² which results in four times higher hydrogen production per m² cell area than for AEL [63]. However, the cost of PEM is considerably higher than the cost of AEL, the investment needed for PEM is at least two times the investment of AEL resulting in a price of approximately 2000 €/kW_{el} [67, 66]. This is partly due to the rare and expensive raw materials which include platinum group metals such as iridium [63, 65]. The operating hours of PEM stack are in the range of 60,000 – 100,000 h with degradation rate 0.5 - 2.5 %/a. The lifetime of PEM is therefore comparable to the lifetime of AEL. The efficiency of PEM electrolyser varies in the range of 60-68 % [63].

The mechanism of the electrolyser differs from AEL so that water is split to oxygen, protons and electrons at anode. Protons then transfer through the membrane to cathode where they, together with the electrons from external circuit, are converted to hydrogen. [64] The chemical equations of anode and cathode are presented below in equations (4) and (5).



PEM's operating temperature varies between 20-100 °C and it can operate in pressures above 100 bar. This could be advantageous in a case where hydrogen is directed into pressurized storage because the produced hydrogen is already pressurized and large compressors are not needed. The electrolyte that is typically used is a solid polymer membrane called Nafion. [67]

One major advantage of PEM electrolyser is its great dynamic properties. When compared to AEL, PEM has wider load range and faster ramp-up and start-up times. The partial load of PEM can be reduced even to 0 - 5 % and overload is also possible [67, 75]. Minimum load of 0 % is possible because of the low gas permeability of the membrane. However, when operated at high pressures, the gas contamination in low current densities could be an issue for PEM as well. The overload operation is dependent on the nominal current density, and its long term effects on the degradation rate have not been investigated yet. [63]

Recent studies show that intermittent operation of PEM may even increase its durability and lifetime. Decreased current densities reduce the voltage degradation rate. Therefore, part-load operation of PEM can increase its lifetime. However, the change in degradation rate is dependent on the length of the ramping interval. Short 10-minute intervals resulted in higher degradation rate than longer 6-hour intervals. Nevertheless, more research is still needed to understand the effect of transient operation on the whole systems lifetime. [63]

Because of the wide load range, shutdowns are less frequent. Nevertheless, the start-up time is in the range of seconds to minutes, depending on whether it is a cold or a warm start-up. This is already very fast and therefore, shutdowns do not cause significant problems as with AEL. Cold start-up takes 5-10 minutes and warm start-up less than 10 seconds. [75] In addition, the ramp rate speed can vary in the range of 10-100 %/s [66]. The high ramp rate is caused by the ability of the proton transport to respond quickly to power fluctuations [62]. Because of these properties, PEM can be coupled with transient or intermittent systems without any major issues.

4.3 Solid Oxide Electrolysis

Solid Oxide Electrolysis (SOE), also called high temperature electrolysis, is the least mature technology of the three main electrolysis technologies. The advantage of the high temperature is that the amount of electricity needed decreases when part of the energy input can be provided with the high temperature heat. Because of this the electrical efficiency can exceed 100 % which makes this electrolyser technology very attractive. [66] There is only limited information about the costs of SOE because of the low maturity of them but it was predicted that their cost would be around 1000 €/kW_{el} in 2030 [67]. Their stack lifetime is estimated to be 1-2 years at the moment which is considerably shorter than that of AEL or PEM. The degradation rate was assumed to be 3 - 50 %/a. [75] Current density of SOE can reach 1 A/cm² and it is limited by degradation issues [63].

SOE operates with the reverse processes of solid oxide fuel cell. Water molecules are decomposed on the cathode where hydrogen and oxygen anions are produced. Oxygen anion acts as the charge carrier and travels to anode where it is oxidized and oxygen is produced. [66] The reactions occurring at cathode and anode are presented below in equations (6) and (7), respectively.



The operating temperature of SOE is considerably higher than that of other electrolyser types, it varies between 500-1000 °C and steam is used instead of liquid water. [64, 66] Operating pressure of SOE is usually ambient but also pressurised operation up to 15 bars has been studied [63]. However, ambient pressure is preferred because high pressure decreases the electrochemical performance of the electrolyser,

especially at high current densities [77]. The solid oxide electrolyte that is used is yttria stabilized zirconia (YSZ) because of its good ionic conductivity at high temperatures [62].

There are still large gaps in the knowledge of dynamic performance of SOE, however some estimations have been done for its start-up times and minimum part-load. Its cold start-up time takes hours and its warm start-up lasts 15 minutes. [75] As the operating temperature of SOE is very high, warm start-ups are preferred to avoid heating up the electrolyser to those temperatures [63]. The start-up times are significantly slower than for PEM and is in the same range with AEL but taking slightly more time to start. [75, 63] The start-up time is limited due to high temperature and the difference in thermal expansion coefficients of the components. [65] The load range of SOE is wide because its minimum part-load can reduce even to 0 %. According to preliminary studies, transient operation of SOE does not affect the level of degradation as with AEL and therefore, the lifetime of the electrolyser remains unchanged. [75, 63] More investigation of the whole SOE system is needed to have deeper insight on the dynamic operation of the complex thermal management [63]. The dynamic properties of each electrolyser technology are summarised in Table 5.

Table 5: Dynamic properties of different electrolyser technologies.

Electrolyser Technology	Ramp rate	Warm / Cold start-up	Minimum load
AEL	20 %/s	1 - 5 min / 0.5 - 2 h	15 - 20 %
PEM	10 - 100 %/s	<10 s / 5 - 10 min	0 - 5 %
SOE	-	15 min / hours	0 %

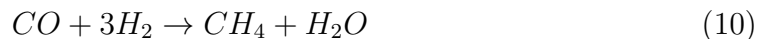
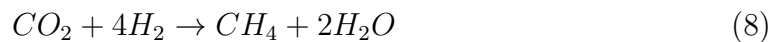
5 Synthesis

Synthesis is the component of PtX process where the produced hydrogen and captured carbon dioxide are converted into various products. PtX products are essential for tackling climate change because the objective is that these renewable products would replace their fossil fuel- based alternatives without a need for major changes in the infrastructure. These fossil fuel- based products are widely used in different industrial sectors and therefore the effects of the replacement would be significant. Examples of these industrial sectors are transportation, chemical and fertilizer industries. [78]

The transient operation of an electrolyser and a CO₂ capture unit affect also the operation of the synthesis reactor. [67] Therefore, also the dynamic performance of the synthesis reactor is important to review. In this chapter, methane synthesis and its dynamics are described in more detail and the dynamics of other synthesis processes, such as methanol and Fischer-Tropsch (FT) are shortly presented.

5.1 Methane

Methanation can be divided into catalytic or thermochemical and biological methanation. In both processes, carbon dioxide and hydrogen react to form methane and water. This is an exothermic reaction and the main reaction equation is presented in equation (8). In catalytic methanation, the process is called Sabatier process and in biological one it is called hydrogenotrophic methanogenesis. Hydrogenotrophic methanogenesis is a multistep process with many interfaces. [79] A competing reaction for methane production in catalytic methanation is the reverse water-gas shift reaction, where CO₂ and hydrogen react to CO and water. The Sabatier reaction could also be seen as the combination of water-gas shift reaction and CO hydrogenation. [67] These reactions are presented in equations (9) and (10), respectively. In addition, other reactions such as formation of higher hydrocarbons and alcohols or coke formation can take place depending on the catalysts and conditions. [80]



The main difference between the methanation processes is the catalysts. Catalytic methanation uses metal catalysts whereas biological methanation utilizes biological catalysts such as methanogenic micro-organisms. The process of catalytic methanation has been known since 1902, and is widely used in the industry today, whereas biological methanation is still in the pilot scale. [79, 67]

5.1.1 Catalytic Methanation

Catalytic methanation is operated at temperatures of 200 to 700 °C and pressures of 1 to 100 bar depending on the chosen reactor type. Many different catalysts have been

researched and could be used to increase the rate of the reaction. These catalysts include metals such as Ni, Ru, Rh and Co. Of these, nickel is seen as the optimum choice because of its good selectivity to methane, its low price and relatively high activity. Multiple reactor types have been used for the catalytic methanation, for example, fixed-bed, fluidized-bed, structured and three-phase reactors. [67, 81] Of which, fixed-bed reactors are the most mature at least for steady state operation. The dynamic operation of the adiabatic and cooled fixed-bed reactors have gained a lot of interest, being the most mature technologies [57]. Therefore, they are the main focus also in this thesis.

Adiabatic fixed-bed reactors have higher maturity level and lower cost than cooled fixed-bed reactors [81]. However, cooled fixed-bed reactors are simpler and have a better controllability of heat release and CO₂ conversion [82, 67]. In addition, the cold start-up of the cooled fixed-bed reactor is faster than that of the adiabatic one. This is because the operating temperature of the cooled reactor is lower and therefore the heating of the reactor does not take as long. [83] High temperatures of adiabatic reactors are, however, also advantageous because they increase reaction rates. Nevertheless, sufficient reaction rates are achieved also in cooled reactors but with more moderate product gas temperatures and lower thermal stress of the catalyst. Both adiabatic and cooled fixed-bed reactors consist usually of multiple reactors in series, for adiabatic reactors, the number of reactor stages is usually higher. [81] The process diagram of adiabatic reactors in series with product gas recycling is shown in Figure 14.

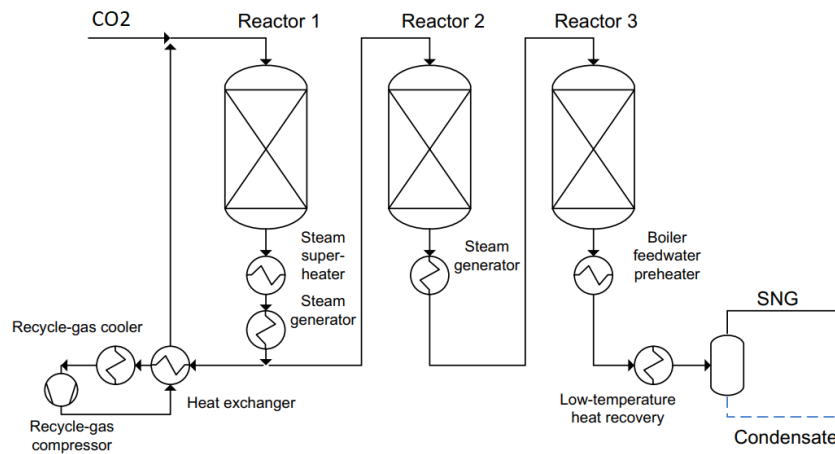


Figure 14: Adiabatic reactors in series with product recycling. Modified from [81].

It has been proven that methanation reaction can be operated dynamically because the chemistry and mass transfers react rapidly to the load changes. The flexibility of the reactors is therefore determined only by the process control systems and not the chemistry of the reaction. As mentioned, the Sabatier reaction is highly exothermic, about 2 MW of heat per m³ catalyst bed has to be removed from the reactor. Therefore, temperature control is in major role in the operation of the reactor to prevent catalyst sintering, cracking or carbon deposition. Catalyst deactivation is

an unwanted but inevitable event that has a great impact on the rate of the reaction. Therefore, it is desirable to delay the deactivation as long as possible. In dynamic operation, the importance of the temperature control is emphasized because the load changes usually result in large temperature changes. As there are no catalysts that could withstand high temperatures for long times, the reactor should have a fast response to the increasing temperature. [67] Maximum temperature that nickel catalyst can withstand is estimated to be 550 - 650 °C [84].

Typical disturbances caused by transient operation of methanation in fixed-bed reactors are travelling hot spot formation and wrong-way behaviour. These are responses to changes in the input parameters such as inlet flow, temperature or pressure. [85] They are caused by the high thermal resistance of the bed that causes the thermal wave to propagate significantly slower than the mass wave inside the reactor. Another enabling factor of these disturbances is the fact that reaction rate is a function of temperature in fixed-bed reactors. [85, 81] Travelling hot spot means a high local temperature that travels downstream of the reactor by convection. It is caused by an increase in the feed flow rate or change in the inlet concentrations. [85] Wrong-way behaviour occurs after abrupt changes in the inlet temperature or inlet flow rate. An example of wrong-way behaviour is that when decreasing the inlet temperature of the reactor, the operating temperature increases. This happens because the reaction rate decreases due to lower inlet temperature in the bed inlet causing more reactants to propagate downstream. The propagated reactants accumulate and increase the reaction rate downstream and the exothermic reaction causes the temperature to rise. [86, 85] These responses are disadvantageous because they can cause thermal instabilities, runaways, loss of selectivity, lower yields or catalyst deactivation [87, 85]. In the context of inlet flow changes, it has been identified that reducing the flow in cooled fix-bed reactors leads to more unstable thermal activity whereas increase in the flow increases the stability [88, 83].

Unstable thermal behaviour inside the reactor during transient operation is disadvantageous also for the quality of methane. The effects of temperature and pressure to CO₂ conversion and methane yield are presented in Figure 15. At first, the CO₂ conversion starts to decrease when temperature increases due to the exothermic nature of the reaction, setting the equilibrium to the reactants side. However, at higher temperatures, the conversion starts to increase. This is because at higher temperatures, endothermic reverse water-gas shift reaction is preferred and CO₂ is converted into CO rather than methane. Methane yield therefore decreases continuously with increasing temperature. Higher pressures reduce or slow down the effect of high temperatures. This is due to methanation being a mole-reducing reaction which is favored at high pressures. [89] Lower conversion of CO₂ to methane causes the methane content in the product gas to reduce and makes the product incompatible with the natural gas grid requirements that were described in Chapter 2. Therefore, control strategies are needed to minimize the temperature increase in the reactor during load changes.

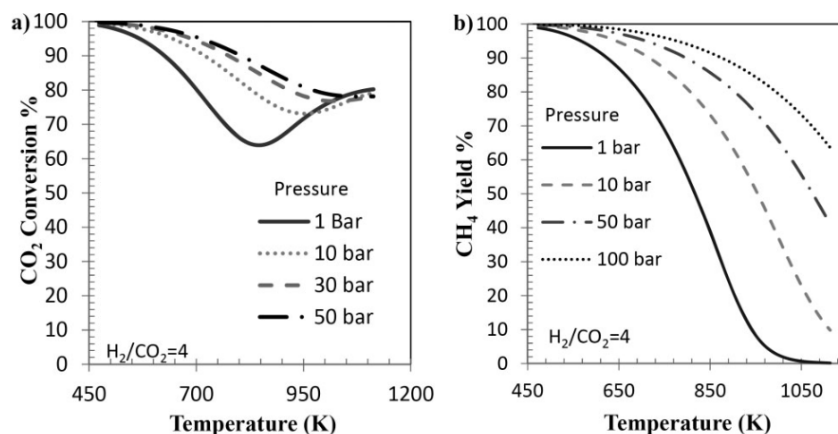


Figure 15: Effect of reactor temperature and pressure to a) CO₂ conversion and b) methane yield [89].

Different methods to minimize the effect of temperature disturbances have been developed, examples of these methods are product gas recycling, CO₂ staging, adapting of coolant temperature in cooled fixed-bed reactors and catalyst dilution [90, 91, 88]. Product gas recycling helps to keep the temperature of the reactor lower and limits the acceleration of the reaction as the reactant concentration in the inlet feed is reduced and heat is removed from the reactor. The best result of transient performance is achieved when the recycle ratio is adapted dynamically. [92] Recycle ratio is the ratio of recycle flow to the pure feed flow and typically its value varies between 0.5 to 3 [87]. Fortunately, product gas recycling has been adapted to most commercial adiabatic reactors already and sometimes used also for cooled fixed-bed reactors [81]. The optimal recycle ratio for adiabatic reactors decreases with increasing flow rate. This is because both increasing flow rate and high recycle rate reduce the residence and shift the reaction zone towards the reactor outlet. Therefore, increasing flow rate can be compensated with lower recycle rate to shift the reaction zone back and fully utilize the reactor volume. For cooled fixed-bed reactors, the higher the recycle ratio, the better temperature control in the reactor. However, with increasing recycle ratio, the conversion to methane drops. [83] Therefore, a recycle ratio of 0.05 to 0.1 was proposed by Matthischke et al. [83] to avoid thermal catalyst deactivation but also to keep the conversion as high as possible. In another study, Matthischke et al. [92] used a ramp rate of 0.83 - 1.4 %/min for an experimental laboratory scale fixed-bed reactor with product circulation.

CO₂ staging is a method where only part of the CO₂ feed is fed to the first reactor. The rest of the feed bypasses it and is fed to the following reactors in series. This method assists in the temperature control as the pure reactant feed to the reactors is limited. Giglio et al. [91] simulated the effect of CO₂ staging on partial load and hot start-up of multi-tubular cooled fixed-bed reactor with three reactor stages. First, a fraction of 39 mol-% of CO₂ flow was fed to the first reactor stage and the rest was fed to the second reactor. When the load was decreased to 80 %, a temperature change was observed in all of the reactors. Temperature increase occurred in the first two reactors, whereas temperature was decreased in the last

reactor. Temperature increases were caused by the lower convective heat transport and reduced heat transfer to the coolant medium. This can be regarded as wrong-way behaviour. The highest increase was in the first reactor where the reactants were not yet converted to methane and thus a higher reaction rate was achieved. The temperature profile of the first reactor during load reduction is presented in Figure 16. In the last reactor, the CO_2 conversion was already at a high enough level that the reaction rate decreased which in turn decreased the temperature. The maximum temperature of the first reactor was $520\text{ }^\circ\text{C}$, which is close to the maximum acceptability limit that was set to $550\text{ }^\circ\text{C}$. However, the temperature limit was not exceeded and therefore the load reduction was successful. Lower partial loads were reached by changing the CO_2 fraction to each reactor. The lower the load, the lower the fraction to the first reactor. Under part load of 65 %, the feed was divided into three fractions and some of the CO_2 was fed straight to the third reactor. With this procedure, a minimum load of 45 % and ramp rate of 46 %/min were achieved without exceeding the maximum temperature limit. [91]

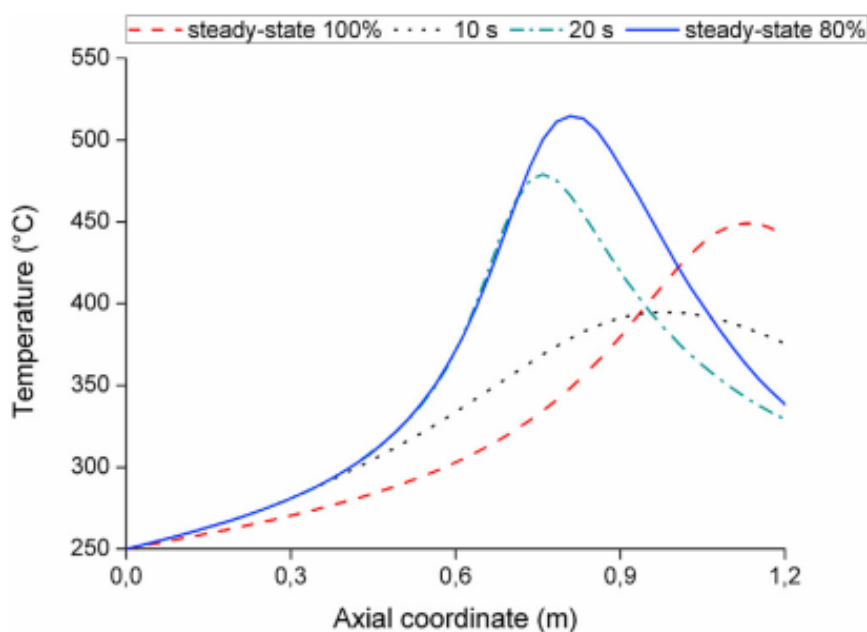


Figure 16: Temperature profile of the first reactor during load reduction to 80 % [91].

Coolant temperature can be adapted to the changing inlet flow rate in cooled fixed-bed reactors to reach higher temperature control. When the inlet flow is decreased, it initiates wrong-way behaviour and causes temperature to increase. In order to avoid temperatures that cause catalyst deactivation and large conversion losses, the coolant temperature could be decreased. [88] Fischer & Freund [88] studied load reduction in a wall-cooled tubular fixed-bed reactor with coolant temperature control. They noticed that a load reduction of 50 % could be achieved with this control method without activating wrong-way behaviour. Temperature profiles of the reactor and coolant during load reduction are presented in Figure 17. Additionally,

a model with multiple random load steps between 50 and 100 % was conducted successfully. However, instant step changes were assumed and ramp rates were not included in the study. In addition, it was mentioned that the efficiency of this method is highly dependent on the time delay of the temperature change in the coolant that is described with time constant and dead time. In this optimization model time delay of 10 seconds and dead time of 5 seconds were used.

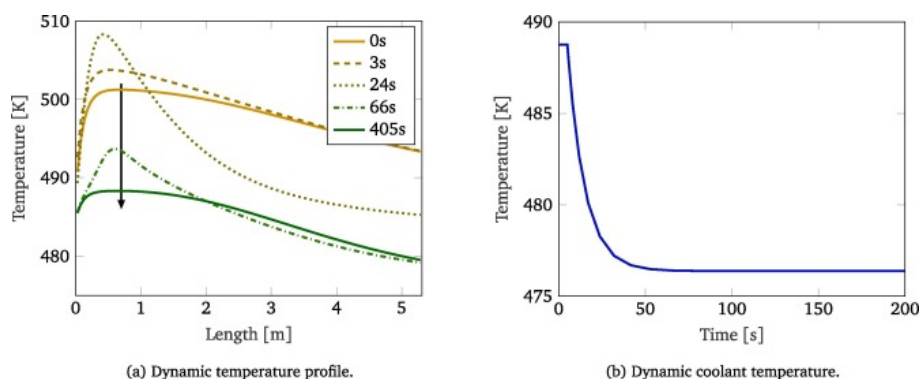


Figure 17: Temperature profiles of reactor and coolant during load reduction to 50 % [88]

Catalyst dilution is another method to control temperature variations in the reactor when inlet flow is changed. In practise, catalyst dilution is done by changing some of the catalyst pellets with inert pellets to reduce the local volumetric activity of the catalyst and thus also decrease the reaction rate and temperature release. [93] This means, however, that the reactor size should be increased to reach the targeted conversion rates [84]. Catalyst dilution should be combined with some other control mechanism, such as product gas recycling or coolant temperature -control, to ensure necessary flexibility against load changes [90, 84]. An experimental Power-to-Methane facility HELMETH used catalyst bed dilution as a temperature control method in a cooled-fixed bed reactor and reached minimum load of 20 %. They noticed that temperature rises the most in the inlet of the reactor when gas inflow is changed and therefore diluted only the first third of the catalyst bed. This way, the reactor size is not increased as much and the conversion and product gas quality are improved. They were also able to perform a hot start-up from 250 °C in approximately 3 minutes. [94]

Another catalyst dilution method has been studied by Zimmermann et al. [95], it is called core-shell catalyst dilution. In this method, catalyst pellets are covered with inert shells that limit the activity of the catalyst by changing the rate-determining step to the diffusion through the cell at high temperatures. At low temperatures, the thin cell does not affect the reaction rate as much. A significantly smaller reactor size is required in this method than in the fixed-bed dilution method. In addition, much better temperature control is achieved with core-shell catalyst dilution. When CO₂ flow rate was varied between 30 - 100 %, the fixed-bed dilution method resulted in quite large temperature variations and hot spot behaviour. In the core-shell dilution method, a new steady state temperature was reached quickly without travelling hot

spot behaviour. The temperature control was improved even further by implementing two segments with different shell thicknesses. This way, temperature did not change during the whole operation period. However, higher conversion was reached with uniform shell thickness.

An important factor in the transient operation of methanation is the start-up time. It needs to be considered if the reactor can be shut-down and restarted if there is no hydrogen flowing into the reactor. Before the shutdown of the reactor, it should be flushed with hydrogen or an inert gas to ensure catalyst preservation. In addition, the temperature of the reactor should be kept above 200 °C to avoid formation of nickel carbonyls from nickel catalyst. [67, 96] Also, thermal ramp should be considered because if the reactor is heated up too quickly, it causes thermal stress within the reactor. A maximum of 50 °C/h heat ramp was proposed by Frank et al. [97].

Fache et al. [96] studied the start-up of multi-tubular cooled fixed-bed reactor with catalyst dilution and noticed a linearity between the start-up time and idle period. After short idle periods, the reactor can be ignited spontaneously without an external heat source because of the high thermal inertia of the bed and the exothermic nature of the reaction. If the idle period is long enough, the temperature of the reactor has already decreased to an extent where the heat of the reaction is not enough and external heat source is required to heat up the reactor. A ramp rate of 3.3 %/s was used to increase the flow rate from zero to nominal. The start-up was concluded to be complete when methane flow rate reached 90 % of its design value. A warm start-up was still possible after 6 hours of idle time when the insulation thickness was 0.1 meters. The restart time was then measured to be 38 minutes. If the insulation thickness was reduced to 0.05 m, the maximum idle time that allows for warm start-up was 3 hours and a restart time of 25 minutes was obtained. For both thicknesses, the start-up time after 30 minutes of idle time was 5-6 minutes. After some time steps, the spontaneous restart gets slower than the restart with external heating because of the slowly decreasing temperature in the reactor. Therefore, it could be advantageous to use external heating after longer idle periods even though it would otherwise be unnecessary. Alternatively, it is possible to speed up the spontaneous restart by recycling the product gas or heating the reactor with the product that is not completely converted and therefore incompatible with the product requirements.

Bremer et al. [82] studied the coolant temperature - control strategy during start-up in cooled fixed-bed reactor. They noticed that without any optimization or control, the temperature rises above maximum acceptability limit during start-up. Therefore, they suggested that the start-up should be controlled by varying the coolant temperature. In this study, the flow rate was kept constant. Inlet gas temperature was set to 127 °C which was also then the temperature of the reactor at time zero. The best result was obtained when the coolant temperature was chosen so that it equals the steady state solution of dynamic optimization. The control trajectories are presented in Figure 18. The coolant temperature was set to maximum at the beginning to initiate the reaction. When the reaction rate started to increase, the coolant temperature was decreased to remove the excess heat from the reaction.

Methane conversion reached steady state after 13.3 minutes.

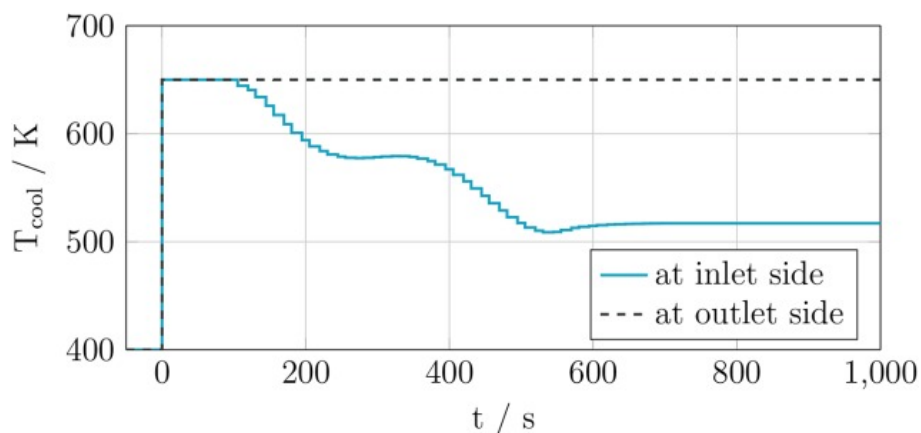
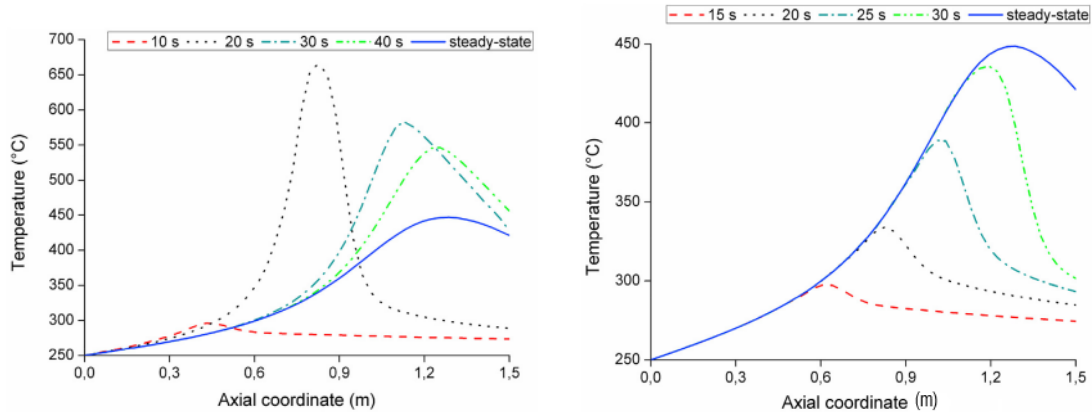


Figure 18: Control trajectories for coolant temperature during start-up [82].

A warm start-up was modelled for the same reactor design with CO₂ staging as previously described from Giglio et al. [91]. The three reactors were in a standby mode and temperature equaled the temperature of the coolant, which was 240 °C. Here, the start-up process was complete when the methane content of the product gas reached 95 mol-% on dry basis. In the first strategy, all of the reactors were started simultaneously. This way, all of the reactors reached steady state within 60 seconds. However, problem with increasing temperature in the second reactor was observed. The temperature had a peak at 650 °C which leads to damages in the catalyst. The temperature peak was a result of increasing reactant flow to the second reactor because the reaction had not reached steady state in the first one. Therefore, all of the unreacted reactants were fed to the second reactor and the inlet value was increased significantly from the design value. Reaction rate and temperature were thus increased. The second strategy results in longer start-up time, 130 seconds, but better temperature control. The reactors were started one-by-one after the previous one had reached steady state. This way the inlet concentrations match the design values. Comparison of the temperature profiles in the second reactor for both strategies are presented in Figure 19. It can be clearly seen that the first strategy results in a travelling hot spot behaviour, whereas, it is avoided in the second strategy.



(a) Temperature profile with strategy 1. (b) Temperature profile with strategy 2.

Figure 19: Comparison of reactor 2 temperature profiles with different start-up strategies [91].

All the control strategies and their dynamic features, including ramp rates, minimum loads and start-up times, are summarized in Table 6. Warm start-up was considered if the standby temperature was above 200 °C. Ramp rates were calculated from the warm start-up times if they were not stated separately in the study, which may be overly optimistic due to the difference between optimized warm start-up and random load change [75]. This is the case in studies of Giglio et al. [91] and Fache et al. [96]. Therefore, the ramp rate from the study of Mattischke et al. [92] seems the most realistic. Minimum loads and start-up times are in the same magnitude for all of the studies with slight differences that may have been caused by different control methods. In the study by Fache et al. [96], the warm start-up time had the highest value because the standby times were increased and spontaneous start-up without external heating was measured. Temperature control methods are important for minimizing the negative effect on methane quality during transient operation. However, temperature increase was measured in almost all of the control strategies which implies to changes in the methane yield.

Table 6: Summary of different control methods for catalytic methanation and their dynamic properties.

Control method	Reactor type	Ramp rate	Minimum load	Warm/Cold start-up	Source
Gas recycling	Recycle	0.83 - 1.4 %/min	-	-	[92]
Gas recycling	Adiabatic	-	-	6.5 min/-	[83]
CO ₂ staging	Cooled	46 %/min	45 %	130 s/-	[91]
Coolant temperature	Cooled	-	-	-/13.3 min	[82]
Coolant temperature	Cooled	-	50 %	-	[88]
Catalyst dilution (bed)	Cooled	-	20 %	3 min/-	[94]
Catalyst dilution (bed)	Cooled	3.3 %/s	-	5 - 38 min/-	[96]
Catalyst dilution (core-shell)	Cooled	-	30 %	-	[95]

5.1.2 Biological Methanation

In biological methanation, the micro-organisms anaerobically metabolize the carbon dioxide and hydrogen and use the released energy for their growth [67]. The methane production is catalysed by autotrophic hydrogenotrophic methanogenic Archae [98]. The operation temperature is between 20 to 70 °C and the pressure is mostly ambient. The micro-organisms are present in a fermentation broth and therefore the methanation reaction occurs in a aqueous solution. The reaction rate of the biological methanation is lower compared to the catalytic one due to the lower temperatures and lower mass transfer coefficient. In addition, the flow rate for biological methanation is low and to increase it, significantly larger reactor units are required. [67]

Biological methanation can be divided into in-situ and ex-situ processes. In in-situ process, the methanation reactor is combined with a biomass digester which produces the CO₂. In ex-situ process, the carbon dioxide is fed to the reactor from some external source, for example carbon capture unit. Ex-situ configuration provides more flexibility to the process. [67, 98] The focus in this thesis is on the ex-situ process.

Biological methanation is usually performed in continuous stirred-tank reactors (CSTRs). However, also fixed-bed, trickle-bed and membrane reactors have been investigated. The rate limiting step in all of these reactors is the gaseous hydrogen transfer to the liquid solution. Generally, trickle-bed reactors (TBRs) show better mass transfer performance than CSTRs. Methane formation rate is quite low for some of the reactors. Higher methane formation rate results generally in relatively lower methane content in the product. [67] In this chapter, CSTRs and trickle-bed reactors are reviewed because of the commonness of the CSTRs and the promising features of the trickle-bed reactor. The flow diagrams of both reactors are presented

in Figure 20.

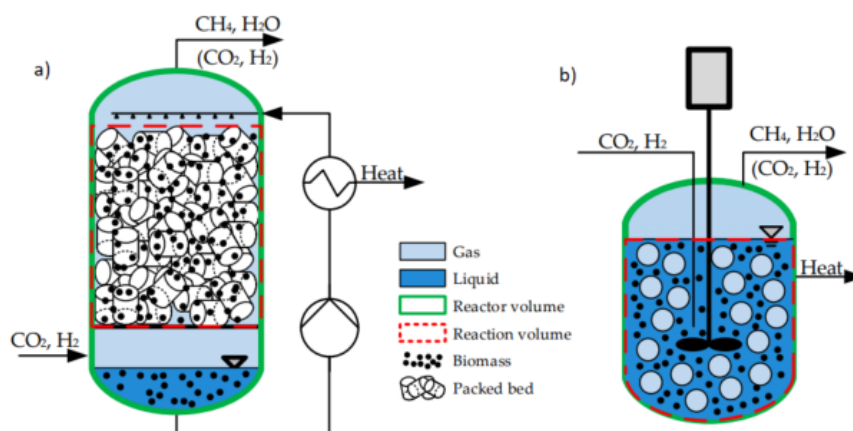


Figure 20: Flow diagrams of a) TBR and b) CSTR [79].

As mentioned above, the main challenge of biological methanation is gas-liquid mass transfer of hydrogen gas. However, it is important that mass transfer is the one factor limiting the reaction in mixed-culture reactors because if hydrogen amount in the liquid solution would increase faster than the conversion rate of it, volatile fatty acids would accumulate in reactor. This would cause acidification of the reactor broth which would result in decreased microbial activity. [99] In addition, faster CO_2 conversion caused by increased amount of hydrogen would result in increase in the pH of the solution [100]. Nevertheless, successful experiments of stable operation with enhanced mass transfer have been reported [99]. The mass transfer of hydrogen can be improved by increasing the mass transfer coefficient, specific surface area or the concentration gradient between the phases [79]. In CSTRs, the mass transfer coefficient can be increased by increasing the stirring rate which also increases the electricity consumption. Larger surface area can be achieved with optimized impeller design that reduces the bubble size. Concentration gradient can be increased with higher operating pressures. [99, 79] In the context of dynamic operation, increased flow rate of hydrogen causes the mass transfer to diminish and therefore more hydrogen passes through the reactor and the conversion efficiency is reduced [75]. Therefore, mass transfer improvements are especially required for the transient operation.

As the temperature of biological methanation is considerably lower than that of catalytic methanation, temperature control inside the reactor is not as large of an issue. It has been reported that there is no limitation of minimum load based on biology. However, it is argued that the operation is not feasible under loads when the electricity consumption exceeds the energy content of the produced methane. Therefore, an approximation of minimum load of 10 % was made for CSTRs. In addition, an immediate shutdown was reported to be possible without negative effects as well as start-up after 560 hours of standby. [67]

In a study from a project called STORE&GO, experimental results of biological methanation in a CSTR reactor showed that minimum load of 40 % was possible.

Ramp rates of 1.8 - 5.5 %/min were achieved in this study. The limiting factor in the load rate changes is the Archaea's adaptation to the new conditions. After the load change step, the biocatalyst requires an adaptation period before the next step could be performed. These load change rates are enabled by low gas hourly space velocity (GHSV) value and the liquid phase that acts as a buffer to the changes. A cold start-up time of 15 minutes was achieved in this study. [101]

Trickle-bed reactors have been investigated recently because of their ability to enhance the gas-liquid mass transfer of hydrogen without increasing electricity consumption. Their ability is based on a packing/carrier material that increases the interphase area per reactor volume for the mass transfer. [102] Comparison of different parameters of CSTRs and TBRs are presented in Table 7. It can be seen that the mass transfer coefficient and effective surface area, meaning specific surface area divided by the reactor volume, of TBR are in the same range as for CSTR but the power input is significantly lower.

Table 7: Comparison of CSTR and TBR reactors [79].

Parameter	CSTR	TBR
Mass transfer coefficient (m/s)	0.3 - 4 x 10 ⁻⁴	0.4 - 2 x 10 ⁻⁴
Effective surface area (m ⁻¹)	100 - 1500	60 - 640
Volume specific power input (Wh/m ³)	50	4.3

The flexible operation of TBRs has also been studied recently. Changes in the pH of the reactor are problematic also for flexible operation of trickle-bed reactors. Sudden increased water production can dilute the nutrients in the trickling-bed liquid and cause the pH to decrease. [100, 102, 103] However, it is possible to exchange the liquid regularly to minimize the effect of liquid dilution [104]. Additionally, increased flow rate of CO₂ can decrease the pH as well as the acetate formation due to increased hydrogen mass transfer to the liquid. Multiple studies show that below pH of 6.2 the gas conversion reduces significantly due to decreased activity of the biocatalyst. [100, 102, 103]

Sposob & Wahid [104] studied the effect of reactor current configuration on load changes in a laboratory-scale thermophilic trickle-bed reactor. The configuration is called counter-current if hydrogen and carbon dioxide are fed at the reactor bottom, and concurrent if they are fed from the top. The results show that counter-current reactors achieve higher and more stable methane content in the product gas for all loads. Concurrent configurations result in lower methane production because the reactants are fed from the top, and therefore, they remove the liquid from the reactor packing much faster than in counter-current configuration. This can result in poorer nutrient access and biofilm drying. Even in the counter-current reactors, that show more stable performance, the methane content decreases with higher flows of hydrogen and CO₂. In this study, no process optimization was used. Therefore,

methane content in higher loads could be increased with changes in the operation conditions, such as recirculation rate or hydraulic retention time. In addition, pH stabilization was not needed because cow manure was used as the liquid phase. The advantages of cow manure are that it does not require pH maintenance or mineral supplementation.

Strübing et al. [103] performed experimental studies on a pilot-scale thermophilic trickle-bed reactor and concluded that hot start up after 30-minute standby was possible without issues in the gas conversion. The desired conversion rate was achieved in 26 minutes. However, an instant start-up after 24-hour cold standby resulted in decreased methane content in the product gas. The cold start-up had to be performed in four steps during 60-minute time period to avoid these conversion issues. These steps were necessary for the Archae to adapt to the new environment as in the CSTR reactor. The ramp rate used varied between steps and was in the range of 0.6 and 1.1 %/min including the adaptation. [103] In another study by the same authors [100], it was shown that longer standbys, meaning timespan of days, are not possible in higher temperatures due to low conservation of methanogens in those temperatures. Methane content at 230 minutes after reinstating the gas feed, after 2-day standby at 55 °C, was only 72 %. It took 12.4 hours for the methane content to reach the target of 96 %. Therefore, hot start-up is preferred after short standbys to achieve faster start-up but after standbys longer than one day, hot start-up is not feasible or possible depending on the timespan of the standby.

As stated previously, the minimum load of biological methanation is mainly limited by the electricity consumption of the process [67]. Because the electricity consumption of trickle-bed reactors is about one tenth of consumption of CSTRs [79], the minimum load of trickle-bed reactors could be significantly lower than that of CSTRs which was estimated to be 10 %.

5.2 Alternative Synthesis Technologies

Power-to-x includes multiple other synthesis technologies in addition to PtM. These technologies are also important to develop and research due to the large area of applications where the products can be utilized instead of fossil fuels. In this chapter, methanol and Fischer-Tropsch synthesis and their dynamic properties are shortly reviewed. This review is done to give wider perspective of how well does dynamic capabilities of PtM compare to those of other PtX technologies.

5.2.1 Methanol

Methanol synthesis has traditionally used syngas as a raw material. However, also carbon dioxide can be used as a raw material or carbon monoxide can react to carbon dioxide via RWGS-reaction which will then react to methanol. It has been researched if the methanol synthesis occurs mainly via CO₂ or CO hydrogenation and nowadays most scientist agree that CO₂ hydrogenation is the dominant reaction. Therefore, research related to raw CO₂ hydrogenation has been accelerating recently. Both hydrogenation reactions release energy, CO hydrogenation being the most exothermic

reaction. The synthesis requires temperatures of 200 - 300 °C and pressures of 50 - 100 bars. The catalysts that are used in most cases are based on CuO and ZnO with carrier of Al₂O₃ (CZA), however, specific catalysts for CO₂ are investigated. [105]

Dynamic operation of methanol synthesis is not yet state-of-the-art and only few research studies discuss dynamic aspects of the synthesis. However, due to methanol synthesis being an exothermic process that is quite similar to methane synthesis, thermal runaways and catalyst sintering are issues for this synthesis, too, when changing the load. [106, 107] Critical temperature for CZA catalyst, above which the damages occur, is 300 °C [107]. Further research is required to obtain more detailed information about the thermal behaviour and possible control methods during load changes. Dynamic simulation of CO₂ to methanol from ViteSSe project implied a possible ramp up from 20 to 100 % in 6 - 7 minutes. An experimental project called LPMeOH could achieve 5 %/min ramp rate and it worked with alternating feed compositions and in on/off operation. However, after a restart of the operation, a slow increase in the conversion has been noticed in a few studies. It takes about 60 - 80 hours to increase the conversion from 90 % to steady state. [105] Currently, there is no theoretical or experimental data available about the load range of methanol synthesis, however, an assumption of 10 % for the minimum load was made by Chen et al. [108].

5.2.2 Fischer-Tropsch

Fischer-Tropsch is a pathway to convert syngas into various liquid hydrocarbons. The products vary by the length of the carbon chain depending on the process conditions. The development of the process started in the 1920s after the research related Sabatier reaction was published. The synthesis is usually operated at temperatures of 150 - 350 °C. Higher temperatures may lead to undesired shorter carbon chains, catalyst deactivation and carbon deposits. The synthesis is divided into low- and high-temperature synthesis based on what products are desired. Low temperature FT produces higher hydrocarbons in a temperature range of 180 - 250 °C, and high temperature FT is for short hydrocarbons and temperatures of 300 - 350 °C are used for it. The synthesis is usually operated at moderate pressures, up to 30 bar. Too high pressures cause also catalyst deactivation and by coke formation. The synthesis uses Fe- or Co- based catalysts and the H₂/CO ratio depends on the catalyst used. As with methane and methanol synthesis, CO₂ can also be used as a feedstock. [105, 109]

The dynamic operation of FT-synthesis has been investigated slightly more than that of methanol synthesis, however, not as deeply as methanation. FT-synthesis is also exothermic and therefore temperature control is also in a crucial part of the dynamic operation of FT synthesis. However, the temperature control could be easier in a liquid phase synthesis. In addition to temperature variations, it has been investigated if the dynamic operation affects to the produced products of the process. [105, 109] However, it has been concluded that hydrogen pulsing, meaning the variable hydrogen inlet flow, could be possible without major problems within certain limits and it could also be used as a process enhancement method. This idea

has been researched a lot in the literature but concrete systems and results are still missing. [109]

When comparing the information related to dynamic capabilities of FT and methanol synthesis to methation, it can be concluded that the research related to dynamics of methanation has been more of a hot topic recently. There is not much information to be found related to transient operation of FT and methanol synthesis. However, this may change in the future when the dynamic properties become more relevant due to increasing amount of RE. Based on the information obtained from the few studies related to FT and methanol synthesis, methanol synthesis seems to have equal dynamic capabilities as methanation and FT could have even better properties. However, as mentioned, this needs to be researched more to obtain experimental results of the process behaviour during transient operation.

6 Hydrogen Storage

When considering the flexible operation of PtM, intermediate storage facility for hydrogen is required to allow for the components of PtM to run independently. As mentioned in the previous chapters, the PtM components have very different dynamic features. Electrolysers have considerably faster ramp rates and lower loads than methanation or CO₂ capture. Therefore, intermediate hydrogen storage is needed to enable cost optimization of electrolyser operation while maintaining the synthesis capacity and quality. In this chapter, the main storage technologies for hydrogen are shortly reviewed.

Hydrogen can be stored in different forms: compressed, liquefied or material-based storages. Liquefied hydrogen requires an extremely low temperature, -253 °C. Achieving this temperature in a hydrogen storage application consumes considerable amount of energy. In addition, there is a risk for hydrogen boil-offs in the liquefied storage, which can result in hydrogen and thus economical losses and in some cases even in a safety hazard. Material-based storages include for example metal hydrides and liquid organic hydrogen carriers (LOHCs). [110, 111] Material-based storages are interesting options for safer long-time storage or hydrogen transportation because hydrogen can not leak from these storages without external heat input. However, for buffer storage, they might not be feasible as they require a lot of energy to release the hydrogen and the release rate is quite slow. [112, 113] In addition, the CAPEX of large material-based hydrogen storages, especially the one of metal hydrides, is high due to the small capacities of the storage units [114]. Compressed hydrogen storage is the focus of this thesis because only a short-time storage is required for the PtM process and fast charge and discharge are necessary. In addition, discharged hydrogen is already in pressurised and gaseous form which is advantageous for the methanation feed. [111]

Under compressed hydrogen storage, there are multiple different categories as well. Compressed hydrogen can be stored for example in vessels, geological storages or in other underground facilities. Of these options, storage vessels are the main focus of this thesis because geological and other underground storages usually require certain geological structures which are unlikely to be found on the process site. Storage vessels suffer from hydrogen embrittlement issues with certain metal types. Hydrogen embrittlement is a phenomenon where hydrogen weakens the surrounding metal and causes hydrogen to leak and to form explosive mixtures with oxygen. However, different materials have been developed to avoid or prolong the embrittlement, for example composite materials and steels with low carbon content. [110, 115] More information on hydrogen embrittlement can be found in [116].

Hydrogen has extremely low volumetric density whereas its gravimetric density is quite high. Due to the low volumetric density, hydrogen occupies a significant amount of space and therefore, compression of hydrogen is more energy-intensive than for example compression of methane. Volumetric storage density is used to describe the amount of hydrogen in kilograms that can be stored in one cubic meter of storage. The storage density is linearly dependent on the pressure of the storage and based on the ideal gas law. The volumetric storage density can be calculated as

shown in Equation (11). In this equation, $\rho_{storage}$ is the volumetric storage density, p is the storage pressure in bars and temperature is assumed to be ambient. [110]

$$\rho_{storage} = 0.0807 \frac{kg}{bar \cdot m^3} \cdot p \quad (11)$$

However, hydrogen differs from an ideal gas significantly because it spreads to a larger area than predicted in the ideal gas law. Therefore, a compressibility factor (Z), which describes the ratio of ideal mass of hydrogen to the real mass, should be included in the ideal gas law. The ideal gas law with compressibility factor is shown in Equation (12), where V is volume of the storage, n is the amount of substance, T is the temperature and R is the gas constant. The volumetric storage density equation was derived from the new ideal gas law and updated to its form in Equation (13).

$$pV = nZRT \quad (12)$$

$$\rho_{storage} = 0.0807 \frac{kg}{bar \cdot m^3} \cdot \frac{p}{Z} \quad (13)$$

The value of compressibility factor depends on the storage pressure and temperature [110]. The values for it in different temperatures and pressures are shown in Figure 21.

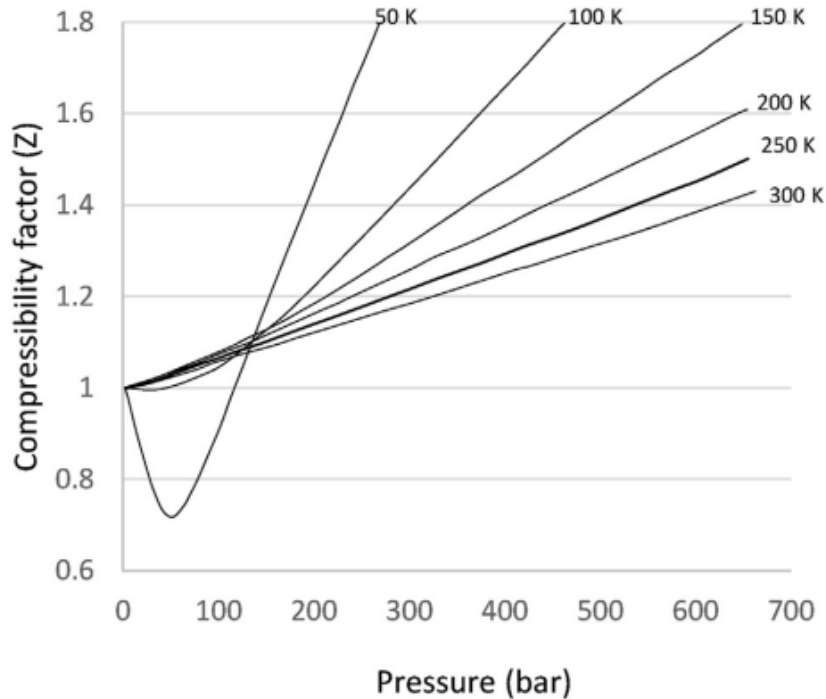


Figure 21: Compressibility factor for hydrogen in different pressures and temperatures [110].

Hydrogen can be stored in storage vessels in pressures up to 700 - 900 bars [111, 115]. Higher pressures are more beneficial because they increase the volumetric storage density. However, the compression of hydrogen becomes more energy intensive as pressure is increased. The compression requires about 5 - 20 % of LHV based energy content of hydrogen depending on the final pressure of the storage [117]. The highest possible pressure is limited in some cases due to the materials used in the storage and their ability to withstand the pressure. Stationary vessels that are usually used in large-scale applications are called type I and type II vessels. [110] These storage vessels, especially type I, have the highest maturity and lowest cost. Their gravimetric capacity is the lowest due to the metal parts, however it is not an issue for a stationary storage. [118] Type I storage is an all-metal storage that is made from carbon steel or low-alloy steel. Type II has a load-bearing metal liner hoop around the main cylindrical body. The liner is also partially wrapped with a fiber resin composite. Type I vessel can withstand 500 bar pressure but is operated usually at 200 - 300 bars, and the size of it is commonly in the range of 2.5 - 50 m³. Type II does not have pressure limitations and it is more durable and lighter than type I vessel. Type III and type IV storage vessels are even lighter due to their composite parts but their cost is also higher. They are advantageous in mobile applications but they are not the focus of this thesis. [110, 115]

7 Dynamic Modelling

Modelling and simulation are important tools to imitate real-life situations and gain knowledge of various systems without needing to build them in real-life. This is time efficient and cost-effective method to test different systems and their functionality. In dynamic modelling, the variables are time-dependent, meaning their value will change over time and therefore, their rate of change is not equal to zero [119]. The time derivative of these variables is shown in Equation (14).

$$\frac{\partial}{\partial t} \neq 0 \quad (14)$$

Taking dynamic aspects into account usually increases the complexity of the model but also increases the ability of the model to imitate a concrete system [119]. Steady state models are used as simpler method to gain basic knowledge of a system, however actual steady state rarely occurs in real life and therefore those models are not entirely accurate. Dynamic simulation gives a more detailed overview of the development of the process variables over time. This enables process improvements such as optimization of process design variables or control strategies. With dynamic simulation, the safety of the process can also be improved by studying the behaviour of the process in hazardous conditions. Additionally, start-up and shut-down behaviour, which are mandatory for example for process maintenance, can only be studied with dynamic models. Therefore, dynamic simulation adds significant value on top of the basic understanding given by the steady state models. [120] However, due to the complexity of dynamic models, they are more time-consuming to create and they can also include some simplifications that do not apply in real life. Dynamic systems can be divided into discrete and continuous systems. In discrete systems, the values of the variables change only at certain times whereas in continuous systems, the changes are smooth and happen continuously. [121] In this chapter, state-of-the-art dynamic modelling related to PtM is presented and the used simulation software is introduced.

7.1 State-of-the-Art Dynamic Modelling

Many research articles about dynamic modelling of PtM have been published in the recent years. Plenty of these articles include models of individual components of the PtM process and their dynamic capabilities. However, some models have also been made about the dynamic operation of the whole process. In addition, the cost optimization of the operation was included in few of the studies. Recent studies related to dynamic modelling of carbon capture and methanation were reviewed in Chapters 3.3 and 5.1. In this chapter, state-of-the-art dynamic models of electrolysers and whole PtM process are shortly reviewed.

Sakas et al. [122] created an industrial size alkaline water electrolyser model in Simulink environment. The simulation was zero-dimensional and consisted of dynamic mass and energy balances for the whole electrolyser plant. The model was validated with an experimental data from industry, and it was concluded that the

model predicts the thermal behaviour of the electrolyser with accuracy of 98.7 % and the mass balances correctly represent the mass flows at full load. However, at lower loads, the mass flows predicted by the model differ from the actual ones from the industrial plant. In a model created by David et al. [123], the controllability of gas production under dynamic operation was studied. The model was a phenomenological based semiphysical model for a self-pressurized alkaline electrolyser, and it was based on mass and energy balances in MATLAB. This model also successfully replicated an experimental electrolyser assembly. Zheng et al. [124] created a model for cost optimization of electrolyser operation with hydrogen storage. The model is also able to describe the efficiency changes, temperature variation and state transitions during the dynamic operation. However, the accuracy decreases with lower load levels. In addition to alkaline electrolysers, also PEM electrolysers have been modelled dynamically. For example, Sood et al. [125] modelled a dynamic PEM electrolyser with auxiliaries, that could be easily scaled to fit different sizes. The average error between the model results and experimental data was 5 %.

Uchman et al. [126] studied a PtM plant that is powered dynamically by wind energy in their Simulink model. The wind energy was assumed to be excess energy and therefore it was used only at night time when the demand is otherwise lower. The objective of the study was to find operational limitations for the process by changing the electrolyser capacity, hydrogen storage capacity and power generated by the wind farm. The optimal configuration was concluded to be 4 MW electrolyser powered with 10 MW wind farm. Increasing the storage size had a positive effect on the utilization time of the methanation. Economic potential of the dynamic operation was not included in this study.

Gorre et al. [7] created a Simulink model where they minimized the gas production costs of dynamic PtM process by changing the hydrogen storage size. The optimal storage size was found for fixed methanation capacity as well as for an optimal configuration of storage size and methanation capacity. Different power sources, wind energy, solar energy and grid utilization, in the form of grid control, were modelled. From the model, the needed storage capacity differences between different electricity origins were observed. It was concluded that solar energy requires larger storage capacity as the electricity generation has longer gaps in the daily cycle, whereas wind energy does not require as large storage capacity due to its more frequent variations in generation of electricity. Methanation capacity was larger for wind energy than for solar energy. An important conclusion was that dynamic operation with hydrogen storage could decrease the costs as much as 17 % in some cases and that the configuration should be chosen based on an analysis of the electricity supply. This model, however did not take into account the dependency of electrolyser efficiency on the load level. In addition, the electricity costs were assumed to be constant for the whole operation period and the production costs were optimized by minimizing the CAPEX of the process.

Inkeri et al. [127] studied the effect of dynamic properties of methanation reactor, hydrogen storage and full load hours on the efficiency of the process. The electrolyser operation was controlled with three methods: spot, wind and solar. In the spot control method, the electrolyser was run on full load or shut down depending on

the electricity price in the spot market. The price threshold was varied between 5 - 60 €/MWh to obtain a wide range of different full load hours. The wind and solar control methods utilized the excess electricity from these sources to power the electrolyser. It was concluded that the higher the full load hours and the larger the storage, the more the operation resembles steady state operation efficiency-wise and the smaller the effect of the reactor dynamic properties becomes. Maximum standby time, maximum thermal ramp and cooling rate of the reactor had the strongest effect to the process efficiency in the cases of wind and solar when the full load hours were low. In the case of spot control, the difference of the parameters was only seen as the variation of maximum efficiency with maximum thermal ramp. In conclusion, this study focused more on the dynamic ability of the reactor rather than cost optimization of electrolyser operation.

Qi et al. [128] proposed and modelled an alternative method to respond to the intermittent nature of renewable energy: intermediate liquid CO₂ energy storage, LCES. LCES is a thermo-mechanical storage that uses compressors and turbines to store and create electricity. CO₂ was used as a working fluid in the storage. The storage could therefore be used as a buffer for electricity and CO₂. SOE was used in the model and it was powered with renewable electricity. When the generation of renewables was low, electricity was used from the LCES storage. This way, both the electrolyser and methanation could be operated steadily. The efficiency of the total process was calculated to be 41.3 % and the LCOSNG value was 166 €/MWh for the year 2021. However, this was not dynamic simulation in practise, but only an alternative solution for the issues caused by intermittent nature of renewable electricity generation.

The dynamic simulations that were described here are summarized in Table 8. These studies correspond to only a minor part of the academic literature that is written on this topic. However, to the current knowledge of the writer, no simulation has been made about optimization of electricity cost of the electrolyser based on variable electricity prices and with multiple load levels. In addition, demand response payments have not been included in previous studies about dynamic operation. The process model of this thesis is presented in detail in Chapter 8.

Table 8: State-of-the-art of dynamic simulation of PtM.

Publication	Authors	Year	Modelling tool	Components modelled
Dynamic energy and mass balance model for an industrial alkaline water electrolyzer plant process	Georgios Sakas, Alejandro Ibanez-Rioja, Vesa Ruuskanen, Antti Kosonen, Jero Ahola and Olli Bergmann	2021	MATLAB, Simulink	Electrolyser (AEL)
Dynamic modelling of alkaline self-pressurized electrolyzers: a phenomenological-based semiphysical approach	Martín David, Hernán Alvarez, Carlos Ocampo-Martinez and Ricardo Sánchez-Peña	2020	MATLAB	Electrolyser (AEL)
Optimal day-ahead dispatch of an alkaline electrolyser system concerning thermal-electric properties and state-transitional dynamics	Yi Zheng, Shi You, Henrik W. Bindner and Marie Münster	2022	MATLAB	Electrolyser (AEL), Hydrogen storage
Generic Dynamical Model of PEM Electrolyser under Intermittent Sources	Sumit Sood, Om Prakash, Mahdi Boukerdja, Jean-Yves Dieulot, Belkacem Ould-Bouamama, Mathieu Bressel and Anne-Lise Gehin	2020	Symbol-Shakti, MATLAB, Simulink	Electrolyser (PEM)
Significance of methanation reactor dynamics on the annual efficiency of Power-to-Gas -system	Eero Inkeri, Tero Tynjälä and Hannu Karjunen	2021	MATLAB	Power source, Electrolyser, Hydrogen storage, Methanation
Cost benefits of optimizing hydrogen storage and methanation capacities for Power-to-Gas plants in dynamic operation	Jachin Gorre, Fabian Ruossa, Hannu Karjunen, Johannes Schaffert and Tero Tynjälä	2020	MATLAB, Monte-Carlo simulation method	Power source, Electrolyser, Hydrogen storage, Methanation
The analysis of dynamic operation of Power-to-SNG system with hydrogen generator powered with renewable energy, hydrogen storage and methanation unit	Wojciech Uchman, Anna Skorek-Osikowska, Michał Jurczyk and Daniel Węcel	2020	MATLAB, Simulink	Power source, Electrolyser (AEM), Hydrogen storage, Methanation

7.2 Simulation Software

The simulation software that was chosen for this thesis is Simulink. Simulink is a simulation tool that is a part of MATLAB software environment. MATLAB is a commercial environment that has wide online user support. Simulink simulation software is widely used in scientific communities as can be seen from Table 8, which is one reason why it was chosen. Another reason for the choice was the ability to easily simulate both continuous and discrete systems. Simulink's benefits are its easy model constructing method and the readability of the model. Simulink provides multiple different blocks for generic functions out of which the model can be constructed. In addition, user can define functions by herself via MATLAB code. The readability of the model is better when it consists of blocks instead of mathematical equations or plain code, which is important for possible further developments of the model. Additionally, the software can process large data sets easily and quickly. Another essential feature of Simulink in regards to this thesis is the possibility to use Matlab Optimization Toolbox in the simulation. Optimization of the model parameters is easier when it can be conducted under the same environment. In short, this simulation software was chosen because it is a widely used and easy-to-use tool that is a part of large software environment with multiple useful features.

8 Methods

This chapter includes description of the methodology of the experimental part of this thesis. The experimental part is divided into a Simulink model and an economic analysis of the process. The results from the model are used as input parameters for the economic analysis. First, the logic and the components of the process model are described in detail and then the assumptions and equations used in the economic analysis are presented.

8.1 Process Model

In this chapter, the Simulink model that was created and utilized in this thesis is described. The model was used to study the feasibility of transient Power-to-Methane operation and it consists of electrolyser, hydrogen storage, carbon capture and methanation. However, the main focus is on the electrolyser and the hydrogen storage. The time step of the model is one hour. The purpose of the model was to study transient operation of electrolyser and how the costs of the process could be reduced with that operation method. With regards to the cost minimization, optimal operation method and hydrogen storage size were found with which the highest cost reductions were achieved. Hydrogen storage enables transient operation of the electrolyser and thus decreases the electricity costs. However, the hydrogen storage itself and the compression of hydrogen create more expenses. Therefore, an optimized storage size should be found to make sure that the difference between electricity cost reductions and the cost of the storage is the most favorable for the economic feasibility of the PtM process. The optimal operation method determines when the load of the electrolyser is changed to reach the lowest operation costs for certain storage size. The logic of the model is presented next and then the parameters for each unit are described in more detail.

The operation logic of the model is that the load of the electrolyser is varied based on electricity price for each hour. The load is changed by varying the current density of the electrolyser which consequently affects the produced hydrogen mass flow according to Equation 1. Low electricity prices are utilized in such a way that at electrolyser full load, hydrogen is produced to storage. It was decided, that maximum hydrogen flow to the methanation is 80 % of the maximum hydrogen flow from the electrolyser. Therefore, 20% of the maximum hydrogen flow is stored. Hydrogen mass flow at electrolyser full load determines the synthesis maximum capacity and the required carbon dioxide flow, assuming stoichiometric reaction and 100 % conversion. Hydrogen mass flows each hour also affects to the status of the storage, meaning the amount of hydrogen it holds each hour. If the hydrogen mass flow is above the maximum flow to the methanation, hydrogen is added to storage and in an opposite scenario, hydrogen is taken from the storage. Summarized diagram of the process logic is presented in Figure 22.

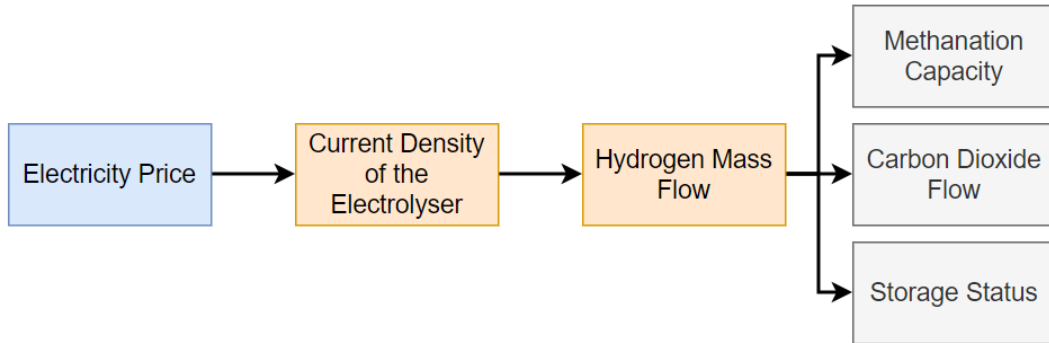


Figure 22: Summarized operation logic diagram of the process.

The logic behind the operation of the storage is illustrated in Figure 23. First, the model checks if the hydrogen flow is sufficient to run the methanation at full load. When the methanation full load is possible with the produced hydrogen, and there is hydrogen left over after the process, the storage is charged, whereas if there was no left over hydrogen, the storage status would stay constant. After each charging period, the status of the storage is checked to see if it is above a threshold value. If the storage was too full, the electrolyser load would be decreased. In another scenario, where the hydrogen flow is not sufficient for methanation full load, the storage is utilized. The amount of hydrogen taken from the storage corresponds either to the amount needed to cover the methanation full load, or to the amount that is left in the storage if it is less than needed for full load. In the latter case, methanation is run with part-load and excess CO_2 is sent to a long-time storage. However, in practise, emptying of the hydrogen storage is avoided. When the amount of hydrogen approaches zero, the load of the electrolyser is increased, regardless of the electricity price at that moment. With this action, it is ensured that there is always enough hydrogen in the storage to cover the needs of the methanation.

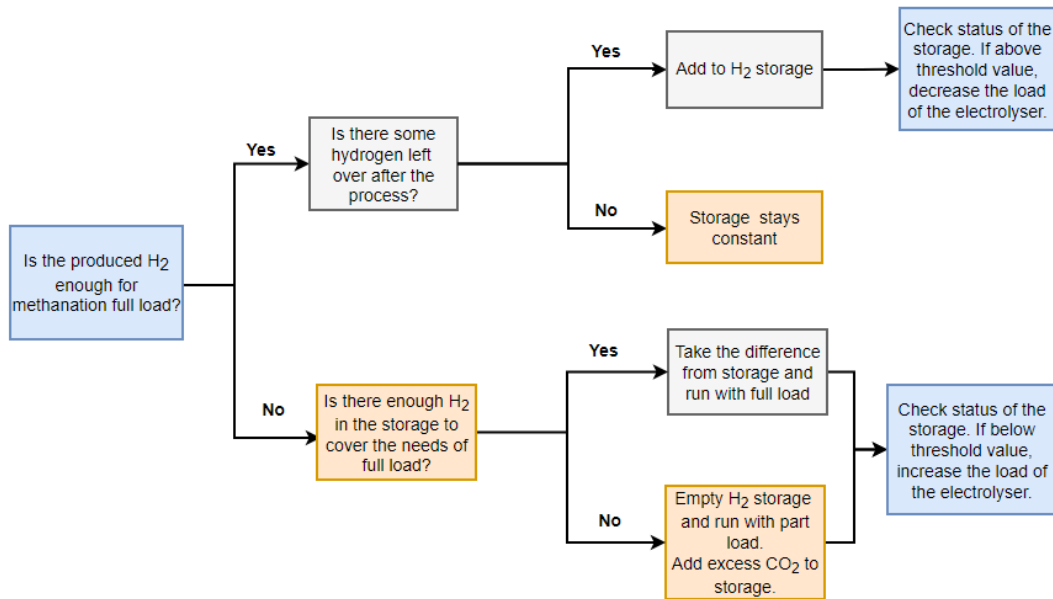


Figure 23: Logic diagram of the hydrogen storage model.

The control mechanisms of the process are presented in a simplified PI-diagram in Figure 24. The valve to the hydrogen storage opens if the hydrogen flow exceeds the maximum flow to methanation. Similarly, the valve from hydrogen storage opens when there is not enough hydrogen flowing to the reactor. A control mechanism that prevents emptying or overfilling of the hydrogen storage by changing the electrolyser load is also presented in the below figure. Carbon dioxide flow is controlled with one valve. If the hydrogen flow to methanation corresponds to part-load flow, the valve to CO₂ storage is opened and excess CO₂ is stored. No CO₂ is taken out of the storage.

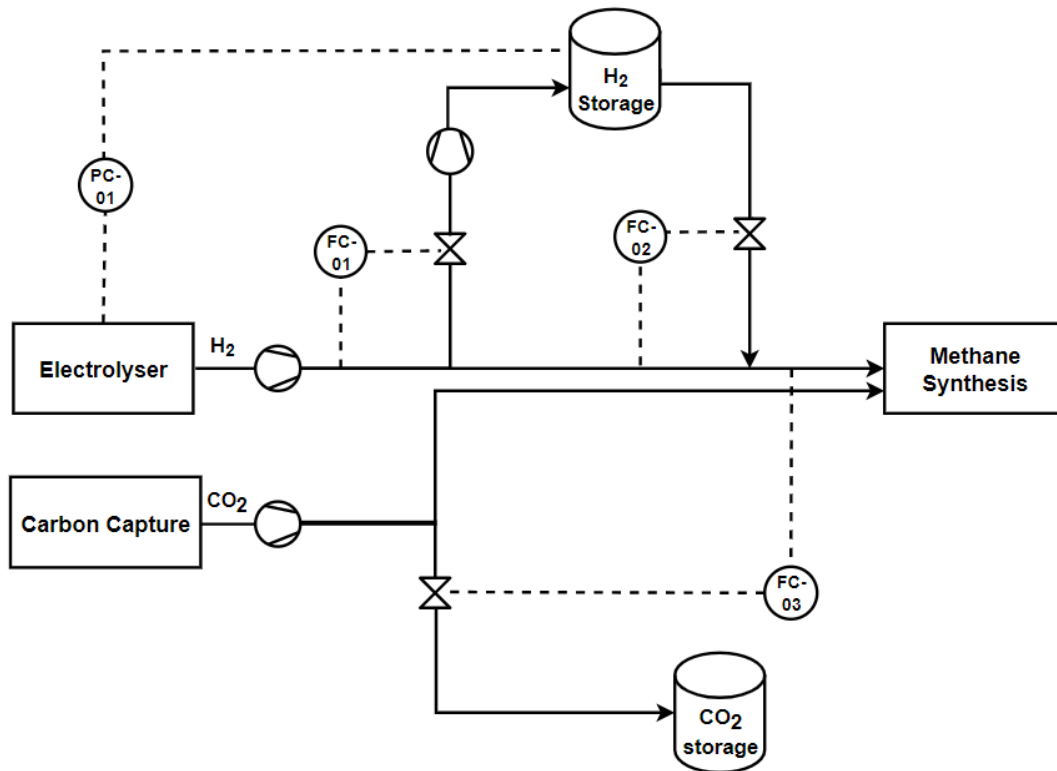


Figure 24: Simplified PI-diagram of the control mechanisms.

Finally, the flow sheet of the model is presented in Figure 25. The model takes the electricity data points from excel spreadsheet, that is colored with turquoise, and compares them to the price load limits. The load of the electrolyser and the produced hydrogen are determined in the light blue area. The described logic of the hydrogen storage is modelled in the green part. The yellow area contains calculations of the electricity consumption, full load hours and demand response payments. The maximum hydrogen flow to the methanation as well as methanation capacity and flow of produced methane are calculated in the dark purple area. With that information, the required flue gas flow is determined in the dark blue part in the top right corner. The stability of the methanation is confirmed with the model inside the light purple part.

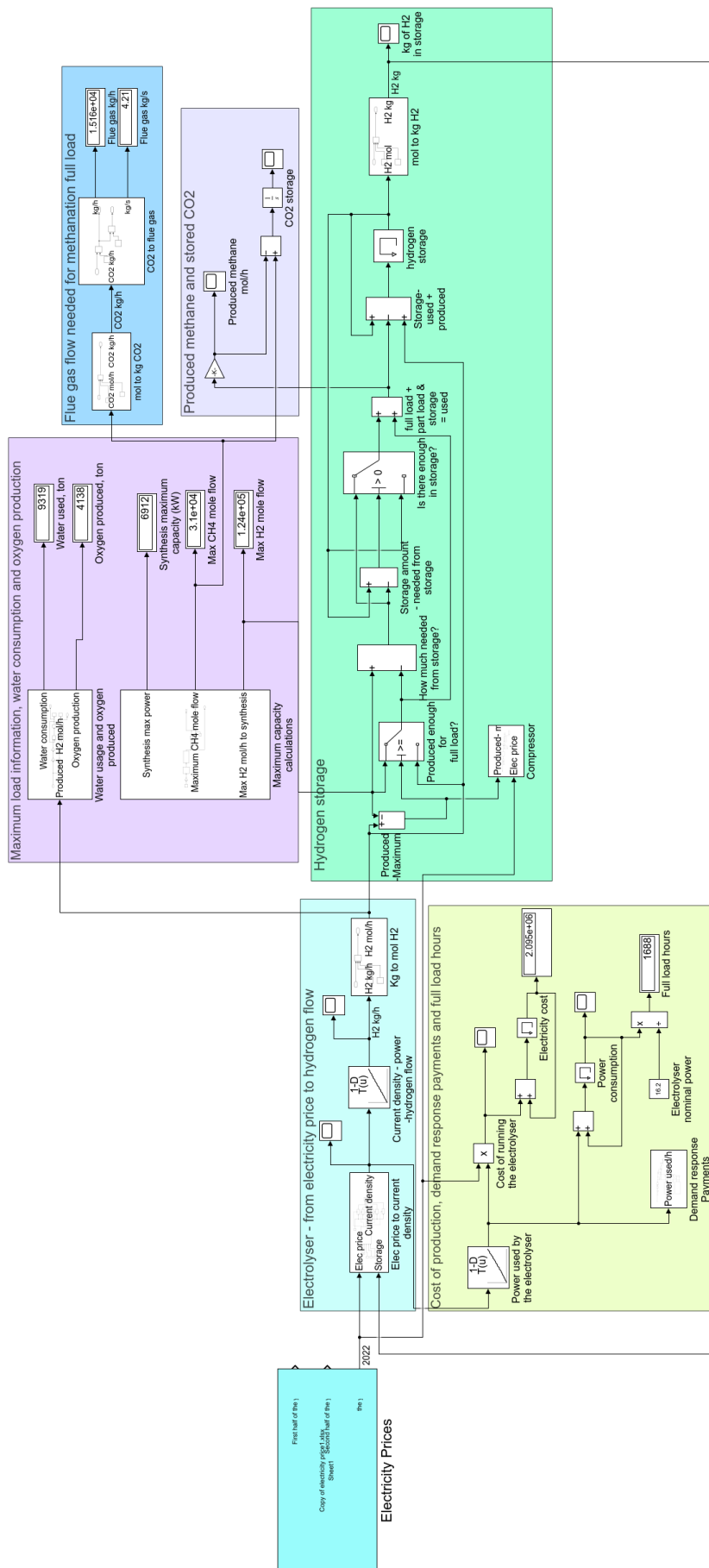


Figure 25: Flow sheet of the model.

8.1.1 Water Electrolysis

The chosen electrolyser technology is alkaline water electrolyser. Even though AEL has poorer dynamic properties than PEM electrolyser, the properties are significantly better than those of methanation reactor. In addition, the model uses timescale of one hour. Therefore, ramp rate of 20 %/s can be considered as instant change in the load. AEL is the most mature and the most inexpensive technology and therefore it was chosen instead of PEM. Results from an Aspen plus model of AEL by Jambur & Lähdemäki [129] was used as the input for this model. The maximum electrical power of the electrolyser is 16.2 MW. It has 8 stacks which all consist of 150 cells. It is operated at temperature of 80 °C and pressure of 1 bar. The full load power-based efficiency of the electrolyser is 64 %. The main parameters of the electrolyser are presented in Table 9. The parameters that are load-specific have the full load value in this Table.

Table 9: Main parameters of AEL electrolyser used in the model.

Parameter	Value
Power (MW)	16.2
Efficiency (%)	64
Temperature (°C)	80
Pressure (bar)	1
Number of Stacks	8
Minimum load (%)	20
Current density (A/m ²)	4000
Mass flow (kg/h)	312.8

The load of the electrolyser was varied between 20 - 100 % corresponding to current densities of 800 - 4000 A/m². Electrolyser shut-downs were not considered in this model, because of the long cold start-up times of AEL or alternatively, extra heating required to keep the electrolyser warm. The load was changed according to the Finnish spot electricity price on a particular hour. Therefore, price-load -limits were set. The limits specify an electricity price where a specific load is used. To simplify the model and the readability, four load levels were used: 20 %, 50 %, 80 % and 100 %. These loads were chosen because they are divided quite evenly through the load range of AEL. The load-specific parameters are presented for each load in Table 10. The price-load limits for each load level were determined through optimization and will be discussed in sections 8.1.6 and 9.1.

Table 10: Load specific parameters of the AEL electrolyser.

Load	20 %	50 %	80 %	100 %
Power (MW)	1.2	7.3	12.5	16.2
Efficiency (%)	77	71	66	64
Current density (A/m ²)	800	2000	3200	4000
Mass flow (kg/h)	61.3	155.7	250.0	312.8

8.1.2 Hydrogen storage

The hydrogen storage was chosen to be type II pressurised vessel. This vessel type was chosen because the lack of pressure limitations of it. The storage was assumed to be operated at 500 bars and the temperature to be ambient. The charge and discharge times of the storage were presumed to be negligible. The compressor was assumed to consume 15 % of the LHV-based energy content of hydrogen, which is about 5 kWh/kg.

The compressibility factor is about 1.3 according to Figure 21 in the chosen conditions. The volumetric density of the storage is then 31 kg/m³ according to Equation 13. One pressure vessel bundle has a size of 50 Nm³ which can fit up to 1550 kg of hydrogen in the described conditions. Five different storage capacities were modelled: 0 kg, 1550 kg, 3100 kg, 4650 kg and 6200 kg. That is, the modelled storage requires 0 - 4 vessel bundles.

8.1.3 Carbon capture

In Chapter 3 it was stated that the transient operation of carbon capture is possible with certain limitations. However, in this model the carbon capture is kept stable. That is, the flue gas flow was assumed to be stable and electricity generation from power plants was not increased by ramping down the carbon capture. This decision was made because carbon capture load reduction contradicts emission reduction goals. In addition, there is an economical benefit of capturing the carbon. EU emissions trading system allows industries to sell their emission allowances if there are some left over. Reducing emissions with carbon capture creates left over allowances that can be sold with the prevailing carbon price. Therefore, economic and environmental benefits are achieved with stable carbon capture whereas only economic benefit is obtained with transient operation. However, transient operation may be necessary in a case where flue gas flow is fluctuating. In this thesis, data from Finland was utilized and the flue gas flow from power plants is quite stable.

The required flue gas flow rate was calculated from the maximum hydrogen flow to methanation. Stoichiometric reaction was assumed and therefore carbon dioxide mole flow was one fourth of the hydrogen mole flow. The concentration of carbon dioxide was assumed to be 10 % in the flue gas and 90 % of the CO₂ was presumed to be captured. With these assumptions a flue gas flow rate of 4.2 kg/s is needed to feed sufficient amount of carbon dioxide to the methanation reactor. This flue gas flow is obtained from a 8 MW forest residue boiler.

8.1.4 Methanation

The considered methanation technology is catalytic methanation. The market requirements for SNG from sector coupling were described in Chapter 2.2 and summarised in Table 2. Important factors that needed to be taken into account in grid injection were the methane quality and the predictability of the product quantities. Chapter 5 presented the dynamic features of methane synthesis and it was noticeable that sudden variations in the inflow rates cause instabilities and conversion reductions in the reactor. This model does not take into account the chemical reactions inside the reactor in detail but only assumes 100 % conversion, and therefore a simplification was made to keep the methanation steady to ensure high quality and steady production of SNG throughout the year. The stability was achieved with the hydrogen storage. The control mechanism between the storage and electrolyser load is important to avoid part-load operation of methanation.

Hydrogen inflow to the reactor corresponds to 80 % of the maximum hydrogen production. Assuming 100 % conversion and stoichiometric reaction, the mass flow of produced SNG is 498 kg/h. The LHV-based power of the methanation is then 6.9 MW.

8.1.5 Demand Response Payments

Demand response payments from the Finnish frequency containment reserve for disturbances were calculated for each electricity price mix in the model. Actual data for the acquired capacity and hourly prices of that reserve from Fingrid were utilized for each year. FCR-D was chosen as the utilized reserve because it has the second largest share of demand response participation in Finland and the minimum bid that is required to participate is only 1 MW. In the balancing energy market, which has the largest share of demand response, the minimum bid is as high as 5 MW which means that the payments would not be received when the load is reduced from maximum load (16.2 MW) to 80 % load (12.5 MW). Therefore, more frequent payments are achieved with FCR-D. In the model, it is assumed that when the acquired capacity of the reserve for a particular hour is equal or higher than the load reduction of that hour, the bid will be approved and the hourly price will be paid for the amount of load reduced. The assumption of the bid approval may be overly optimistic as usually there are more bids than acquired capacity and therefore all of the bids will not be approved. Nevertheless, this assumption was made for simplification.

8.1.6 Methodology and Model validation

The scenarios that were used to run the model were different electricity price mixes. Three mixes were compiled from Finnish hourly electricity price data from years 2021 and 2022. The year of 2021 was divided into two parts because the prices in the first part of the year were quite low and stable whereas in the second part, larger variations occurred and the prices were extremely high. The year 2022 has different price evolution than either of the mixes from 2021; the prices are not as high as

in the second part of 2021 but the frequency of the price variation is higher. The scenarios used are called 2021a, 2021b and 2022. The prices are presented in Figure 2b. The timescales of these mixes are not the same: 2022, being the ongoing year, is shorter than the mixes from 2021. This will be taken into account by extrapolating the electricity prices of all of the chosen timescales to a whole year. It was assumed that the electricity price trend during the chosen timescale would be recurring until a year has passed. Electricity from the national grid was assumed but renewable origin of the electricity can be confirmed with certificates. More information related to the certificates can be found from example in [130].

The electricity costs were minimized for each scenario with Matlab Optimization Toolbox by varying electricity price limits that determine the load of the electrolyser. The limits were introduced to the model as shown in Equation (15). $L1$, $L2$ and $L3$ are the electricity price limits. $L1$ is the lowest price limit, $L2$ the second lowest and $L3$ is the highest. M and N are variables that represent the difference between the limits. The optimization tool finds values for $L1$, M and N , from which $L2$ and $L3$ can be calculated. Constrains set for design variables $L1$, M and N are that all of them should find values in the range of 0 - 200 €/MWh.

$$\begin{aligned} L2 &= L1 + M \\ L3 &= L2 + N \end{aligned} \tag{15}$$

The optimization was conducted so that the electricity costs were minimized for set storage sizes: 0 kg, 1550 kg, 3100 kg, 4650 kg and 6200 kg. In the case with 0 kg storage, the electrolyser was run with constant load. The no storage -case was used as a baseline scenario against which results from the other cases were compared. In the cases where hydrogen storage was used, the electrolyser load was decreased to 20 % when hydrogen amount in the storage approached the upper limit. Similarly, the load was increased to 80 % if the storage decreases below a threshold value. The value of 80 % was chosen because at that load, the hydrogen flow required to methanation is supplied from the electrolyser without needing to discharge the storage. These load changes were done regardless of the electricity price. Therefore, the storage status was considered a priority before the electricity price. Factors affecting the electrolyser load and which load level is used at a particular situation are presented in Table 11.

Table 11: Factors affecting the load level of the electrolyser.

Electrolyser Load Level				
Hydrogen in Storage (kg)	20 %	50 %	80 %	100 %
<500			X	
>~Maximum Capacity	X			
Electricity Price (€/MWh)	20 %	50 %	80 %	100 %
<L1				X
L1 <x <L2			X	
L2 <x <L3		X		
>L3	X			

The model was validated with mass balances around multiple configurations. With this validation method, the conservation of material in the system will be ensured. The first mass balance is around the produced hydrogen, shown in Equation (16). A mass balance was also created for the storage system, that is presented in Equation (17). Variables $m_{H_2,n}$ and $m_{H_2,n-1}$ stand for hydrogen amount in the storage at current hour and hydrogen amount in the storage at previous hour, respectively. Finally, mass balance around the Sabatier reaction is presented in Equation (18). All of these equations for each hour were proven to be true in the model and therefore no mass is created or lost in the system.

$$\dot{m}_{H_2,prod} = \dot{m}_{H_2,used} + \dot{m}_{H_2,stored} \quad (16)$$

$$m_{H_2,n} = m_{H_2,n-1} + \dot{m}_{H_2,stored} - \dot{m}_{H_2,fromstorage} \quad (17)$$

$$\dot{m}_{CH_4,prod} + \dot{m}_{H_2O,prod} = \dot{m}_{H_2,used} + \dot{m}_{CO_2,used} \quad (18)$$

8.2 Economic analysis

In this chapter, the methods for economic analysis are presented. For each scenario, operating and capital expenditures, levelized cost of synthetic natural gas and net present value are calculated. With these values, the feasibility of transient operation of PtM can be discussed in more detail. The comparison cases for the transient case are the no storage case and a PPA-case. In the PPA-case a steady operation with stable electricity price is assumed. The input values for the calculations for each unit of the system are presented in Tables 12, 13, 14 and 15. Uniform discount rate of 6 % was used and lifetime of the operation was set to 20 years.

Table 12: Input parameters for economic calculations for the electrolyser.

Electrolyser			
Parameter	Value	Unit	Source
CAPEX	750	€/kW	[68, 69, 70]
Stack change	50	% of CAPEX	[70]
Fixed OPEX	47.5	€/kW	[71]
Water price	0.69	€/ton	[131]
O ₂ selling price	87.74	€/ton	[132]

Table 13: Input parameters for economic calculations for the storage system.

Storage & Compressor			
Parameter	Value	Unit	Source
CAPEX of storage	559	€/kg	[133]
Fixed OPEX of storage	1	% of CAPEX	[7]
CAPEX of compressor	0.3	M€	[134]
Fixed OPEX of compressor	2	% of CAPEX	[133]
Electricity consumption of compressor	15	% of H ₂ LHV	Estimation, [117]

Table 14: Input parameters for economic calculations for methanation.

Methanation			
Parameter	Value	Unit	Source
CAPEX	450	€/kW	[7]
Fixed OPEX	3	% of CAPEX	[7]
SNG selling price	132	€/MWh	Estimation, [13, 17]

Table 15: Input parameters for economic calculations for carbon capture.

Carbon Capture			
Parameter	Value	Unit	Source
LCOCO ₂	75	€/t CO ₂	Estimation, [7, 135, 136]
EU ETS price	80	€/t CO ₂	Estimation, [137]

Capital expenditures describe the investment costs of the system. These costs are therefore paid in the beginning of the system lifetime. In these calculations, it is

assumed that the capital costs were divided for the first two years, after which the operation started. The CAPEX for the electrolyser is estimated to be 750 €/kW from literature values that vary between 500 - 1100 €/kW [68, 69, 70, 71]. The investment cost of methanation is 450 €/kW according to [7] and storage CAPEX was set to 559 €/kg according to [133]. No economics of scale was included in the calculations for the storage due to the modularity of the storage vessels. The costs of the storage vary significantly, approximately in the range of 200 - 1500 €/kg [134] and only a little information is available on the specifics of the type of storage. Some sources mentioned that the costs of the storage increases with the storage pressure [138], however, this was not evident in the literature values [134]. The storage CAPEX cost was chosen based on estimation that the type of storage that was chosen is cheaper than composite vessels and therefore the cost is not from the highest end. However, due to the high storage pressure, the cost is not from the lowest end either. The CAPEX of the hydrogen compressor was calculated based on equations from [134]. With Equation (19), the power of the compressor was calculated resulting in a value of 315 kW. Then, with Equation (20), the cost of the compressor was estimated. The lifetime of the compressor is set to 15 years [134] after which a new compressor has to be purchased. The cost of carbon capture was included in the economic analysis as a levelized cost of carbon dioxide.

$$P_{comp} = \dot{m} \cdot \frac{ZTR}{M\eta} \cdot \frac{N\gamma}{\gamma - 1} \cdot \left(\frac{p_{out}}{p_{in}}^{\frac{\gamma-1}{N\gamma}} - 1 \right) \quad (19)$$

$$CAPEX_{comp} = 15000 \cdot \left(\frac{P_{comp}}{10} \right)^{0.9} \quad (20)$$

Within these Equations:

- P_{comp} is the power of the compressor in kW
- \dot{m} is the mass flow rate to the compressor: 0.02 kg/s
- Z is the hydrogen compressibility factor: 1.3
- T is the temperature: 298 K
- R is the ideal gas constant: 8.314 J / (K mol)
- M is the molar mass of hydrogen: 2.016 g/mol
- η is the compressor efficiency: set to 75 %
- N is the number of compressor stages: set to 3
- γ is the diatomic constant factor: 1.4
- p_{in} is the inlet pressure of the compressor: 1 bar
- p_{out} is the outlet pressure of the compressor: 500 bar

The operating expenditures, or OPEX, are the yearly expenses from running and maintaining the operation. OPEX can be divided into fixed and variable expenses. Fixed OPEX stays constant throughout the operation and variable expenses differ depending on the time. For the electrolyser, fixed expenses are for example, labor costs and maintenance whereas variable costs are electricity costs and water usage. These variable expenses change depending on the load of the electrolyser at each hour.

Fixed OPEX is assumed to be CAPEX-based for methanation, storage and compressor. Meaning that the fixed OPEX corresponds to some percentage of the CAPEX of that unit. Cooling and heating costs were included in the fixed OPEX because it was assumed that the cost of them does not vary with load changes. The CAPEX-based percentages for the fixed OPEX are 1 %, 2 % and 3 % for storage, compressor and methanation, respectively. The fixed OPEX of the electrolyser is assumed to be 47.5 €/kW [71]. In addition, the stack change of the electrolyser is included as a yearly fixed maintenance cost equaling 50 % of the CAPEX cost divided for twenty years, which results in 0.3 M€/a.

Another fixed cost for each scenario is the cost of carbon capture. The cost of carbon capture was included in the calculations as the cost of captured carbon, or the levelized cost of carbon capture. This cost includes both CAPEX and OPEX for the carbon capture and an estimation of its value was made based on literature findings [7, 136, 135]. The estimation for the cost of carbon capture is 75 €/t CO₂ which equals to about 10 M€/a. However, the carbon credit achieved by reducing the CO₂ emissions is estimated to be 80 €/t CO₂ currently [137], which is higher than the cost of captured carbon. Therefore, payments are received from the carbon capture operation and it shows as an income in the calculations. The amount of the income is about 0.7 M€/a.

Variable OPEX consists of the electricity cost of the electrolyser, water usage of the electrolyser and electricity cost of the compressor. The electricity costs for each case are presented in Chapter 9.1. The water usage is assumed to be 200 % of the stoichiometric need and the cost of water is 0.69 €/ton according to [131]. Electricity consumption of the compressor is assumed to be 15 % of the LHV of hydrogen due to the high storage pressure. This corresponds to about 5 kWh/kg.

Levelized cost of synthetic natural gas was calculated to compare the effects of electricity cost reductions and CAPEX increase to the feasibility of the process. Levelized cost of energy is used to calculate the average net present cost of the product over the lifetime of the system. It is calculated by dividing the discounted costs over the lifetime by the amount of discounted production of SNG. The calculation formula is shown in Equation (21), where i is the operation year and r is the discount rate. The costs are equal to discounted CAPEX and OPEX and discounted payments received from CO₂ capture, selling of O₂ and demand response participation are subtracted from the costs. The remaining costs are divided by the discounted amount of produced SNG. Revenues from carbon capture and selling of oxygen are calculated from LCOCO₂, EU ETS price and oxygen selling price values that are shown in Tables 12 and 15. The LCOSNG of the different electricity price mixes were compared to steady operation method with stable electricity price in the form of wind generation based PPA.

$$LCOSNG = \frac{\sum_{i=0}^{21} \frac{1}{(1+r)^i} \cdot (CAPEX_i + OPEX_i - CO_{2,i} - O_{2,i} - DR_i)}{\frac{1}{(1+r)^i} \cdot SNG_i} \quad (21)$$

In addition to levelized cost of synthetic natural gas, also levelized cost of hydrogen was calculated. LCOH₂ was calculated the same way as LCOSNG in Equation (21)

but only the electrolyser and hydrogen storage were taken into account. Therefore, no carbon capture payments or methanation costs were included. In addition, the costs were divided by the amount of produced hydrogen and not SNG. $LCOH_2$ were calculated because the electrolyser and storage costs correspond to the majority of the costs.

Net present values for all of the cases were calculated. NPV is a measure of profitability and it describes the difference between the present value of future cash inflows and outflows. Positive NPV value means that the project is likely to be profitable, and it is recommended that the investment is made. The calculation formula for cumulative NPV is presented in Equation (22) where again r is the discount rate and i is the particular year of the operation. The NPVs of the dynamic cases were also compared to the steady operation cases with wholesale and PPA prices.

$$NPV = \sum_{i=0}^{21} \frac{SNG_i + O_{2,i} + CO_{2,i} + DR_i - CAPEX_i - OPEX_i}{(i + r)^i} \quad (22)$$

9 Results

The results obtained from the model and the economic analysis are presented and discussed in this chapter. The results from the model consist of electrolyser electricity costs, full load hours of the electrolyser, demand response payments and price-load limits. Economic analysis was conducted with parameters such as capital and operating expenditures, levelized cost of synthetic natural gas and net present value. The assumptions behind the model and economic calculations were presented in Chapter 8.

9.1 Optimized Operation Parameters for the Electrolyser

Results from the optimization of electrolyser operation; price-load limits, electricity costs of the electrolyser, full load hours (FLHs) as well as demand response payments, for electricity price mixes 2021a, 2021b and 2022 are presented in Tables 16, 17 and 18, respectively. These results are discussed in more detail in the following paragraphs.

The price-load limits are shown for each case in Tables 16, 17 and 18. Limits 2 and 3 are calculated from the design variables M and N as was shown in Equation (15). The limits for 2021a are significantly lower than for 2021b or 2022. This is because of the low electricity spot prices of that mix and therefore the possibility to run the electrolyser with significantly lower prices than for 2021b and 2022. The limits were the highest for 2022 with the highest fluctuation in the electricity prices. Because the high fluctuations, the limits have to be higher to be able to produce enough hydrogen. In some of the cases, for example 2021a with 3000 kg storage, the limits 1 and 2 are equal. This is because the optimizer could give the value of 0 to the design variables. If the usage of certain load level was calculated to be ineffective, it could be taken out of use by setting M or N to zero. For the no storage -case, the limits were not determined by the optimization, but were merely chosen in a way that the electrolyser will be operated only at load level 80 %.

Table 16: Results from optimization with electricity price mix 2021a.

2021a						
Storage size (kg)	L1 (€)	L2 (€)	L3 (€)	Electricity Cost (M€/a)	FLH (h/a)	DR Payments (k€/a)
0	-	-	-	5.42	7006	-
1550	54.1	55.9	57.8	5.15	7136	114.4
3100	58.4	58.4	60.0	5.01	7150	98.2
4650	56.2	56.2	59.1	4.92	7148	91.0
6200	53.1	57.6	65.0	4.89	7136	86.9

Table 17: Results from optimization with electricity price mix 2021b.

2021b						
Storage size (kg)	L1 (€)	L2 (€)	L3 (€)	Electricity Cost (M€/a)	FLH (h/a)	DR Payments (k€/a)
0	-	-	-	11.00	7006	-
1550	70.3	84.7	209.2	10.54	7066	<u>29.5</u>
3100	75.8	85.9	102.5	10.36	7084	15.4
4650	74.6	82.3	95.1	10.31	<u>7090</u>	10.9
6200	81.8	86.8	114.4	<u>10.21</u>	<u>7090</u>	13.6

Table 18: Results from optimization with electricity price mix 2022.

2022						
Storage size (kg)	L1 (€)	L2 (€)	L3 (€)	Electricity Cost (M€/a)	FLH (h/a)	DR Payments (k€/a)
0	-	-	-	10.36	7006	-
1550	101.6	101.6	104.5	9.53	7146	<u>24.7</u>
3100	105.6	105.6	124.5	9.07	7167	20.4
4650	82.4	105.2	163.2	8.96	7150	12.8
6200	112.1	112.1	114.3	<u>8.90</u>	<u>7231</u>	16.5

A common trend for the different electricity price mixes, that can be seen from Tables 16, 17 and 18, is that the electricity costs of the cases with storage are all lower than those of the cases with no storage. More specifically, the electricity costs decrease with increasing storage capacity. The lowest costs for each electricity price mix are underlined in the above tables. The electricity costs per kilogram of produced SNG correspond to about 1.12 - 1.24 €/kg for 2021a, 2.34 - 2.52 €/kg for 2021b and 2.04 - 2.38 €/kg for 2022. The comparison of the price development for different electricity price mixes is shown in Figure 26. It can be seen from the figure that the curves are steeper at first and then even out towards the end. Therefore, the most significant electricity cost reductions are achieved when moving from no storage-case to smallest possible storage and only smaller reductions can be reached when changing a medium size storage to a large one. The mix of 2022 has the steepest curve meaning that largest absolute reductions are achieved with that mix. 2022 is the mix with the most frequent fluctuations in the electricity price so it is reasonable that it benefits the most from dynamic operation of the electrolyser. For mix 2021b the electricity costs are higher than for 2022 but the cost reductions are not that significant. This is caused by the fact that 2021b had higher average electricity price but the frequency of the oscillations was not as high. 2021a had low electricity prices and only minor fluctuations and therefore the achieved reductions of that mix are lower than for 2021b and 2022. It can be concluded that, with regard to operational expenses, dynamic operation of the electrolyser is advantageous even in the scenario

where electricity prices are quite stable. However, capital expenses will increase with larger storage capacities and the effect of that to the feasibility of the system will be discussed in Chapters 9.4 and 9.5.

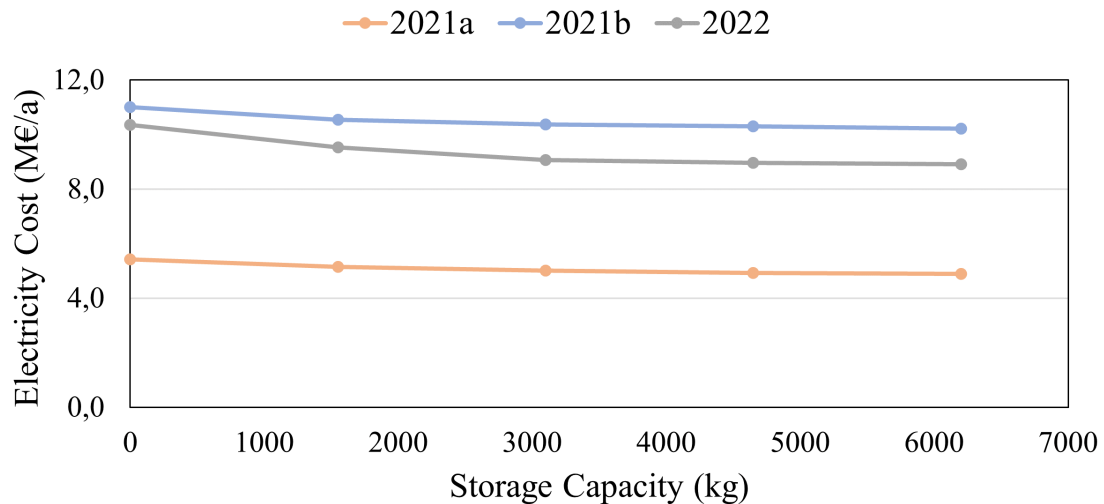


Figure 26: Relation between storage capacity and electricity cost for each electricity price mix.

The cumulative demand response payments for each scenario are presented in Figure 27. The payments vary between approximately 10 000 - 115 000 €/a. The payments are this low, because the times when large payments were paid were not the same as the times of high electricity prices. In other words, there was no need to pay as much when the electricity prices were high because then consumers would presumably lower the load based on the cost reduction achieved with only implicit demand response methods. This is also the reason why the payments achieved in 2021a are significantly higher than for 2021b and 2022. The prices were lower in that scenario and therefore explicit payment methods were needed to balance the consumption. No payments were received in the no storage -case as it was a steady case with no possibility to participate to the demand response market. The highest payments in each electricity price mix were reached with the smallest storage. This is due to the fact that the smaller the storage, the more frequent the filling of it and therefore the more frequent load reductions. When the load reductions are more frequent, more payments are received. In conclusion, the explicit demand response payments should be higher to make a significant difference to the feasibility of the process. To have an idea how much the payments could be at maximum, the electrolyser operation could also be optimized with regard to maximum demand response payments. However, because the cost reductions with implicit demand response method are already quite high, the explicit payments are not necessarily needed to increase the feasibility above the no storage -case. Electrolyser and fuel cell participation to the French reserve markets were studied by Grueger et al. [139]. They observed that the hydrogen production costs could be lowered significantly

with accepting low energy bids. However, the revenue for the fuel cell operation was diminishing. These results are compatible with the results of this thesis: the implicit measures, meaning the electricity cost reductions, increase the feasibility much more than the payments from the reserve market.

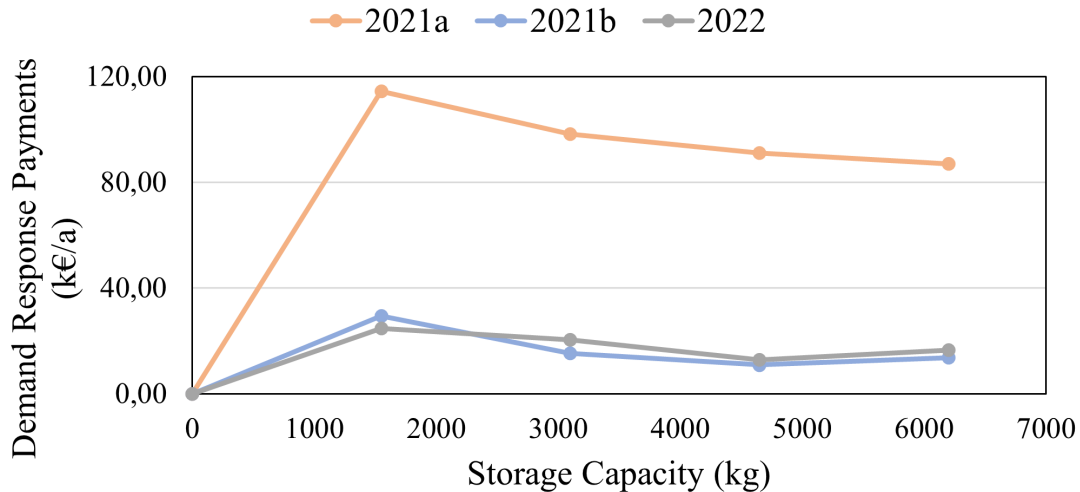


Figure 27: Demand response payments from FCR-D for each electricity price mix.

The full load hours of the electrolyser are presented in Figure 28. It can be seen that the usage of the electrolyser is higher for the cases with storage than for the cases with no storage. However, the FLHs do not increase with increasing storage size in all of the scenarios. This is caused by the controlling method of the load level. The load level is not only dependent on the electricity price but also on the storage status. In addition, the price-load limits vary between the storage sizes and causes the electrolyser operation to be different for each case. Therefore, the FLHs have no clear relation between the storage size and electricity cost. The full load hours correspond to about 80 % utilization degree in a year for all of the mixes which is quite high. The highest full load hours were achieved in mix 2022 due to the high value of limit 1 which enables wide range of full load operation. In a study by Gorre et al. [140] it was noticed that the production costs decrease with higher full load hours. In that study the cost reductions were achieved with lower standby hours and thus higher production rate. In a study by van Leeuwen et al. [134], the electricity costs increased with higher FLHs because it is assumed that with higher utilization rate, more expensive electricity must be used in order to provide enough electricity for the operation. The results obtained here do not follow either of these trends and do not have a clear relation with electricity costs due to the more complicated operation method of the electrolyser.

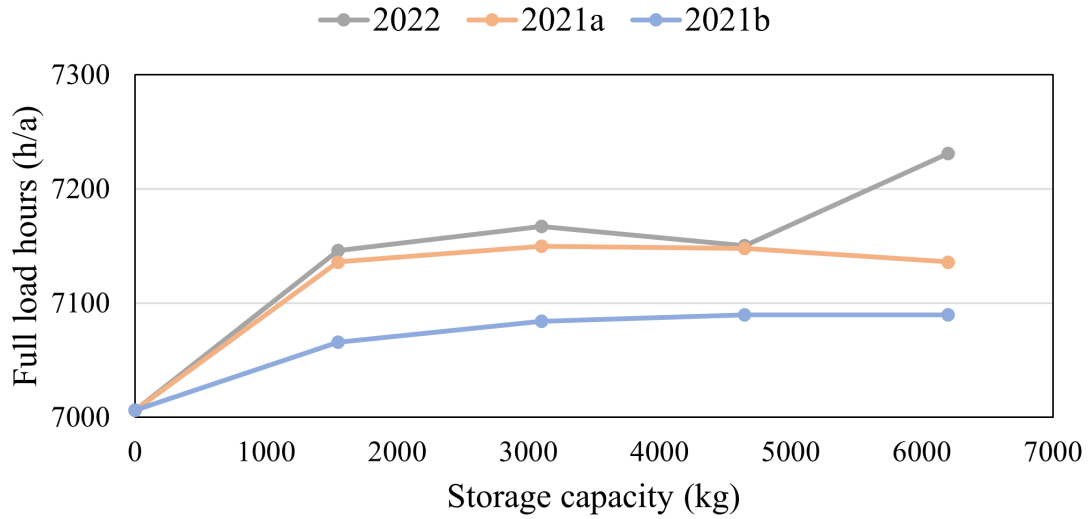


Figure 28: Full load hours for each electricity price mix scenario and storage case.

9.2 Capital Expenditures

Capital costs of storage, compressor, electrolyser and methanation were taken into account in the calculations of CAPEX of the whole process. The capital cost of the compressor was calculated to be about 0.3 M€ with Equation (20), and it was taken into account in the cases with storage. No compressor was included in the case with no storage. The storage CAPEX varied with storage size but electrolyser and methanation CAPEX were the same for each case. The capital expenditures for each case are presented in Table 19. Additionally, the increase of the cost is illustrated in Figure 29.

Table 19: CAPEX for all of the storage capacity cases.

Storage Capacity (kg)	Storage CAPEX (M€)	Compressor CAPEX (M€)	Electrolyser CAPEX (M€)	Methanation CAPEX (M€)	Total (M€)
0 kg	0	0	12.2	3.1	15.3
1550 kg	0.9	0.3			16.5
3100 kg	1.7				17.3
4650 kg	2.6				18.2
6200 kg	3.5				19.1

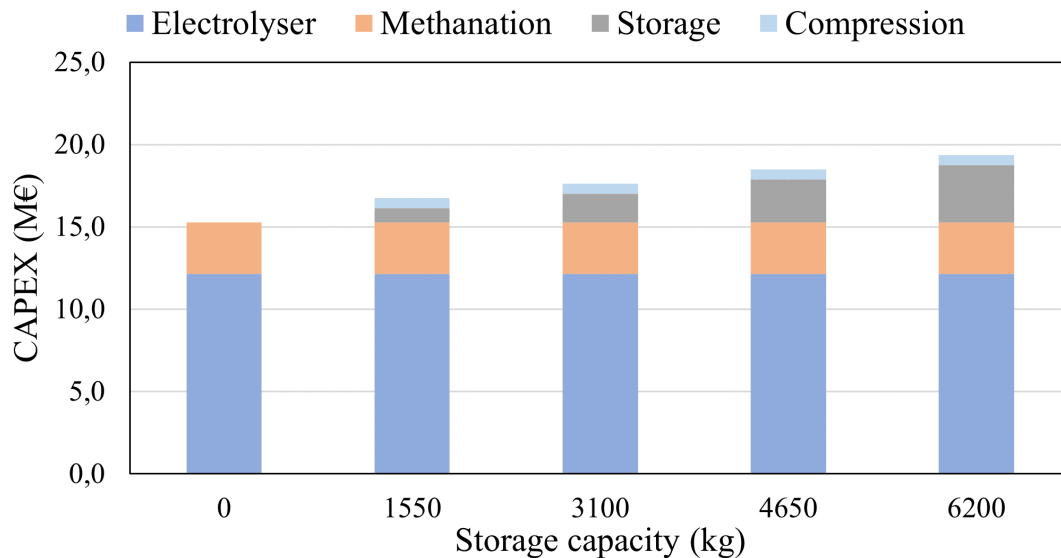


Figure 29: Capital costs for different storage capacities.

From Table 19 and Figure 29, it can be noticed that the difference in the capital expenses between the no storage -case and the 6200 kg storage -case is about 4.1 M€ which corresponds to 27 % of the CAPEX of no storage -case. This is a relatively low increase as the capital cost of the electrolyser is substantially higher. The combined effect of electricity cost reductions and capital cost increase to the production costs of synthetic natural gas are further examined in Chapters 9.4 and 9.5.

9.3 Operating Expenditures

The fixed OPEX values for each storage capacity are presented in Table 20. These costs are equal for each electricity price mix as it is assumed that they are not dependent on the electricity price. Fixed OPEX was dependent on the CAPEX costs in this analysis. Therefore the cost of the fixed OPEX increases slightly with increasing storage capacity due to increase in the CAPEX.

Table 20: Fixed OPEX for all of the storage capacity cases.

Storage Capacity (kg)	Fixed OPEX (M€/a)
0 kg	1.17
1550 kg	1.19
3100 kg	1.20
4650 kg	1.21
6200 kg	1.21

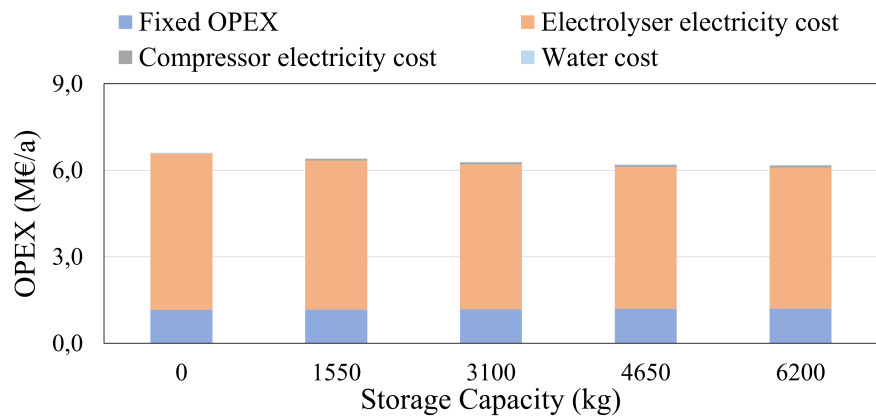
The variable OPEX consists of electricity costs of the electrolyser and compressor and water cost. The water cost is quite constant between the scenarios and cases, the value being about 0.027 M€/a. Compressor cost is slightly higher than the water cost,

it varies between the cases in the range of 0.04 - 0.096 M€/a. The water cost and compressor electricity consumption are not significant parts of the variable OPEX as the electricity cost of the electrolyser is considerably higher. The total variable OPEX costs are presented in Table 21.

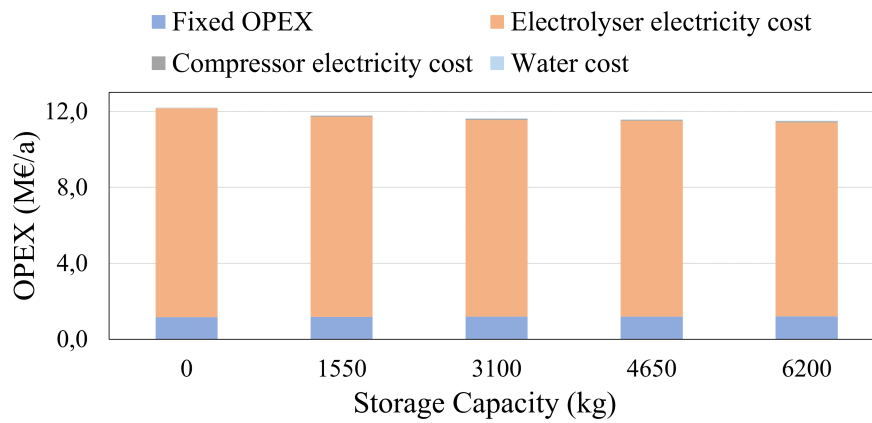
Table 21: Variable OPEX for all of the cases

Mix	2021a	2021b	2022
Storage capacity (kg)	Variable OPEX (M€)	Variable OPEX (M€)	Variable OPEX (M€)
0	5.5	11.0	10.4
1550	5.2	10.6	9.6
3100	5.1	10.4	9.2
4650	5.0	10.4	9.0
6200	5.0	10.3	9.0

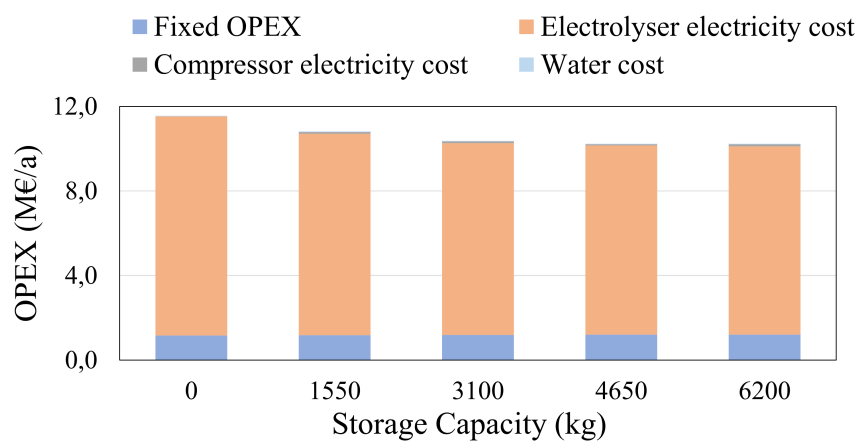
The relation of variable and fixed OPEX for scenarios 2021a, 2021b and 2022 are presented in Figure 30. It is clear that the electricity cost of the electrolyser represents a large majority in the operating costs and it decreases with increasing storage size. Fixed OPEX are the second highest costs, being still significantly smaller than the electrolyser electricity cost. Expenses related to compressor operation and electrolyser water consumption are diminishing and are not clearly visible in Figure 30.



(a) 2021a



(b) 2021b



(c) 2022

Figure 30: Operating costs of different electricity price mixes.

9.4 Levelized Cost of Synthetic Natural Gas

The calculated LCOSNG values in €/MWh for each electricity price mix scenario are presented in Figure 31. The LCOSNGs are compared to the average selling price of natural gas in March 2022 in Figure 31. The value of the average SNG price is 132 €/MWh. The LCOSNGs for 2021a, 2021b and 2022 are about 92 €/MWh, 181.4 €/MWh and 159.5 €/MWh, respectively. There are large variations in the LCOSNG values due to the variations in the electricity prices. Van Leeuwen et al. [134] report LCOSNG values of 79 - 143 €/MWh depending on the electrolyser CAPEX for a plant with 80 % utilization rate and with the most inexpensive electricity mix of that time. Estimating the reference LCOSNG with the same CAPEX, 750 €/kW, that was used in this thesis, results in 90 €/MWh which is comparable with 2021a LCOSNG. To make the process profitable, the production costs should be lower than the selling price of SNG. This is the case only for scenario 2021a with the low electricity prices. Scenarios 2021b and 2022 are not profitable, however, the cases with dynamic operation and storage are more feasible than the steady case without storage. This is the case also for 2021a with the most stable electricity prices, the LCOSNG decreases slightly by 4 €/MWh from the no storage -case. Therefore, it can be concluded that dynamic operation is more feasible than steady operation even with stable electricity prices. Meaning that the electricity cost reductions are higher than the increase in CAPEX costs for all of the electricity price mixes. The feasibility can also be increased even further with optimal storage size.

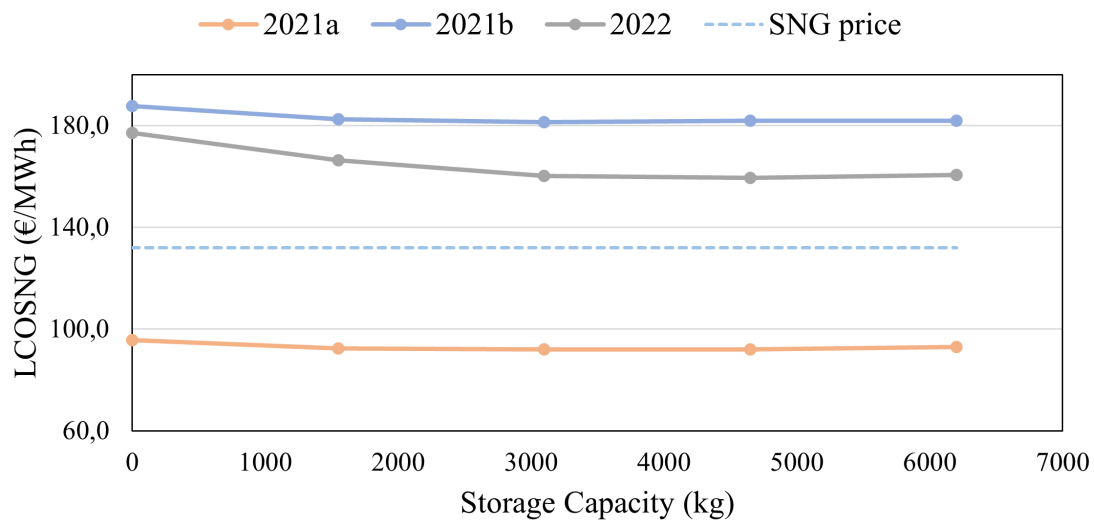


Figure 31: Levelized cost of synthetic natural gas for each electricity price mix compared to the selling price of SNG.

In the no storage -case, the operation of the electrolyser is steady but the electricity prices still vary the same way as in the dynamic cases. Comparison cases with steady operation and stable electricity prices were therefore also included. These cases include average PPA prices from wind generation in Finland and in Europe. The

price of average wind PPAs in 2022 in Finland is 39.5 €/MWh and in Europe it is 64 €/MWh [141, 142]. The comparison of the different cases is shown in Figure 32. The PPA Finland case is the most inexpensive method to produce SNG, after which comes 2021a. PPA Europe is clearly more expensive than 2021a but it is still feasible as the production costs are lower than the selling price of SNG. The PPA prices have had an increasing trend during the years 2021 and 2022 due to the high wholesale prices and it is probable that they will increase even further [141, 142]. In addition PPAs are usually signed for 10 years or more which can be a benefit or a con [142]. It is a beneficial if the wholesale prices keep increasing during the agreement and the bought electricity becomes relatively cheaper. However, in an opposite situation, the bought electricity becomes relatively more expensive if the wholesale prices decrease. Therefore, there is a risk of uncertainty in signing a PPA but currently they are included in the most feasible options. Dynamic operation with wholesale prices is the second most feasible option and the most unfeasible operation method is steady operation with wholesale prices.

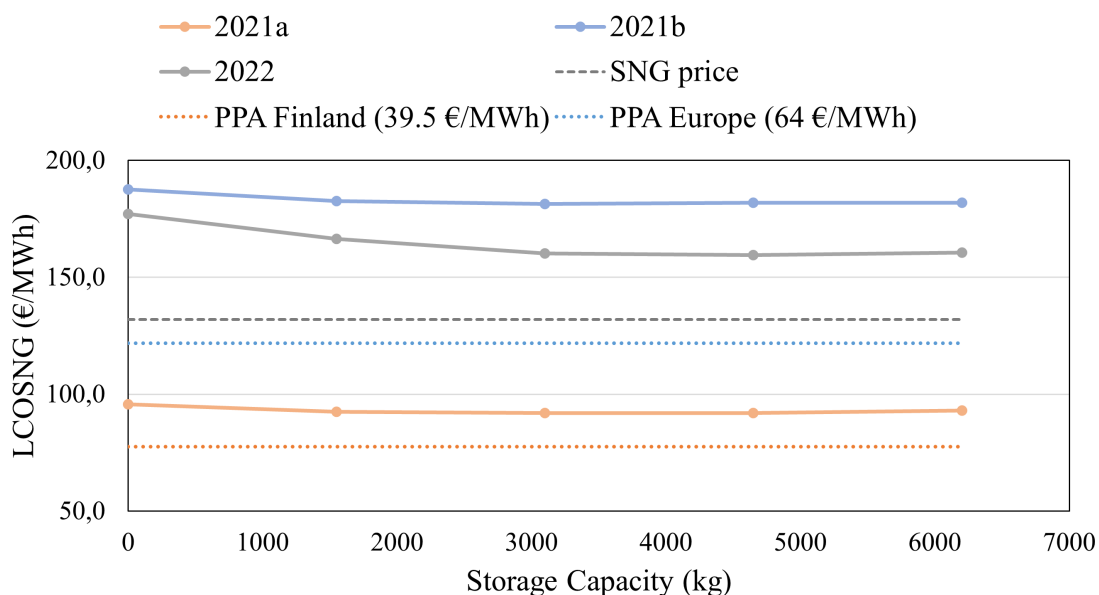
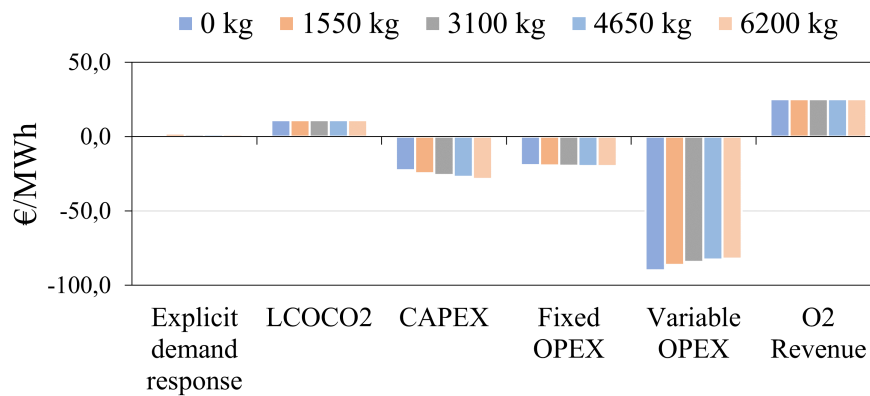


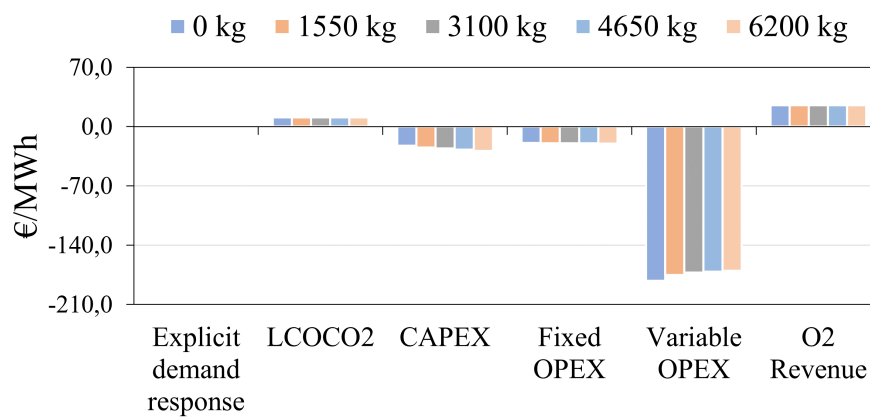
Figure 32: Levelized cost of synthetic natural gas for each electricity price mix compared to PPA scenarios.

To further demonstrate the effect of electricity costs of the electrolyser to the economic feasibility of the process, the factors affecting the LCOSNG were broken down to categories in Figure 33. The categories that have positive value have a decreasing effect on the production costs and the ones with negative value increase the costs. Carbon capture, O₂ revenue and demand response payments have positive values and CAPEX, fixed OPEX and variable OPEX have negative values. As it was mentioned before, demand response payments are very low and therefore hardly visible in Figure 33. The electricity costs are included in the variable OPEX along with water cost, which was significantly smaller than the electricity costs. The share

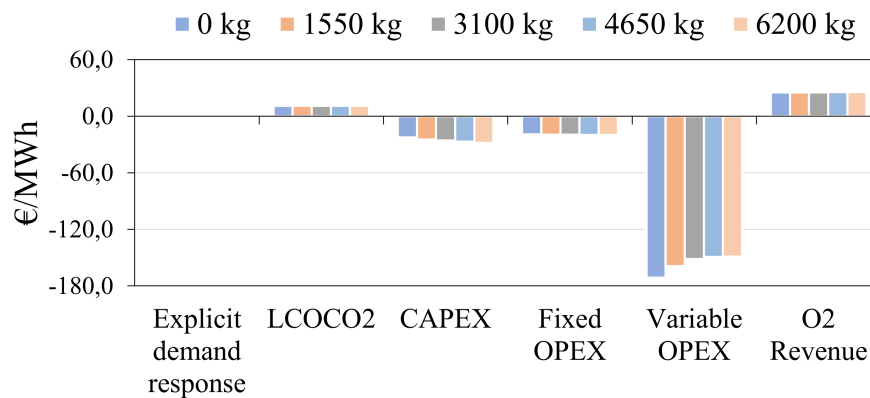
of variable OPEX in the LCOSNG is clearly the highest for all of the cases. The share is about 80 €/MWh for 2021a, 170 €/MWh for 2021b and 150 €/MWh. These costs are on average about 65 %, 79 % and 77 % of the total costs for 2021a, 2021b and 2022, respectively. Therefore, there is a significant importance in decreasing the electricity costs with dynamic operation or alternatively with power purchase agreement. The same conclusion was made by Gorre et al. [140]. They noticed that when electricity price increases above 20 €/MWh, the electricity cost becomes the majority of the gas production costs. The second largest cost contributor was CAPEX in that study which is in line with the results presented here. Water cost had also the smallest effect to the total costs according to their study.



(a) 2021a



(b) 2021b



(c) 2022

Figure 33: Factors affecting the LCOSNG for different electricity price mixes.

The values of $LCOH_2$ for each electricity price mix and for each storage size are presented in Figure 34. These values are not comparable with the LCOSNG values because the produced amount and lower heating values of the fuels are different. However, same trends are visible here than in LCOSNG: the prices decrease from the no storage -case to the dynamic cases and the cost reductions are the highest for

2022. Scenario 2021a has values of approximately 80 €/MWh which corresponds to about 2.7 €/kg. Scenario 2021b has values of about 155 €/MWh which is equal to 5.2 €/kg. The LCOH₂ values for 2022 vary more than in the other cases, the lowest costs being about 135 €/MWh or 4.5 €/kg. These costs determine the minimum selling price of hydrogen to make the hydrogen production feasible. Green hydrogen production costs are reported to range within 2.5 - 6 €/kg or 75 - 180 €/MWh according to KPMG [143]. The results of this thesis are comparable with the values given by KPMG.

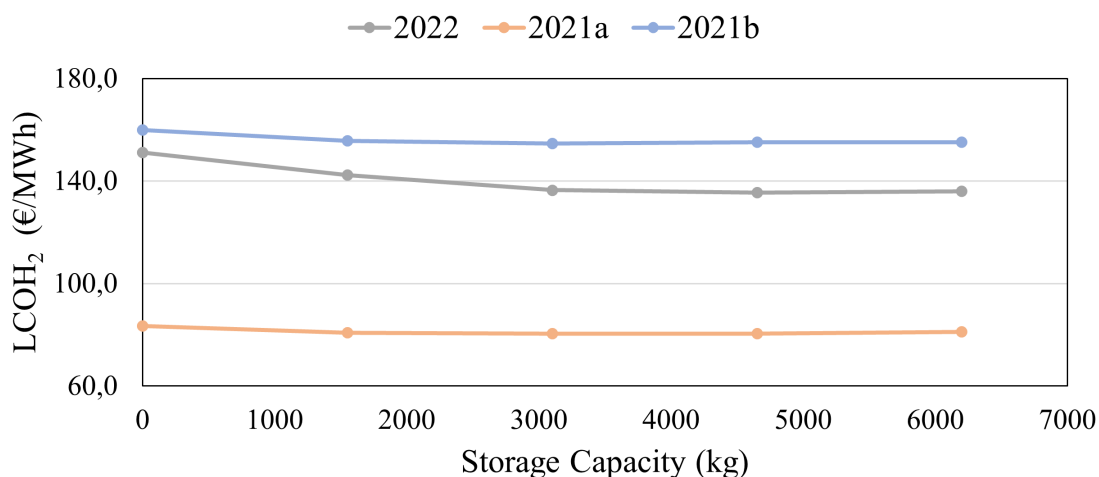


Figure 34: Levelized cost of hydrogen for each electricity price mix.

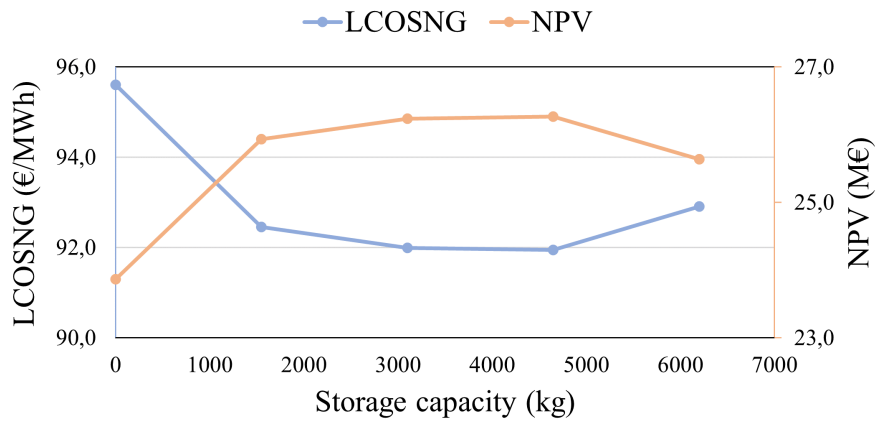
9.5 Net Present Value

Cumulative net present values for each storage case and electricity price mix are presented in Table 22 along with internal rate of return (IRR) values. IRR gives the value of discount rate with which the NPV would reach zero. If the project is well below profitability, IRR can not be calculated. The NPV values presented here confirm the assumption from Chapter 9.4 that the only profitable dynamic electricity price mix is 2021a. The values of that mix are well above zero and therefore the net cash inflows are much larger than the outflows. However, for 2021b and 2022 this is not the case. The highest NPV for 2021b is -32.4 M€ and for 2022 the highest value is -18 M€. This means that these projects did not reach profitability in twenty years and the costs are much higher than the incomes. IRR values for these electricity price mixes could not be calculated due to the low NPV values. For comparison purposes, the NPV of PPA Finland -case was calculated to be 35.7 M€ and for PPA Europe, the NPV was 6.7 M€. The respective IRRs were 27 % and 11 %. These values indicate that both PPA scenarios are profitable.

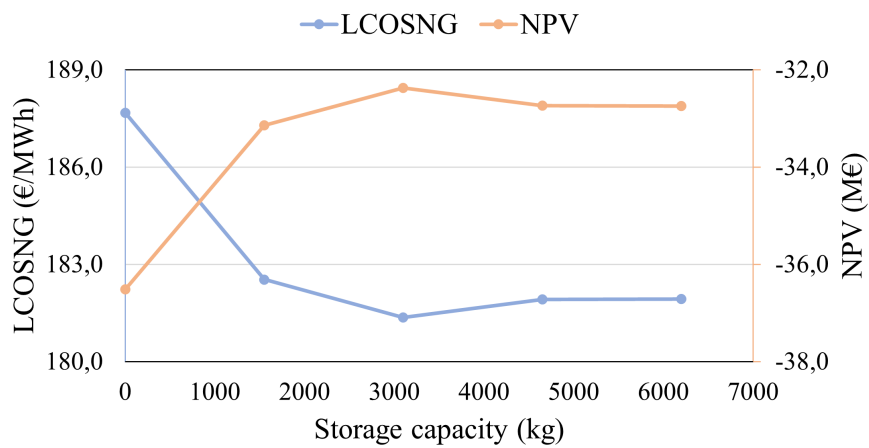
Table 22: NPV and IRR values for each scenario.

Mix Storage capacity (kg)	2021a		2021b		2022	
	NPV (M€)	IRR (%)	NPV (M€)	IRR (%)	NPV (M€)	IRR (%)
0	23.9	20.7	-36.5	-	-29.5	-
1550	25.9	20.9	-33.1	-	-22.6	-
3100	26.2	20.4	-32.4	-	-18.5	-
4650	26.3	19.8	-32.7	-	-18.0	-
6200	25.6	19.0	-32.7	-	-18.8	-

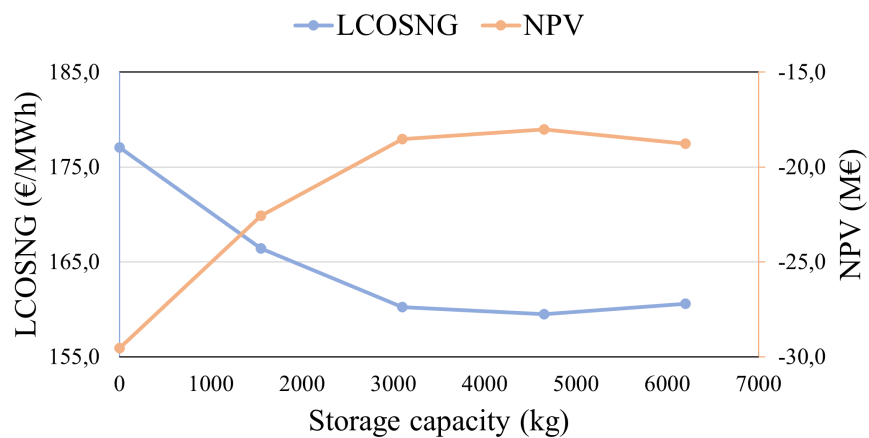
Both NPV and LCOSNG for each electricity price mix are presented in Figure 35 from which the optimal storage size can be concluded. The optimal size is the point in Figure 35 where the production costs are at minimum and where the profitability is the highest. For all of the mixes, the profitability increases steeply to the storage capacity of 3100 kg after which the changes are not as significant. For 2021a and 2022, the profitability increases slightly for 4650 kg storage case and for 6200 kg, the profitability starts to decrease. The mix 2021b behaves differently, as the storage capacity of 3100 kg is the highest point after which the profitability decreases and is then stable between storage sizes 4650 kg and 6200 kg. The difference in behaviour of these mixes is caused by that the electricity cost reductions for 2021b from 3100 kg to 4650 kg storage are not as high as for the other mixes. The CAPEX increase is, however, equal for all of the mixes. Due to low cost reductions, the profitability does not increase after 3100 kg for 2021b. However, the cost reductions between 4650 kg and 6200 kg storages for 2021b are higher than for 2021a or 2022. It can be concluded that 3100 kg storage is optimal for 2021b and 4650 kg storage is optimal for 2021a and 2022. However, for 2021b, when moving past the optimal point, the larger storage capacities do not decrease the profitability as significantly as for the other mixes. For all of the electricity price mixes, the no storage -case is considerably less profitable than the optimal case.



(a) 2021a



(b) 2021b



(c) 2022

Figure 35: NPV and LCOSNG for different electricity price mixes.

The difference between LCOSNG values between the no storage - and optimal case is the largest for 2022. The savings achieved are about 17.6 €/MWh which

corresponds to 10 % of the cost of no storage -case for that mix. For 2021a the same numbers are 3.7 €/MWh and 3.8 % and for 2021b they are equal to 6.3 €/MWh and 3.3 %. Because the electricity cost reductions with storage are the highest for 2022, the total savings achieved are also the largest for that mix. The mix of 2021b has the lowest relative cost savings due to the extremely high electricity prices.

The level of profitability of the process is therefore affected by the dynamic operation. The NPVs of optimal storage capacity cases for dynamic operation, and steady operation with wholesale and PPA prices are compared in Figure 36. From the comparison, it can be seen that dynamic operation of the process can not necessarily make the process profitable even though it is a reasonable method to lower the costs compared to steady operation with wholesale prices. The profitability of the process is mainly affected by electricity prices as was shown in Figure 33 and therefore future electricity prices will determine if the process is feasible or not. The process is not profitable with current, 2022, electricity prices, but with 2021a prices, profitability is reached. The steady scenarios with PPA prices are profitable, PPA Finland having the highest NPV. However, the prices of PPAs have also experienced an increasing trend as have the wholesale prices. If the trend continues, even the PPA scenarios could become unprofitable. Therefore, if there will not be a downturn in the future electricity prices, some other measures such as political, are required to make the transition from fossil fuels to renewable ones possible.

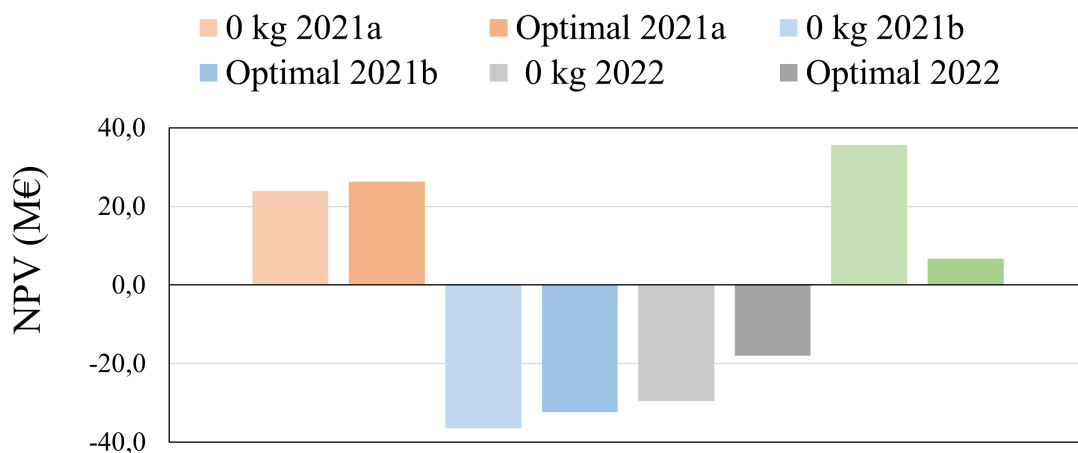


Figure 36: NPVs for optimal dynamic operation cases and different steady operation scenarios.

Sensitivity analyses were also conducted for CAPEX costs and oxygen revenue for the case 2021a with optimal storage size. CAPEX costs of each component were increased to 1.5 times the values used in the economic analysis. This was done because of the high variation of prices in literature and due to possible price increase in the future due to inflation. Oxygen revenue was set to 0 € because of the uncertainty of possible customers for whom to sell the oxygen. The results of the sensitivity analysis are shown in Figure 37. It can be seen that both, CAPEX increase and removing oxygen revenue, have a significant decreasing effect on the

NPV. Removing oxygen revenue results in a lower NPV than increasing CAPEX. The combined effect of these measures decrease the NPV to 0.9 M€. Even though these measures would affect negatively on the profitability of the process, they would not decrease the NPV to below zero in this case. This means that with 2021a electricity prices and 4650 kg storage the process would be feasible even if no oxygen was sold or the investment costs of the process were increased.

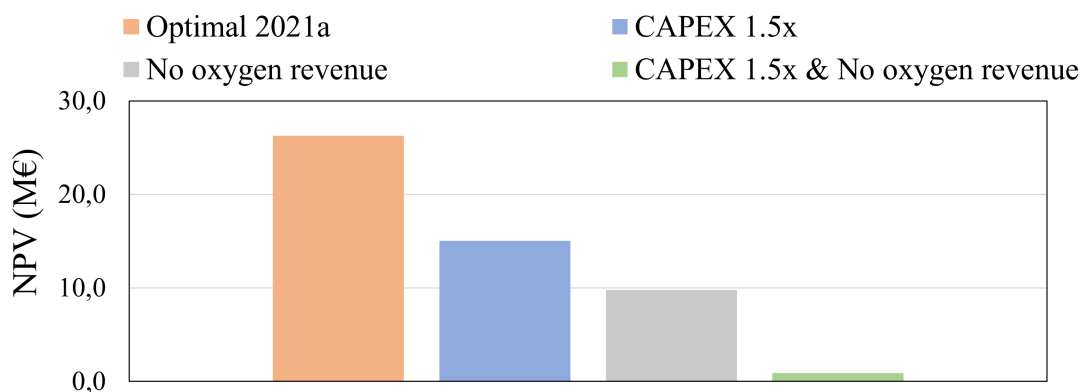


Figure 37: NPV sensitivity analysis for scenario 2021a with optimal storage size.

In addition to electricity prices, CAPEX and oxygen revenue, there are other factors that will have a large effect on the feasibility of the process. These factors include carbon price and natural gas selling price. If both prices stay at high level, the more advantage there is for the expensive SNG production. However, natural gas prices have come down from the record high (over 200 €/MWh) prices during this thesis and are now in the range of 80 - 100 €/MWh [144]. The LCOSNG values for 2021a vary between 92 - 95.6 €/MWh which means that if the selling price was below these values, the NPV of 2021a would decrease to below zero. Therefore, the current natural gas prices are already on the edge of making scenario 2021a unprofitable. The same applies even for the PPA scenarios with LCOSNGs of 78 and 122 €/MWh for Finland and Europe, respectively. With these conclusions, it is highly probable that political measures are needed for the renewable fuels to be able to compete with the fossil ones.

The replacement of fossil natural gas with SNG is highly important in this world situation and thus political methods to improve the profitability of SNG production can be expected. Alone supporting renewable electricity generation and increasing of it can make a major impact to the process feasibility. As it was mentioned, electricity cost reductions from dynamic operation are the highest with volatile electricity prices which are more frequent with VRE. In addition, renewable electricity is cheaper to generate and therefore electricity prices could decrease with higher share of renewable electricity. Due to the necessity of shutting off Russian gas, European commission published REPowerEU-plan to strengthen the European energy security. The plan includes a target to increase the share of renewable electricity to 45 % by 2030. The target was increased from the initial 40 % that was decided in the EU Fit-for-55

package in 2021. In addition, a 200-million-euro additional funding was decided to reserve for research of hydrogen production. [145] These measures are important for accelerating the green transition and making the Power-to-X, including PtM, technologies considerable alternatives for fossil ones.

10 Conclusions

In this thesis, the dynamic capabilities and operation methods of Power-to-Methane were studied. The dynamic capabilities of the process are mainly limited by methanation and CO₂ capture. From these two, amine-based absorption acts as a bottleneck for the process because of its high minimum load and slow start-up time. However, methanation has also poor dynamic properties due to the thermal runaways occurring in the reactor when changing the inlet flow. Thermal runaways cause methane yield and CO₂ conversion to decrease which have a negative impact on the quality of the product. It is debatable if CO₂ is needed to be utilized in a dynamic manner if the flue gas flow to the capture unit is stable. In the scenario where CO₂ is operated steadily due to environmental benefits, the title of bottleneck of the process is held by methanation. On the other hand, electrolyzers show generally very good transient properties. From the top three electrolyser technologies, PEM is the one with the best dynamic capabilities. The dynamic operation of SOE requires more investigation as no ramp rate of SOE was yet known. In addition, the effect of dynamic operation on electrolyser degradation rate has to be researched more closely to be able to estimate the CAPEX costs more accurately.

Market requirements for demand response in the Finnish electricity system and sector coupling in the context of grid injection were reviewed. The requirements related to demand response were minimum load curtailment capacity and ramp requirement for the curtailment. These requirements varied between different market places. However, it was concluded that electrolyzers could participate to almost all of the markets, excluding fast frequency reserve. Requirements related to grid injection were that the production of SNG should be well predicted and that the quality of the product should be at high enough level, more specifically the methane content should be above 95 mol-%. The requirements for grid injection are not always fulfilled during transient operation of methanation due to the reduction in methane yield and CO₂ conversion.

A Simulink model was created to study the dynamic behaviour of the electrolyser. Different electricity price mixes, 2021a, 2021b and 2022, were used as alternative scenarios for the dynamic operation. Under each electricity price mix, five different storage capacities were modelled. One of the storage capacities was 0 kg, and corresponded steady operation. In the cases where dynamic operation method was utilized, the load level of the electrolyser was varied according to the electricity price and remaining storage capacity. The optimal values for the electricity price - load limits were found by minimizing the electricity costs of the electrolyser. For all of the electricity price mixes, the electricity costs decreased with increasing storage size. The full load hours did not have a clear trend between the scenarios, but they were in the same magnitude for all of the cases, approximately 7000 hours per year. The explicit demand response payments from FCR-D were concluded to be extremely small and did not impact the profitability of the process.

The feasibility of electricity price mixes and storage capacities were compared in the economic analysis. Optimal storage size was found for each mix by selecting the case with the lowest total costs. For 2021a and 2022 the optimal storage size

was 4650 kg and for 2021b it was 3100 kg. The LCOSNG values for the electricity price mixes with optimal storage capacity were 92 €/MWh, 181.4 €/MWh and 159.5 €/MWh for 2021a, 2021b and 2022, respectively.

The profitability of the process increased significantly when moving from steady operation to dynamic operation with optimal storage size. The NPVs increased by 10 %, 11 % and 39 % for 2021a, 2021b and 2022, respectively. The reductions in the production costs were 3.8 %, 3.3 % and 10 % for 2021a, 2021b and 2022, respectively. From these values, it can be concluded that there is a significant potential in dynamic operation with regards to cost optimization. However, due to the high electricity prices of 2021b and 2022, the process did not achieve profitability even with dynamic operation. On the other hand, PPA-powered Power-to-Methane process was profitable. Utilizing the average price of wind generation based PPAs from Finland resulted in the most feasible option. Therefore, even though dynamic operation has economic advantage when compared to steady operation with wholesale electricity prices, dynamic operation can not compete with steady operation with PPA with current electricity prices. In addition to electricity cost, natural gas selling price and carbon price will have a large effect on the feasibility of the process, even when PPA is utilized.

From the results of the economic analysis, it can be concluded that the highest cost reductions can be reached with the electricity price mix with the most frequent electricity price variations, meaning mix of 2022. Therefore, there is a possibility to achieve even larger cost savings with dynamic operation in the future, if the generation and price of electricity evolve to be even more volatile. These cost reductions achieved with dynamic operation are one kind of revenue from demand response, called implicit savings. The importance of demand response in the electricity system will increase as the electricity generation will become more and more intermittent. To conclude, the need for demand response and the revenue from it are both going to grow in the future due to increasing share of renewable energy. Therefore, dynamic capabilities of the process are important to take into consideration even though the process is not feasible with the current electricity prices. The profitability of the process can be increased for example with political initiatives, such as REPowerEU, where the target of increasing the share renewable electricity generation was set to 45 %.

Future work possibilities with this topic are for example electrolyser CAPEX optimization and degradation rate studies. As it was seen in Figure 29, the CAPEX of the electrolyser was significantly larger than that of the storage. It would be an interesting aspect to study the same process and decrease the capacity of the electrolyser and increase the storage size to find the optimal configuration of them with which the CAPEX would be reduced. In addition, the effect of dynamic operation to the degradation rate has to be studied more closely to find out if it has a major impact on the CAPEX cost of the AEL. Alternatively, PEM electrolyser could be used because the preliminary studies show that the dynamic operation could even increase its lifetime. However, as PEM is a more expensive technology, it would also increase the CAPEX of the process. A study could be conducted to see which alternative would result in higher CAPEX in dynamic operation. Additionally, the load levels of the electrolyser could be optimized to achieve the highest possible

efficiency, and therefore lower costs, during transient operation. Demand response possibilities could be further studied by implementing other reserves or markets to the model and by optimizing the electrolyser operation by maximizing the explicit payments.

References

- [1] International Energy Agency, IEA. World energy outlook 2021. 2021. <https://www.iea.org/reports/world-energy-outlook-2021>. Online, accessed 31.3.2022.
- [2] International Energy Agency, IEA. Energy fact sheet: Why does Russian oil and gas matter? 2022. <https://www.iea.org/articles/energy-fact-sheet-why-does-russian-oil-and-gas-matter>. Online, accessed 31.3.2022.
- [3] International Energy Agency, IEA. Russian fossil fuel reliance data explorer. 2022. <https://www.iea.org/reports/russian-fossil-fuel-reliance-data-explorer>. Online, accessed 31.3.2022.
- [4] Statistics Finland. Statistics Finland's free-of-charge statistical databases, 12vq – total energy consumption by energy source (all categories), 1970-2021*. 2021. https://pxweb2.stat.fi/PXWeb/pxweb/en/StatFin/StatFin__ehk/statfin_ehk_pxt_12vq.px. Online, accessed 10.5.2022.
- [5] International Energy Agency, IEA. A 10-point plan to reduce the European Union's reliance on Russian natural gas. 2022. <https://www.iea.org/reports/a-10-point-plan-to-reduce-the-european-unions-reliance-on-russian-natural-gas>. Online, accessed 31.3.2022.
- [6] International Energy Agency, IEA. Gas market report, Q3-2021. 2021. <https://www.iea.org/reports/gas-market-report-q3-2021>. Online, accessed 31.3.2022.
- [7] Jachin Gorre, Fabian Ruoss, Hannu Karjunen, Johannes Schaffert, and Tero Tynjälä. Cost benefits of optimizing hydrogen storage and methanation capacities for Power-to-Gas plants in dynamic operation. *Applied Energy*, 257:113967, 2020.
- [8] Jannik Burre, Dominik Bongartz, Luisa Brée, Kosan Roh, and Alexander Mitsos. Power-to-X: between electricity storage, e-production, and demand side management. *Chemie Ingenieur Technik*, 92(1-2):74–84, 2020.
- [9] Bruna Rego de Vasconcelos and Jean-Michel Lavoie. Recent advances in Power-to-X technology for the production of fuels and chemicals. *Frontiers in chemistry*, page 392, 2019.
- [10] Christina Wulf, Petra Zapp, and Andrea Schreiber. Review of Power-to-X demonstration projects in Europe. *Frontiers in Energy Research*, page 191, 2020.

- [11] Jordi Guilera, Joan Ramon Morante, and Teresa Andreu. Economic viability of SNG production from power and CO₂. *Energy Conversion and Management*, 162:218–224, 2018.
- [12] Yousef SH Najjar. Hydrogen safety: The road toward green technology. *International Journal of Hydrogen Energy*, 38(25):10716–10728, 2013.
- [13] European Gas Hub. European gas prices strongly up as Russia will seek payment in roubles. 2022. <https://www.europeangashub.com/european-gas-prices-strongly-up-as-russia-will-seek-payment-in-roubles.html>. Online; accessed 28.3.2022.
- [14] International Energy Agency, IEA. Gas market report, Q1 2022. 2022. <https://www.iea.org/reports/gas-market-report-q1-2022>. Online; accessed 28.3.2022.
- [15] International Energy Agency, IEA. Electricity market report - January 2022. 2022. <https://www.iea.org/reports/electricity-market-report-january-2022>. Online; accessed 28.3.2022.
- [16] Sarah Brown. Soaring fossil gas costs responsible for EU electricity price increase. 2021. <https://ember-climate.org/insights/research/soaring-fossil-gas-costs-responsible-for-eu-electricity-price-increase/>. Online; accessed 1.6.2022.
- [17] European Energy Exchange, EEX. Spot market data. 2022. <https://www.powernext.com/spot-market-data>. Online; accessed 28.3.2022.
- [18] Nord Pool. Historical market data. 2022. <https://www.nordpoolgroup.com/historical-market-data/>. Online; accessed 28.3.2022.
- [19] Theresa Müller and Dominik Möst. Demand response potential: available when needed? *Energy Policy*, 115:181–198, 2018.
- [20] HA Aalami, M Parsa Moghaddam, and GR Yousefi. Demand response modeling considering interruptible/curtailable loads and capacity market programs. *Applied Energy*, 87(1):243–250, 2010.
- [21] SEDC Smart Energy Demand Coalition. Explicit demand response in Europe, mapping the markets 2017. 2017. <https://smarten.eu/wp-content/uploads/2017/04/SEDC-Explicit-Demand-Response-in-Europe-Mapping-the-Markets-2017.pdf>. Online; accessed 4.4.2022.
- [22] Jacopo Torriti, Mohamed G Hassan, and Matthew Leach. Demand response experience in Europe: Policies, programmes and implementation. *Energy*, 35(4):1575–1583, 2010.

- [23] FinGrid. TSO report on balancing in accordance with article 60 of commission regulation (EU) 2017/2195 of 23 november 2017 establishing a guideline on electricity balancing. 2022. <https://www.fingrid.fi/globalassets/dokumentit/fi/sahkomarkkinat/reservit/ebgl60-tso-report-on-balancing-2022.pdf>. Online, accessed 5.4.2022.
- [24] FinGrid. Reserve products and reserve market places. 2022. <https://www.fingrid.fi/globalassets/dokumentit/fi/sahkomarkkinat/reservit/reserve-products-and-reserve-market-places.pdf>. Online, accessed 5.4.2022.
- [25] FinGrid. Demand-side management. 2022. <https://www.fingrid.fi/en/electricity-market/market-integration/the-future-of-the-electricity-markets/demand-side-management/>. Online, accessed 5.4.2022.
- [26] Kreetta Manninen. Rakennuksen kysyntäjoustomallinnuksen vaatimusten määrittäminen. 2017. https://lutpub.lut.fi/bitstream/handle/10024/134517/Diplomityo_Manninen_Kreetta.pdf?sequence=2. Online, accessed 7.4.2022.
- [27] FinGrid. Säätosähkö- ja säätökapasiteettimarkkinat. 2022. <https://www.fingrid.fi/sahkomarkkinat/reservit-ja-saatosahko/saatosahko--ja-saatokapasiteettimarkkinat/>. Online, accessed 6.4.2022.
- [28] FinGrid. Taajuusohjattu käyttö- ja häiriöreservi. 2022. <https://www.fingrid.fi/sahkomarkkinat/reservit-ja-saatosahko/taajuusohjattu-kaytto--ja-hairioreservi/>. Online, accessed 6.4.2022.
- [29] FinGrid. Frequency containment reserves (FCR-N, FCR-D up and FCR-D down), transactions in the hourly and yearly markets. 2022. <https://www.fingrid.fi/en/electricity-market/electricity-market-information/reserve-market-information/frequency-controlled-disturbance-reserve/>. Online, accessed 6.4.2022.
- [30] FinGrid. Volume and price of balancing energy. 2022. <https://www.fingrid.fi/en/electricity-market/electricity-market-information/reserve-market-information/balancing-power-price/#price-of-balancing-power>. Online, accessed 6.4.2022.
- [31] FinGrid. Fast frequency reserve. 2022. <https://www.fingrid.fi/en/electricity-market/electricity-market-information/reserve-market-information/fast-frequency-reserve/>. Online, accessed 6.4.2022.

- [32] Suomen Tuulivoimayhdistys. Pitkäaikainen sähkönostosopimus (PPA). 2022. <https://tuulivoimayhdistys.fi/tietoa-tuulivoimasta-2/tietopankki/pitkaaikainen-sahkonostosopimus-ppa>. Online, accessed 19.4.2022.
- [33] Mohammad Sadegh Javadi and Amin Javadinasab. Power purchasing agreements in modern power system. *Journal of American Science*, 7(6):164–169, 2011.
- [34] Jason Johns and Jennifer Martin. The law of wind: A guide to business and legal issues. Chapter 7: Power purchase agreements and environmental attributes. 2018.
- [35] Jasmine Ramsebner, Reinhard Haas, Amela Ajanovic, and Martin Wietschel. The sector coupling concept: A critical review. *Wiley Interdisciplinary Reviews: Energy and Environment*, 10(4):e396, 2021.
- [36] Biovoima. Gas transportation containers. 2019. <https://biovoima.com/en/solutions/gas-transportation-containers>. Online, accessed 15.4.2022.
- [37] GasGrid Finland. Kaasun siirtoverkosto. 2022. <https://gasgrid.fi/kaasuverkosto/kaasun-siirtoverkosto/>. Online, accessed 15.4.2022.
- [38] GasGrid Finland. What is flowing in our pipelines? 2022. <https://gasgrid.fi/en/gas-network/what-is-flowing-in-our-pipelines/>. Online, accessed 19.4.2022.
- [39] GasGrid Finland. Kaasunsiirron säännöt, versio 3.0. 2022. https://gasgrid.fi/wp-content/uploads/Kaasunsiirron-saannot-3.0_clean.pdf. Online, accessed 19.4.2022.
- [40] GasGrid Finland. Market model. 2022. <https://gasgrid.fi/en/gas-market/market-model/>. Online, accessed 19.4.2022.
- [41] Tabbi Wilberforce, AG Olabi, Enas Taha Sayed, Khaled Elsaid, and Mohammad Ali Abdelkareem. Progress in carbon capture technologies. *Science of The Total Environment*, 761:143203, 2021.
- [42] Ahmed Al-Mamoori, Anirudh Krishnamurthy, Ali A Rownaghi, and Fateme Rezaei. Carbon capture and utilization update. *Energy Technology*, 5(6):834–849, 2017.
- [43] International Energy Agency, IEA. Global energy review: CO₂ emissions in 2021. 2022. <https://iea.blob.core.windows.net/assets/c3086240-732b-4f6a-89d7-db01be018f5e/GlobalEnergyReviewCO2Emissionsin2021.pdf>. Online, accessed 30.3.2022.

- [44] Zhiwu Henry Liang, Wichitpan Rongwong, Helei Liu, Kaiyun Fu, Hongxia Gao, Fan Cao, Rui Zhang, Teerawat Sema, Amr Henni, Kazi Sumon, et al. Recent progress and new developments in post-combustion carbon-capture technology with amine based solvents. *International Journal of Greenhouse Gas Control*, 40:26–54, 2015.
- [45] Jon Gibbins and Hannah Chalmers. Carbon capture and storage. *Energy policy*, 36(12):4317–4322, 2008.
- [46] Najmus S Sifat and Yousef Haseli. A critical review of CO₂ capture technologies and prospects for clean power generation. *Energies*, 12(21):4143, 2019.
- [47] Fernando Vega, Mercedes Cano, Sara Camino, Luz M Gallego Fernández, Esmeralda Portillo, and Benito Navarrete. Solvents for carbon dioxide capture. *Carbon dioxide chemistry, capture and oil recovery*, pages 142–163, 2018.
- [48] Cheng-Hsiu Yu, Chih-Hung Huang, Chung-Sung Tan, et al. A review of CO₂ capture by absorption and adsorption. *Aerosol and Air Quality Research*, 12(5):745–769, 2012.
- [49] Firoz Alam Chowdhury, Hidetaka Yamada, Takayuki Higashii, Yoichi Matsuzaki, and Shingo Kazama. Synthesis and characterization of new absorbents for CO₂ capture. *Energy Procedia*, 37:265–272, 2013.
- [50] Sandrine Martin, Helene Lepaumier, Dominique Picq, Jean Kittel, Theodorus de Bruin, Abdelaziz Faraj, and Pierre-Louis Carrette. New amines for CO₂ capture. IV. degradation, corrosion, and quantitative structure property relationship model. *Industrial & engineering chemistry research*, 51(18):6283–6289, 2012.
- [51] Thanita Nittaya, Peter L Douglas, Eric Croiset, and Luis A Ricardez-Sandoval. Dynamic modelling and control of MEA absorption processes for CO₂ capture from power plants. *Fuel*, 116:672–691, 2014.
- [52] Patrick Eser, Antriksh Singh, Ndaona Chokani, and Reza S Abhari. Effect of increased renewables generation on operation of thermal power plants. *Applied Energy*, 164:723–732, 2016.
- [53] International Energy Agency, IEA. The role of CCUS in low-carbon power systems. 2020. https://iea.blob.core.windows.net/assets/ccdc6b3-f6dd-4f9a-98c3-8366f4671427/The_role_of_CCUS_in_low-carbon_power_systems.pdf. Online, accessed 31.3.2022.
- [54] Yu-Jeng Lin, Chun-Cheng Chang, David Shan-Hill Wong, Shi-Shang Jang, and Jenq-Jang Ou. Control strategies for flexible operation of power plant integrated with CO₂ capture plant. In *Computer Aided Chemical Engineering*, volume 30, pages 237–241. Elsevier, 2012.

- [55] Fingrid. Sähköjärjestelmän tila, tuotanto suomessa. 2022. <https://www.fingrid.fi/sahkomarkkinat/sahkojarjestelman-tila/>. Online; accessed 3.6.2022.
- [56] Stuart M Cohen, Gary T Rochelle, and Michael E Webber. Optimal operation of flexible post-combustion CO₂ capture in response to volatile electricity prices. *Energy Procedia*, 4:2604–2611, 2011.
- [57] Felix Herrmann, Marcus Grünwald, and Julia Riese. Flexibility of Power-to-Gas plants: A case study. *Chemie Ingenieur Technik*, 92(12):1983–1991, 2020.
- [58] Mai Bui, Paul Tait, Mathieu Lucquiaud, and Niall Mac Dowell. Dynamic operation and modelling of amine-based CO₂ capture at pilot scale. *International Journal of Greenhouse Gas Control*, 79:134–153, 2018.
- [59] Evgenia Mechleri, Adekola Lawal, Alfredo Ramos, John Davison, and Niall Mac Dowell. Process control strategies for flexible operation of post-combustion CO₂ capture plants. *International Journal of Greenhouse Gas Control*, 57:14–25, 2017.
- [60] Howoun Jung, Dasom Im, Seongmin Heo, Boeun Kim, and Jay H Lee. Dynamic analysis and linear model predictive control for operational flexibility of post-combustion CO₂ capture processes. *Computers & Chemical Engineering*, 140:106968, 2020.
- [61] Thomas Marx-Schubach and Gerhard Schmitz. Optimizing the start-up process of post-combustion capture plants by varying the solvent flow rate. In *12th International Modelica Conference*, volume 132, pages 121–130, 2017.
- [62] Alfredo Ursua, Luis M Gandia, and Pablo Sanchis. Hydrogen production from water electrolysis: current status and future trends. *Proceedings of the IEEE*, 100(2):410–426, 2011.
- [63] Alexander Buttler and Hartmut Spliethoff. Current status of water electrolysis for energy storage, grid balancing and sector coupling via Power-to-Gas and Power-to-Liquids: A review. *Renewable and Sustainable Energy Reviews*, 82:2440–2454, 2018.
- [64] S Shiva Kumar and V Himabindu. Hydrogen production by PEM water electrolysis—a review. *Materials Science for Energy Technologies*, 2(3):442–454, 2019.
- [65] SA Grigoriev, VN Fateev, DG Bessarabov, and P Millet. Current status, research trends, and challenges in water electrolysis science and technology. *International Journal of Hydrogen Energy*, 45(49):26036–26058, 2020.

- [66] Sebastian Schiebahn, Thomas Grube, Martin Robinius, Vanessa Tietze, Bhunesh Kumar, and Detlef Stolten. Power to gas: Technological overview, systems analysis and economic assessment for a case study in Germany. *International journal of hydrogen energy*, 40(12):4285–4294, 2015.
- [67] Manuel Götz, Jonathan Lefebvre, Friedemann Mörs, Amy McDaniel Koch, Frank Graf, Siegfried Bajohr, Rainer Reimert, and Thomas Kolb. Renewable Power-to-Gas: A technological and economic review. *Renewable energy*, 85:1371–1390, 2016.
- [68] Andreas Zauner, Hans Böhm, Daniel C. Rosenfeld, and Robert Tichler. Innovative large-scale energy storage technologies and Power-to-Gas concepts after optimisation, D7.7 Analysis on future technology options and on techno-economic optimization. 2019.
- [69] Dohyung Jang, Jaedong Kim, Dongmin Kim, Won-Bi Han, and Sanggyu Kang. Techno-economic analysis and Monte Carlo simulation of green hydrogen production technology through various water electrolysis technologies. *Energy Conversion and Management*, 258:115499, 2022.
- [70] Selma Brynolf, Maria Taljegard, Maria Grahn, and Julia Hansson. Electrofuels for the transport sector: A review of production costs. *Renewable and Sustainable Energy Reviews*, 81:1887–1905, 2018.
- [71] Adam Christensen. Assessment of hydrogen production costs from electrolysis: United States and Europe. *International Council on Clean Transportation: Washington, DC, USA*, pages 1–73, 2020.
- [72] MD Rashid, Mohammed K Al Mesfer, Hamid Naseem, and Mohd Danish. Hydrogen production by water electrolysis: a review of alkaline water electrolysis, PEM water electrolysis and high temperature water electrolysis. *International Journal of Engineering and Advanced Technology*, 2015.
- [73] Rebah Maamouri, Damien Guilbert, Michel Zasadzinski, and Hugues Rafaralahy. Proton exchange membrane water electrolysis: Modeling for hydrogen flow rate control. *International Journal of Hydrogen Energy*, 46(11):7676–7700, 2021.
- [74] Christopher Varela, Mahmoud Mostafa, and Edwin Zondervan. Modeling alkaline water electrolysis for Power-to-X applications: A scheduling approach. *International journal of hydrogen energy*, 46(14):9303–9313, 2021.
- [75] Eero Inkeri. Modelling of component dynamics and system integration in Power-to-Gas process. Lappeenranta-Lahti University of Technology LUT. 2021.
- [76] Floriane Petipas, Qingxi Fu, Annabelle Brisse, and Chakib Bouallou. Transient operation of a solid oxide electrolysis cell. *International journal of hydrogen energy*, 38(7):2957–2964, 2013.

- [77] Ligang Wang, Mar Pérez-Fortes, Hossein Madi, Stefan Diethelm, François Maréchal, et al. Optimal design of solid-oxide electrolyzer based Power-to-Methane systems: A comprehensive comparison between steam electrolysis and co-electrolysis. *Applied Energy*, 211:1060–1079, 2018.
- [78] Rahman Daiyan, Iain MacGill, and Rose Amal. Opportunities and challenges for renewable Power-to-X, 2020.
- [79] Martin Thema, Tobias Weidlich, Manuel Hörl, Annett Bellack, Friedemann Mörs, Florian Hackl, Matthias Kohlmayer, Jasmin Gleich, Carsten Stabenau, Thomas Trabold, et al. Biological CO₂-methanation: An approach to standardization. *Energies*, 12(9):1670, 2019.
- [80] Saeed Sahebdehfar and Maryam Takht Ravanchi. Carbon dioxide utilization for methane production: A thermodynamic analysis. *Journal of Petroleum Science and Engineering*, 134:14–22, 2015.
- [81] Stefan Rönsch, Jens Schneider, Steffi Matthischke, Michael Schlüter, Manuel Götz, Jonathan Lefebvre, Praseeth Prabhakaran, and Siegfried Bajohr. Review on methanation—from fundamentals to current projects. *Fuel*, 166:276–296, 2016.
- [82] Jens Bremer, Karsten HG Rätze, and Kai Sundmacher. CO₂ methanation: Optimal start-up control of a fixed-bed reactor for Power-to-Gas applications. *AIChE Journal*, 63(1):23–31, 2017.
- [83] Steffi Matthischke, Stefan Roensch, and Robert Guttel. Start-up time and load range for the methanation of carbon dioxide in a fixed-bed recycle reactor. *Industrial & Engineering Chemistry Research*, 57(18):6391–6400, 2018.
- [84] Yu-Lung Kao, Po-Hsien Lee, Yu-Ti Tseng, I-Lung Chien, and Jeffrey D Ward. Design, control and comparison of fixed-bed methanation reactor systems for the production of substitute natural gas. *Journal of the Taiwan Institute of Chemical Engineers*, 45(5):2346–2357, 2014.
- [85] Behnam Partopour and Anthony G Dixon. Integrated multiscale modeling of fixed bed reactors: studying the reactor under dynamic reaction conditions. *Chemical Engineering Journal*, 377:119738, 2019.
- [86] Rasmey Try, Alain Bengaouer, Pierre Baurens, and Christian Jallut. Dynamic modeling and simulations of the behavior of a fixed-bed reactor-exchanger used for CO₂ methanation. *AIChE journal*, 64(2):468–480, 2018.
- [87] Steffi Theurich, Stefan Rönsch, and Robert Güttel. Transient flow rate ramps for methanation of carbon dioxide in an adiabatic fixed-bed recycle reactor. *Energy Technology*, 8(3):1901116, 2020.

- [88] Konrad L Fischer and Hannsjörg Freund. On the optimal design of load flexible fixed bed reactors: Integration of dynamics into the design problem. *Chemical Engineering Journal*, 393:124722, 2020.
- [89] Anang Swapnesh, Vimal C Srivastava, and Indra D Mall. Comparative study on thermodynamic analysis of CO₂ utilization reactions. *Chemical Engineering & Technology*, 37(10):1765–1777, 2014.
- [90] Youngmin Jeong, Jonghyun Park, and Myungwan Han. Design and control of a fixed-bed recycle reactor with multicyclic layers: Methanation of carbon dioxide. *Industrial & Engineering Chemistry Research*, 60(12):4650–4667, 2021.
- [91] Emanuele Giglio, Raffaele Pirone, and Samir Bensaid. Dynamic modelling of methanation reactors during start-up and regulation in intermittent Power-to-Gas applications. *Renewable Energy*, 170:1040–1051, 2021.
- [92] Steffi Matthischke, Raphael Krüger, Stefan Rönsch, and Robert Guettel. Unsteady-state methanation of carbon dioxide in a fixed-bed recycle reactor—experimental results for transient flow rate ramps. *Fuel Processing Technology*, 153:87–93, 2016.
- [93] Axel Fache, Frederic Marias, Vincent Guerré, and Stephane Palmade. Optimization of fixed-bed methanation reactors: Safe and efficient operation under transient and steady-state conditions. *Chemical Engineering Science*, 192:1124–1137, 2018.
- [94] Manuel Gruber, Petra Weinbrecht, Linus Biffar, Stefan Harth, Dimosthenis Trimis, Jörg Brabandt, Oliver Posdziech, and Robert Blumentritt. Power-to-Gas through thermal integration of high-temperature steam electrolysis and carbon dioxide methanation-experimental results. *Fuel Processing Technology*, 181:61–74, 2018.
- [95] Ronny Tobias Zimmermann, Jens Bremer, and Kai Sundmacher. Load-flexible fixed-bed reactors by multi-period design optimization. *Chemical Engineering Journal*, 428:130771, 2022.
- [96] Axel Fache, Frédéric Marias, Vincent Guerré, and Stéphane Palmade. Intermittent operation of fixed-bed methanation reactors: a simple relation between start-up time and idle state duration. *Waste and Biomass Valorization*, 11(2):447–463, 2020.
- [97] Elimar Frank, Jachin Gorre, Fabian Ruoss, and Markus J Friedl. Calculation and analysis of efficiencies and annual performances of Power-to-Gas systems. *Applied energy*, 218:217–231, 2018.
- [98] Bernhard Lecker, Lukas Illi, Andreas Lemmer, and Hans Oechsner. Biological hydrogen methanation—a review. *Bioresource technology*, 245:1220–1228, 2017.

- [99] MB Jensen, LDM Ottosen, and MVW Kofoed. H₂ gas-liquid mass transfer: A key element in biological Power-to-Gas methanation. *Renewable and Sustainable Energy Reviews*, 147:111209, 2021.
- [100] Dietmar Strübing, Andreas B Moeller, Bettina Mößnang, Michael Lebuhn, Jörg E Drewes, and Konrad Koch. Anaerobic thermophilic trickle bed reactor as a promising technology for flexible and demand-oriented H₂/CO₂ biomethanation. *Applied Energy*, 232:543–554, 2018.
- [101] Mörs Friedemann, Schlautmann Ruth, Jachin Gorre, and Robin Leonhard. Innovative large-scale energy storage technologies and Power-to-Gas concepts after optimisation, D5.9 Final report on evaluation of technologies and processes. 2020.
- [102] Dietmar Strübing, Bettina Huber, Michael Lebuhn, Jörg E Drewes, and Konrad Koch. High performance biological methanation in a thermophilic anaerobic trickle bed reactor. *Bioresource technology*, 245:1176–1183, 2017.
- [103] Dietmar Strübing, Andreas B Moeller, Bettina Mößnang, Michael Lebuhn, Jörg E Drewes, and Konrad Koch. Load change capability of an anaerobic thermophilic trickle bed reactor for dynamic H₂/CO₂ biomethanation. *Bioresource technology*, 289:121735, 2019.
- [104] Michal Sposob and Radziah Wahid. Comparison and gas loading impact on counter-and concurrent trickle-bed reactor configurations for ex-situ biomethanation. 2021.
- [105] Vincent Dieterich, Alexander Buttler, Andreas Hanel, Hartmut Spliethoff, and Sebastian Fendt. Power-to-Liquid via synthesis of methanol, DME or Fischer-Tropsch-fuels: a review. *Energy & Environmental Science*, 13(10):3207–3252, 2020.
- [106] Florian Nestler, Matthias Krüger, Johannes Full, Max J Hadrich, Robin J White, and Achim Schaadt. Methanol synthesis—industrial challenges within a changing raw material landscape. *Chemie Ingenieur Technik*, 90(10):1409–1418, 2018.
- [107] Alessandro Poluzzi, Giulio Guandalini, Simone Guffanti, Cristina Elsidio, Stefania Moioli, Patrick Huttenhuis, Glenn Rexwinkel, Emanuele Martelli, Gianpiero Groppi, and Matteo C Romano. Flexible power & biomass-to-methanol plants: Design optimization and economic viability of the electrolysis integration. *Fuel*, 310:122113, 2022.
- [108] Chao Chen and Aidong Yang. Power-to-Methanol: The role of process flexibility in the integration of variable renewable energy into chemical production. *Energy Conversion and Management*, 228:113673, 2021.

- [109] Jonas Wentrup, Georg R Pesch, and Jorg Thöming. Dynamic operation of Fischer-Tropsch reactors for Power-to-Liquid concepts: A review. *Renewable and Sustainable Energy Reviews*, 162:112454, 2022.
- [110] Ahmed M Elberry, Jagruti Thakur, Annukka Santasalo-Aarnio, and Martti Larmi. Large-scale compressed hydrogen storage as part of renewable electricity storage systems. *International Journal of Hydrogen Energy*, 46(29):15671–15690, 2021.
- [111] Cevahir Tarhan and Mehmet Ali Çil. A study on hydrogen, the clean energy of the future: Hydrogen storage methods. *Journal of Energy Storage*, 40:102676, 2021.
- [112] Billur Sakintuna, Farida Lamari-Darkrim, and Michael Hirscher. Metal hydride materials for solid hydrogen storage: a review. *International journal of hydrogen energy*, 32(9):1121–1140, 2007.
- [113] Päivi T Aakko-Saksa, Chris Cook, Jari Kiviaho, and Timo Repo. Liquid organic hydrogen carriers for transportation and storing of renewable energy—review and discussion. *Journal of Power Sources*, 396:803–823, 2018.
- [114] G Amica, P Arneodo Larochette, and FC Gennari. Light metal hydride-based hydrogen storage system: economic assessment in Argentina. *International Journal of Hydrogen Energy*, 45(38):18789–18801, 2020.
- [115] Ananya Saraf et al. Techno-economic pricing model for carbon neutral fuels for seasonal energy storage. Master’s thesis at Aalto University. 2022.
- [116] Sandeep Kumar Dwivedi and Manish Vishwakarma. Hydrogen embrittlement in different materials: A review. *International Journal of Hydrogen Energy*, 43(46):21603–21616, 2018.
- [117] Jinyang Zheng, Xianxin Liu, Ping Xu, Pengfei Liu, Yongzhi Zhao, and Jian Yang. Development of high pressure gaseous hydrogen storage technologies. *International Journal of Hydrogen Energy*, 37(1):1048–1057, 2012.
- [118] IA Hassan, Haitham S Ramadan, Mohamed A Saleh, and Daniel Hissel. Hydrogen storage technologies for stationary and mobile applications: Review, analysis and perspectives. *Renewable and Sustainable Energy Reviews*, 149, 2021.
- [119] Alisson V. Brito. *Dynamic Modelling*. InTech, ISBN:953-51-5486-9, 2019.
- [120] Process Ecology. Dynamic process simulation: When do we really need it? 2015. <https://processecology.com/articles/dynamic-process-simulation-when-do-we-really-need-it>. Online; accessed 13.6.2022.

- [121] Michael A. Gray. *Introduction to the simulation of dynamics using simulink*. Chapman Hall/CRC Computational Science. Chapman and Hall/CRC, an imprint of Taylor and Francis, ISBN: 0-429-18430-1, 2010.
- [122] Georgios Sakas, Alejandro Ibáñez-Rioja, Vesa Ruuskanen, Antti Kosonen, Jero Ahola, and Olli Bergmann. Dynamic energy and mass balance model for an industrial alkaline water electrolyzer plant process. *International Journal of Hydrogen Energy*, 47(7):4328–4345, 2022.
- [123] Martín David, Hernán Álvarez, Carlos Ocampo-Martínez, and Ricardo Sánchez-Peña. Dynamic modelling of alkaline self-pressurized electrolyzers: a phenomenological-based semiphysical approach. *International Journal of Hydrogen Energy*, 45(43):22394–22407, 2020.
- [124] Yi Zheng, Shi You, Henrik W Bindner, and Marie Münster. Optimal day-ahead dispatch of an alkaline electrolyser system concerning thermal–electric properties and state-transitional dynamics. *Applied Energy*, 307:118091, 2022.
- [125] Sumit Sood, Om Prakash, Mahdi Boukerdja, Jean-Yves Dieulot, Belkacem Ould-Bouamama, Mathieu Bressel, and Anne-Lise Gehin. Generic dynamical model of PEM electrolyser under intermittent sources. *Energies*, 13(24):6556, 2020.
- [126] Wojciech Uchman, Anna Skorek-Osikowska, Michał Jurczyk, and Daniel Węcel. The analysis of dynamic operation of Power-to-SNG system with hydrogen generator powered with renewable energy, hydrogen storage and methanation unit. *Energy*, 213:118802, 2020.
- [127] Eero Inkeri, Tero Tynjälä, and Hannu Karjunen. Significance of methanation reactor dynamics on the annual efficiency of Power-to-Gas-system. *Renewable Energy*, 163:1113–1126, 2021.
- [128] Meng Qi, Jinwoo Park, Robert Stephen Landon, Jeongdong Kim, Yi Liu, and Il Moon. Continuous and flexible renewable-Power-to-Methane via liquid CO₂ energy storage: Revisiting the techno-economic potential. *Renewable and Sustainable Energy Reviews*, 153:111732, 2022.
- [129] Shivani Jambur and Eerik Lähdemäki. Process model of AEL (Aspen). Wärtsilä Oyj Abp. 2022.
- [130] United States Environmental Protection Agency, EPA. Renewable Energy Certificates (RECs). 2022. <https://www.epa.gov/green-power-markets/renewable-energy-certificates-recs>. Online, accessed 6.7.2022.
- [131] Charlotte Van Leeuwen and Machiel Mulder. Power-to-Gas in electricity markets dominated by renewables. *Applied Energy*, 232:258–272, 2018.

- [132] Remi Chauvy, Lionel Dubois, Paul Lybaert, Diane Thomas, and Guy De Weireld. Production of synthetic natural gas from industrial carbon dioxide. *Applied Energy*, 260:114249, 2020.
- [133] U.S Department of Energy. DOE technical targets for hydrogen delivery. <https://www.energy.gov/eere/fuelcells/doe-technical-targets-hydrogen-delivery>. Online, accessed 11.5.2022.
- [134] Charlotte van Leeuwen and Andreas Zauner. Innovative large-scale energy storage technologies and Power-to-Gas concepts after optimisation. D8.3 Report on the costs involved with PtG technologies and their potentials across the EU. 2018.
- [135] Juho Piispa. Techno-economic analysis and aspen plus process simulation of a Power-to-Gas system integrated to waste incinerator. Master's thesis. Aalto University. 2022.
- [136] Global CCS Institute. Technology readiness and costs of CCS. 2021. <https://www.globalccsinstitute.com/wp-content/uploads/2022/03/CCE-CCS-Technology-Readiness-and-Costs-22-1.pdf>. Online, accessed 11.5.2022.
- [137] European Energy Exchange, EEX. Auction market. 2022. <https://www.eex.com/en/market-data/environmental-markets/auction-market>. Online, accessed 11.5.2022.
- [138] Evangelos Tzimas, C Filiou, SD Peteves, and JB Veyret. Hydrogen storage: state-of-the-art and future perspective. *EU Commission, JRC Petten, EUR 20995EN*, 2003.
- [139] Fabian Grueger, Fabian Möhrke, Martin Robinius, and Detlef Stolten. Early power to gas applications: Reducing wind farm forecast errors and providing secondary control reserve. *Applied energy*, 192:551–562, 2017.
- [140] Jachin Gorre, Felix Ortloff, and Charlotte van Leeuwen. Production costs for synthetic methane in 2030 and 2050 of an optimized Power-to-Gas plant with intermediate hydrogen storage. *Applied Energy*, 253:113594, 2019.
- [141] LevelTen Energy. Q1 2022, PPA price index executive summary, Europe. 2022. <https://www.leveltenenergy.com/ppa>. Online, accessed 24.5.2022.
- [142] LevelTen Energy. Q4 2021, PPA price index, Europe. 2021. <https://www.leveltenenergy.com/post/q4-2021>. Online, accessed 24.5.2022.
- [143] KPMG International. The Hydrogen Trajectory. 2022. <https://home.kpmg/xx/en/home/insights/2020/11/the-hydrogen-trajectory.html>. Online, accessed 11.7.2022.

- [144] European Energy Exchange, EEX. Spot market data. 2022. <https://www.powernext.com/spot-market-data>. Online; accessed 31.5.2022.
- [145] European Comission. Repowereu: A plan to rapidly reduce dependence on Russian fossil fuels and fast forward the green transition. 2022. https://ec.europa.eu/commission/presscorner/detail/en/ip_22_3131. Online; accessed 2.6.2022.